Transition from Laminar to Turbulent Flow

L. Eça

with the help of

Rui Lopes, Serge L. Toxopeus and Maarten Kerkvliet

L. Eça, 9 and 12 April 2021

Contents

- Introduction
- Basic transition onset mechanisms
- Modelling transition from laminar to turbulent flow
  - Empirical correlations
  - e^n method
  - Transport equation(s) models
- Examples of CFD simulations of transitional flows
  - 1st AIAA Transition Workshop
  - AVT-313 Transition Workshop

L. Eça, 9 and 12 April 2021

Introduction

- Flow in pipes showed a change in flow regime:

Reynolds experiment

- Low flow rate (Reynolds number) exhibits a steady flow (laminar regime);
- High flow rate (Reynolds number) exhibits an unsteady flow with a large range of frequencies in the time signal (turbulent regime);

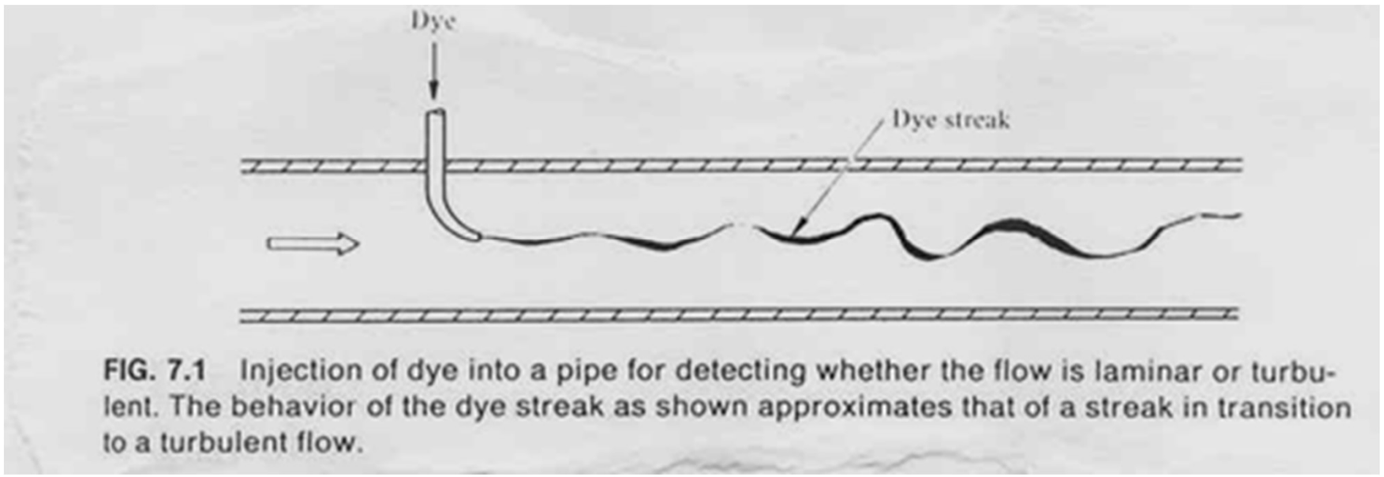

FIG. 7.1 Injection of dye into a pipe for detecting whether the flow is laminar or turbulent. The behavior of the dye streak as shown approximates that of a streak in transition to a turbulent flow.

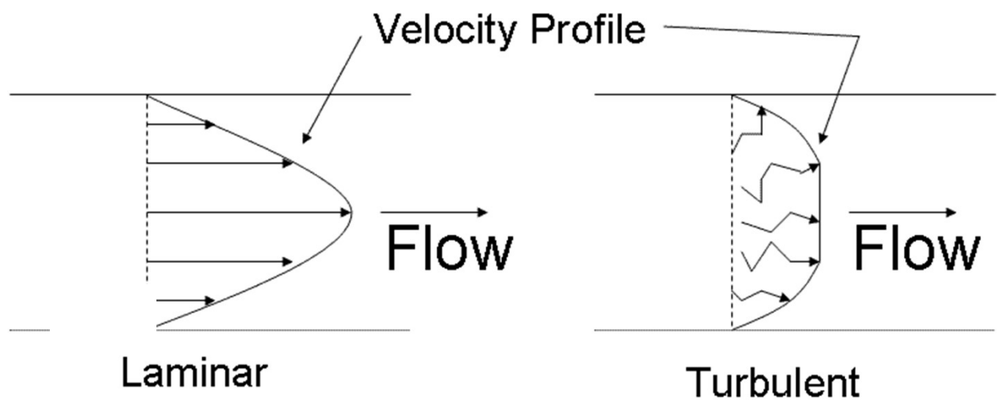

Introduction

- Flow in pipes showed a change in flow regime:

Reynolds experiment

Reynolds number

$$Re = \frac{L_{ref} U_{ref}}{\nu}$$

L_{ref} → Reference length
U_{ref} → Reference velocity
ν → Kinematic viscosity

Pipe flow:

$$Re = \frac{L_{ref} U_{ref}}{\nu}$$

$$L_{ref} = \mathrm{D}$$

$$U_{ref} = U_{avg} = \frac{4Q}{\pi D^2}$$

Introduction

- Flow over a flat plate:

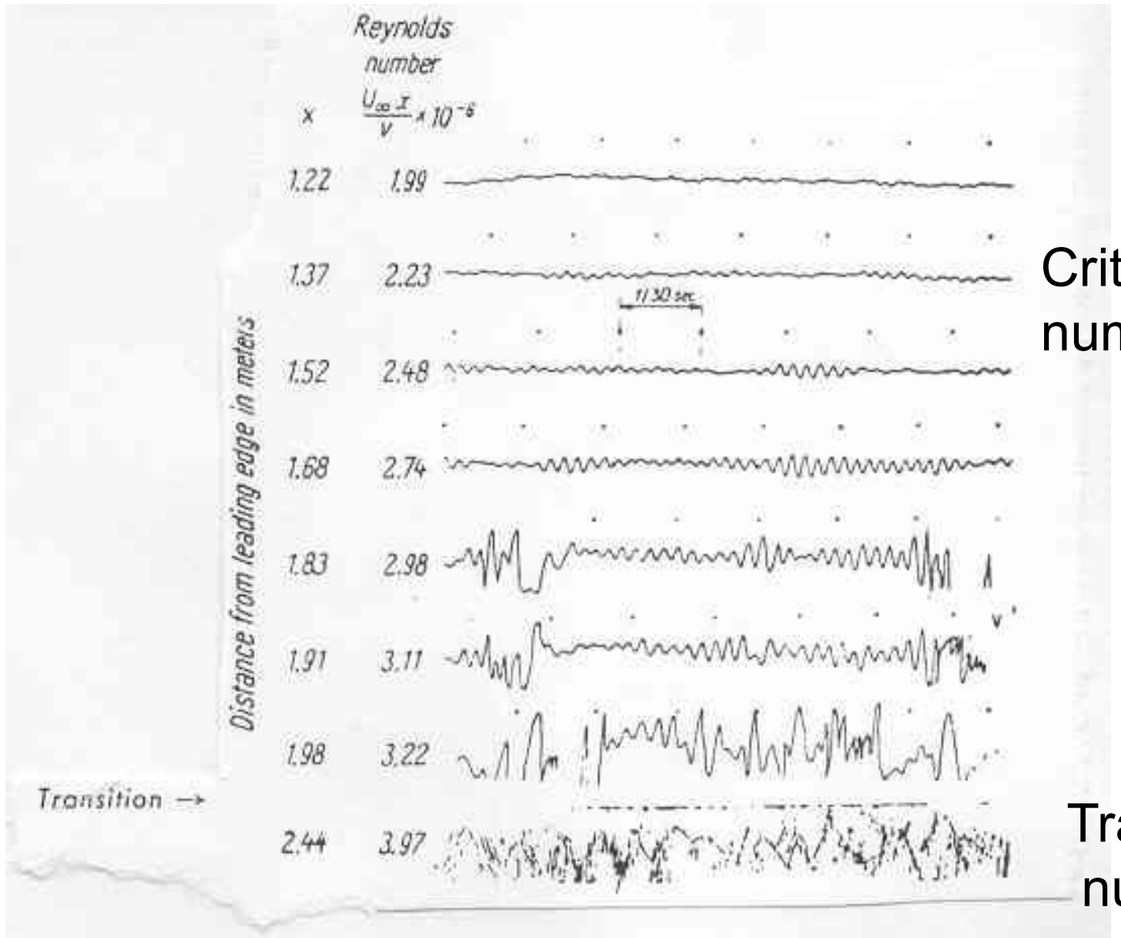

Critical Reynolds number

Transition region

Transition Reynolds number

$$Re = \frac{L_{ref} U_{ref}}{\nu}$$

$$L_{ref} = x$$

$$U_{ref} = U_{ext}$$

- x is the distance to the leading edge

- U_{ext} is the velocity of the external flow

Introduction

- Jet

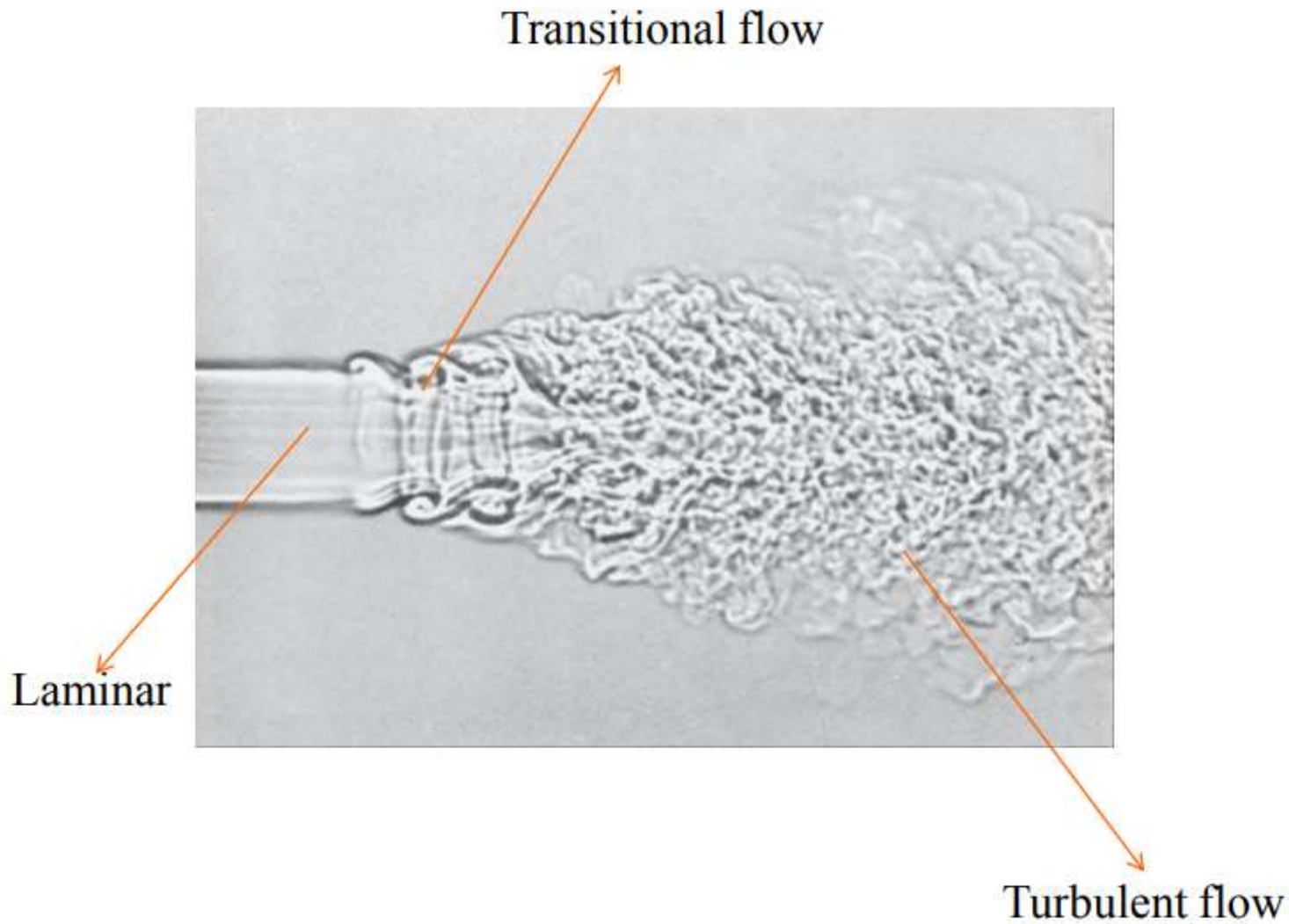

Transition from Laminar to Turbulent Flow

Basic transition onset mechanisms

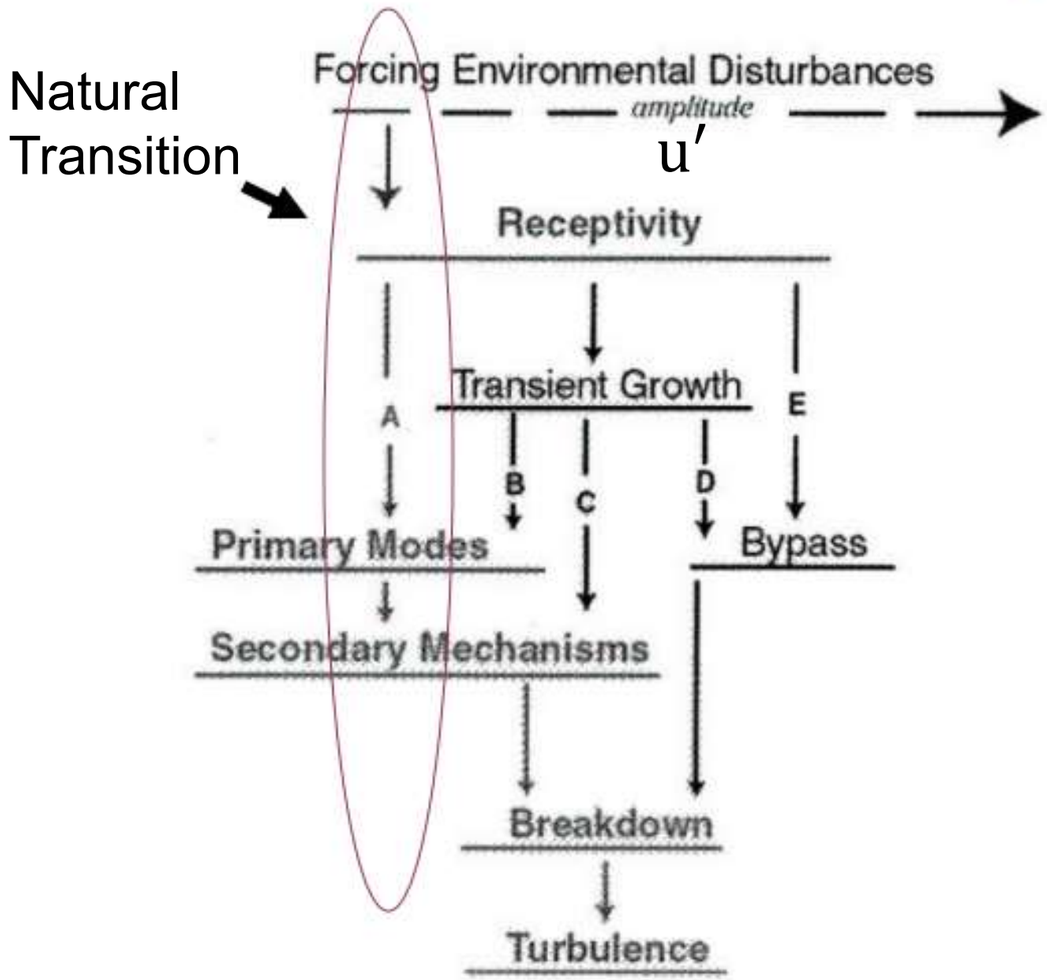

- Receptivity - Disturbances in freestream (sound or vorticity) enter boundary layer as steady and/or unsteady fluctuations of basic state. Establish initial conditions of disturbance amplitude, frequency, phase.

flight, a few wind tunnels $u' < 10^{-3}$

most wind tunnels $< 10^{-2}$

turbulent boundary layer $< 10^{-1}$

turbines/compressors $> 10^{-1}$

Adapted from Prof. Helen Reed, Texas A&M

Basic transition onset mechanisms

- Tollmien-Schlichting (TS) waves (natural transition). Inflection points of velocity profiles cause instability:
  - Pressure gradient in boundary-layers;
  - Free-shear layers;
  - Wakes;
- Separation-induced transition;
- Bypass transition;
- Crossflow (CF) transition (3-D boundary-layers);
- Roughness induced transition;
- …

Modeling transition from laminar to turbulent flow

- Empirical correlations are available to estimate the onset of transition.

$$Re_\theta = 1{,}174\left(1 + \frac{22400}{Re_x}\right)Re_x^{0{,}46} \quad 10^5 < Re_x < 4 \times 10^7$$

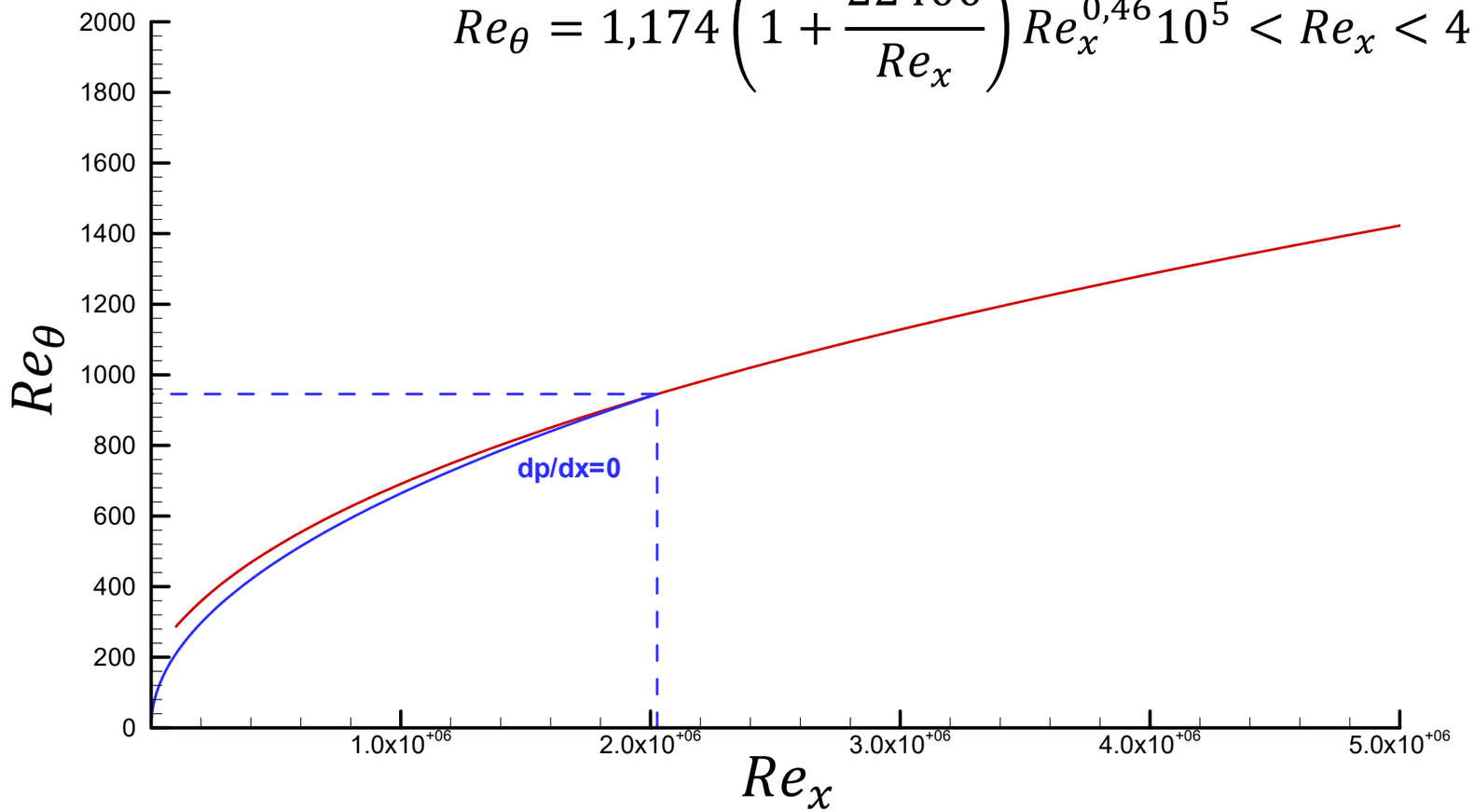

Cebeci & Smith

Modeling transition from laminar to turbulent flow

- Empirical correlations are available to estimate the onset of transition.

$$\log_{10}(Re_x) = -40{,}4557 + 64{,}8066H - 26{,}7538H^2 + 3{,}3819H^3 \quad \text{with} \quad 2.1 < H < 2.8$$

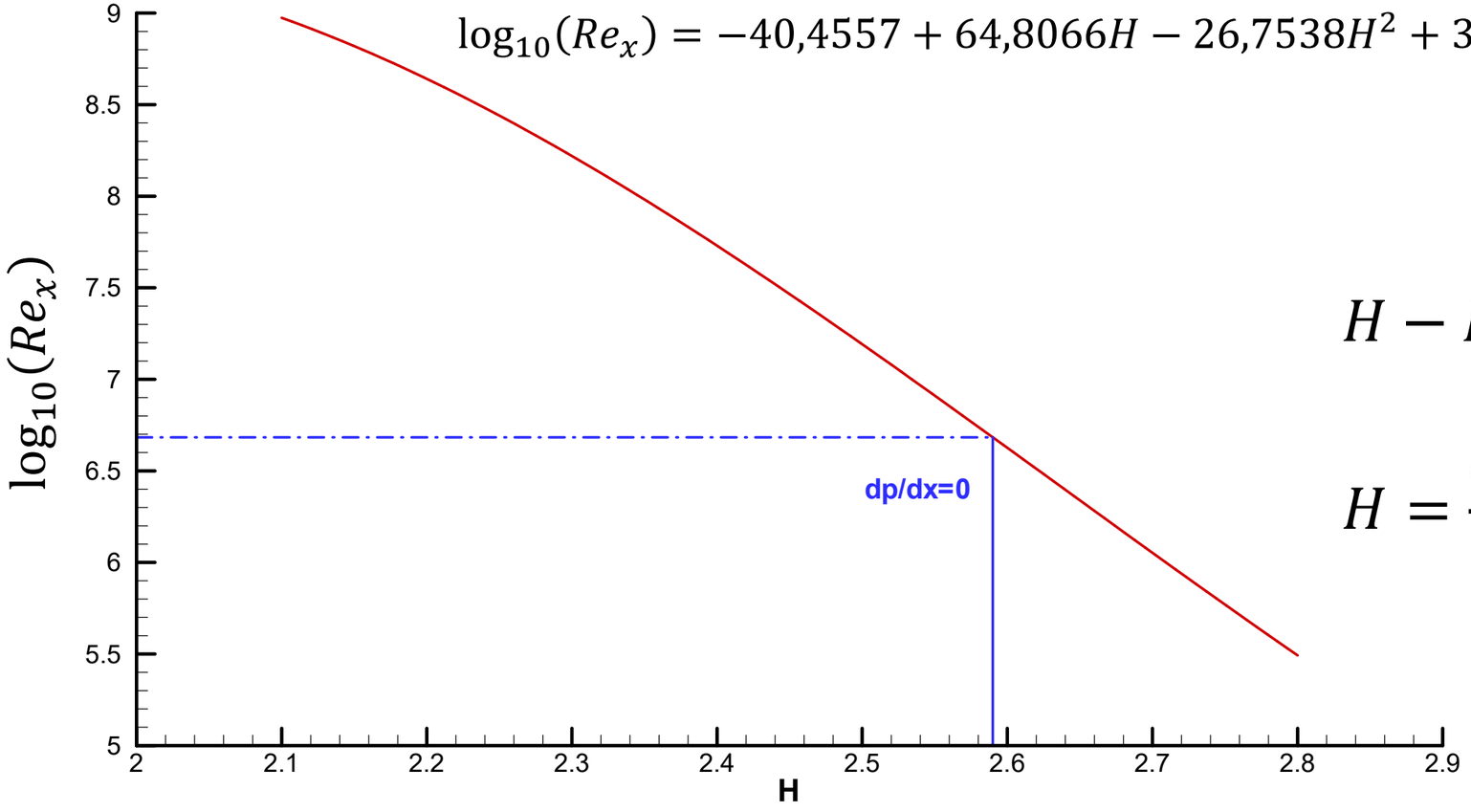

$H - Re_x$ G.Kuiper

$$H = \frac{\delta^*}{\theta}$$

Modeling transition from laminar to turbulent flow

- Change of integral quantities in the transition region is also performed with empirical correlations

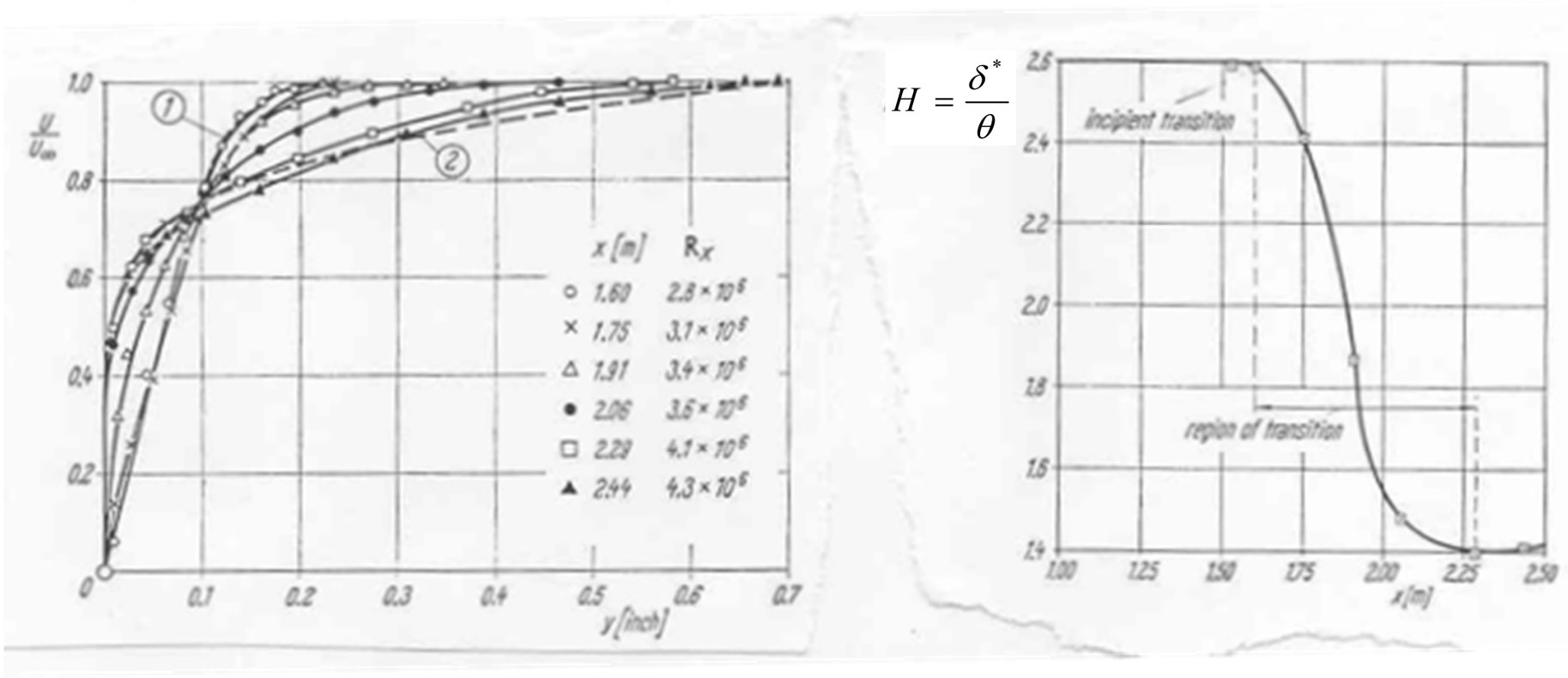

Modeling transition from laminar to turbulent flow

- Change of integral quantities in the transition region is also performed with empirical correlations;
- The shape factor, H, diminishes;
- The momentum thickness, θ, remains approximately constant, if $x_{crit} \simeq x_{trans}$;
- The displacement thickness, δ^*, diminishes;
- The skin friction coefficient, C_f, increases;
- Empirical correlation to determine H at the end of transition to turbulent flow $H = \frac{1{,}4754}{\log_{10}\left(R_{e\theta_{trans}}\right)} + 0{,}9698$

Modeling transition from laminar to turbulent flow

- e^n method based on linear stability theory:
  - It applies to natural transition (and crossflow as well);
  - It computes the local amplification rate of a disturbance along the streamlines using velocity profiles extracted from boundary-layer (CFD) simulations;
  - It requires the specification of a critical n;
  - It determines only the onset of transition.
- Considered a high-fidelity model, but it is not easy to couple it with modern CFD solvers used in engineering applications.

Modeling transition from laminar to turbulent flow

- Low Reynolds numbers turbulence models:
  - Developed for the (time-averaged) Reynolds-Averaged Navier-Stokes equations (RANS);
  - Two main families of 2-equation models ($k-\varepsilon$ and $k-\omega$) have several alternative models available;
  - Most $k-\varepsilon$ models have problems (see C. L. Rumsey, B. A. Petterson Reif, T.B.Gatski);
  - $k-\omega$ models basically calibrated for natural transition on a flat plate.

Modeling transition from laminar to turbulent flow

- Transport equation(s) transition models:
  - Several methods available in the open literature;
  - Extra transport equations solved to handle transition;
  - Underlying RANS turbulence model required;
  - Three different models are presented next:

1. $\gamma - \mathrm{Re}_\theta$ model of R.B. Langtry and F.R.Menter;
2. γ model of F.R.Menter, P.E.Smirnov, T.Liu and R. Avancha;
3. AFT model of J.G.Coder;

- Underlying RANS turbulence model is the $k - \omega$ SST

Modeling transition from laminar to turbulent flow

- $\gamma - \mathrm{Re}_\theta$ model of R.B. Langtry and F.R.Menter

$$\frac{\partial(\rho\gamma)}{\partial t} + \frac{\partial(\rho U_j \gamma)}{\partial x_j} = P_\gamma - E_\gamma + \frac{\partial}{\partial x_j}\left[\left(\mu + \frac{\mu_t}{\sigma_f}\right)\frac{\partial \gamma}{\partial x_j}\right]$$

$$\frac{\partial\left(\rho\hat{R}e_{\theta t}\right)}{\partial t} + \frac{\partial\left(\rho U_j \hat{R}e_{\theta t}\right)}{\partial x_j} = P_{\theta t} + \frac{\partial}{\partial x_j}\left[\sigma_{\theta t}(\mu + \mu_t)\frac{\partial \hat{R}e_{\theta t}}{\partial x_j}\right]$$

$$\gamma_{eff} = \max(\gamma, \gamma_{sep})$$

- Coupling with the $k - \omega$ SST model

$$P_k = \gamma_{eff} P_{k,SST}$$

$$D_k = min\left(max\left(\gamma_{eff}, 0.1\right), 1.0\right) D_{k,SST}.$$

L. Eça, 9 and 12 April 2021

Modeling transition from laminar to turbulent flow

- γ model of F.R.Menter, P.E.Smirnov, T.Liu and R. Avancha

$$\frac{\partial(\rho\gamma)}{\partial t} + \frac{\partial(\rho U_j \gamma)}{\partial x_j} = P_\gamma - E_\gamma + \frac{\partial}{\partial x_j}\left[\left(\mu + \frac{\mu_t}{\sigma_f}\right)\frac{\partial \gamma}{\partial x_j}\right]$$

- Coupling with the $k-\omega$ SST model

$$P_k = \gamma P_{k,SST} + P_k^{lim}$$

$$D_k = max(\gamma, 0.1)\, D_{k,SST}$$

$$P_k^{lim} = 5\max(\gamma - 0.2, 0)(1-\gamma) F_{on}^{lim} \max(3\mu - \mu_t, 0) S\Omega$$

$$F_{on}^{lim} = \min\left(\max\left(\frac{Re_V}{2420} - 1, 0\right), 3\right)$$

L. Eça, 9 and 12 April 2021

Modeling transition from laminar to turbulent flow

- AFT model of J.G.Coder

$$\frac{\partial\left(\rho\tilde{n}\right)}{\partial t}+\frac{\partial\left(\rho U_j\tilde{n}\right)}{\partial x_j}=\rho\Omega F_{crit}F_{growth}\frac{d\tilde{n}}{dRe_{\delta 2}}+\frac{\partial}{\partial x_j}\left[\left(\mu+\mu_t\right)\frac{\partial\tilde{n}}{\partial x_j}\right]$$

- Coupling with the $k-\omega$ SST model

$$\frac{\partial\left(\rho k\right)}{\partial t}+\frac{\partial\left(\rho U_j k\right)}{\partial x_j}=P_k-D_k-P_{trans}+\frac{\partial}{\partial x_j}\left[\left(\mu+\sigma_k\mu_t\right)\frac{\partial k}{\partial x_j}\right]$$

$$P_{trans}=F_1 c_{t5}\mu_t S\left(S-\frac{\left(\mu\chi\right)^2}{\rho\kappa^2 d^2\left(\mu+\mu_t\right)}\right)f_{t2}$$

$$f_{damp}=\frac{\chi^{4.23}}{\chi^{4.23}+7\chi^{3.23}+255}$$

$$\frac{\mu_t}{\mu}=\chi f_{damp}.$$

Modeling transition from laminar to turbulent flow

- Large-Eddy Simulation (LES) can also be used to predict transitional flows. However, there are several challenges:
  - Incompatible with wall models (wall functions) and so griding requirements for wall bounded flows are significant;
  - Subgrid-scale model can influence the outcome;
  - Specification of inlet boundary conditions is not trivial.
- Naturally, Direct Numerical Solution can also be used.
  - Numerical errors (iterative, discretization, statistical and even round-off) have to be diminished to negligible levels;
  - Specification of inlet boundary conditions is not trivial.

1st AIAA Transition Workshop

Case 1 – Zero pressure gradient flat plate

Mach number	0.2
Angle of attack	0°
Reynolds number	200,000 per grid unit
Reference temperature	540 R
Inlet turbulence conditions	Case 1A (T3A): • Inlet turb. intensity = 5.855% • μ_T/μ = 11.9 Case 1B (T3B) • Inlet turb. intensity = 7.216% • μ_T/μ = 99
Comments	Grid resolution studies to be performed using all members of the common grid family for both the T3A and T3B inlet turbulence conditions. Inlet turbulence quantities for participant grids may vary. Participants should report whether or not they use free-stream sustaining terms with the underlying turbulence model.

L. Eça, 9 and 12 April 2021

1st AIAA Transition Workshop

Case 1 – Zero pressure gradient flat plate

Inlet – Everything specified except the pressure;
Bottom – Symmetry and no slip/impermeability conditions;
Top – Symmetry;
Outlet – Pressure imposed.

$Re_L = V_\infty L/\nu = 4\times10^6$

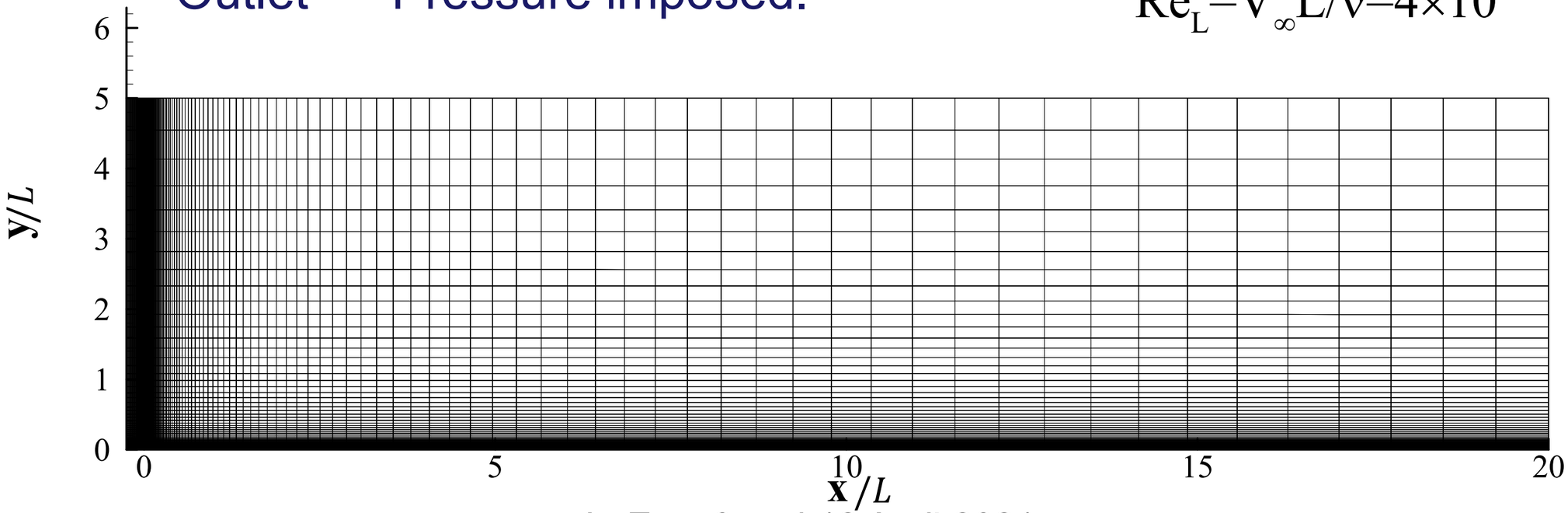

1st AIAA Transition Workshop

Case 1 – Zero pressure gradient flat plate

T3A is a bypass transition test case.

h_i/h_1 identifies the grid refinement ratio.

$h_i/h_1 = 1$ is the finest grid.

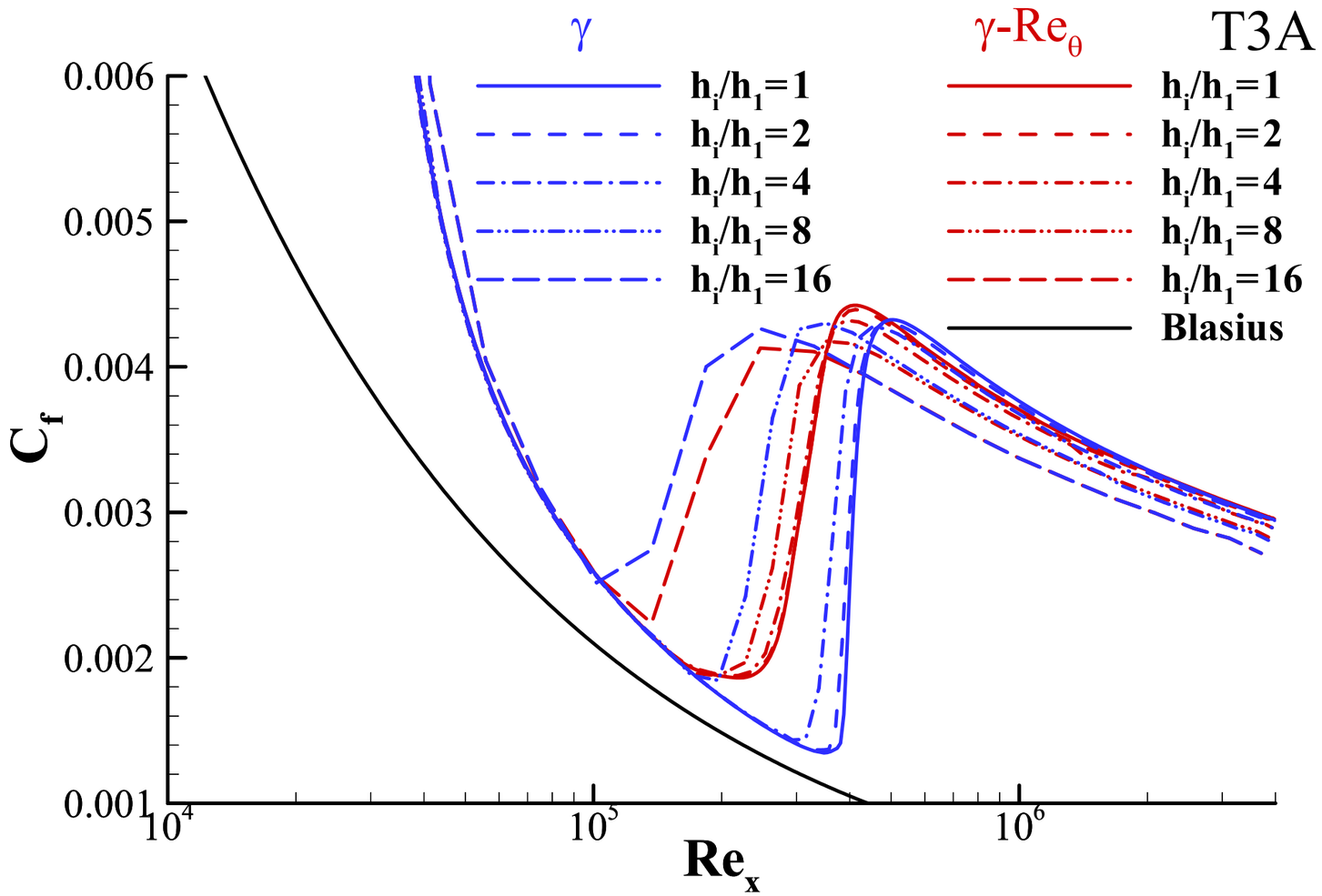

1st AIAA Transition Workshop

Case 1 – Zero pressure gradient flat plate

T3A

AVT results use a different domain size and different inlet conditions for μ_t/μ

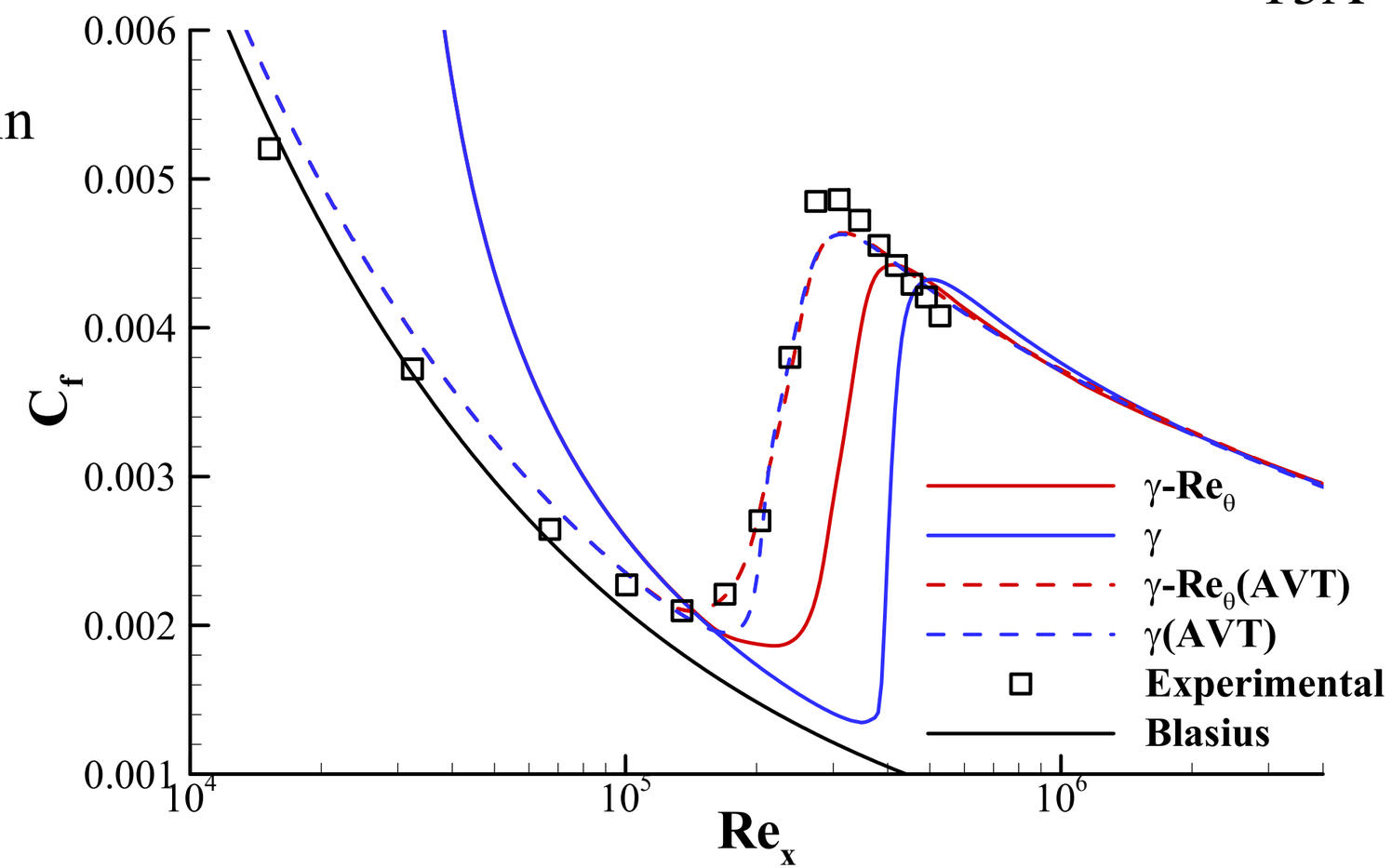

1st AIAA Transition Workshop

Case 1 – Zero pressure gradient flat plate

T3B is a bypass transition test case.

h_i/h_1 identifies the grid refinement ratio.

$h_i/h_1 = 1$ is the finest grid.

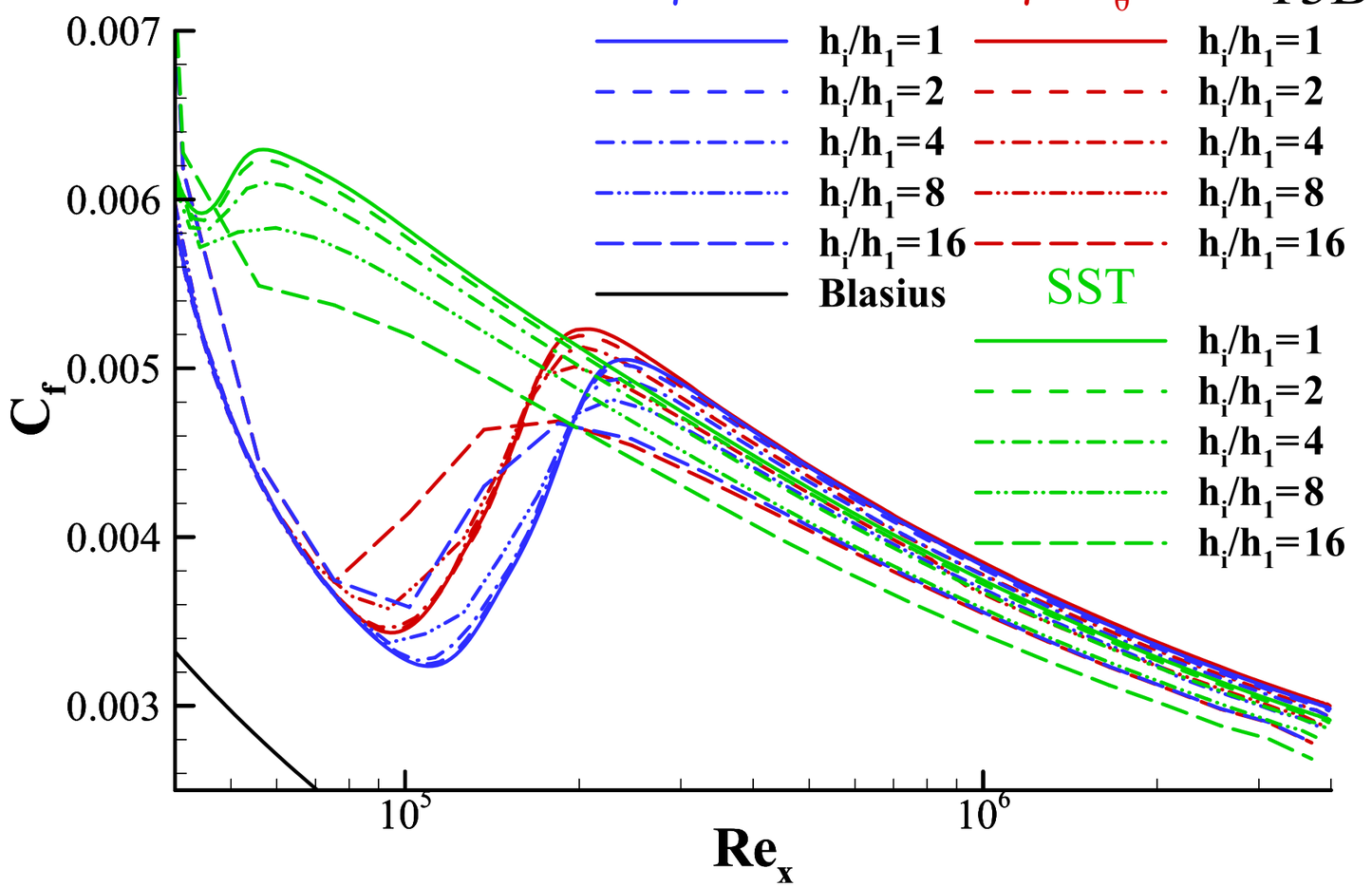

1st AIAA Transition Workshop

Case 1 – Zero pressure gradient flat plate

T3B

T3B is a bypass transition test case.

h_i/h_1 identifies the grid refinement ratio.

$h_i/h_1 = 1$ is the finest grid.

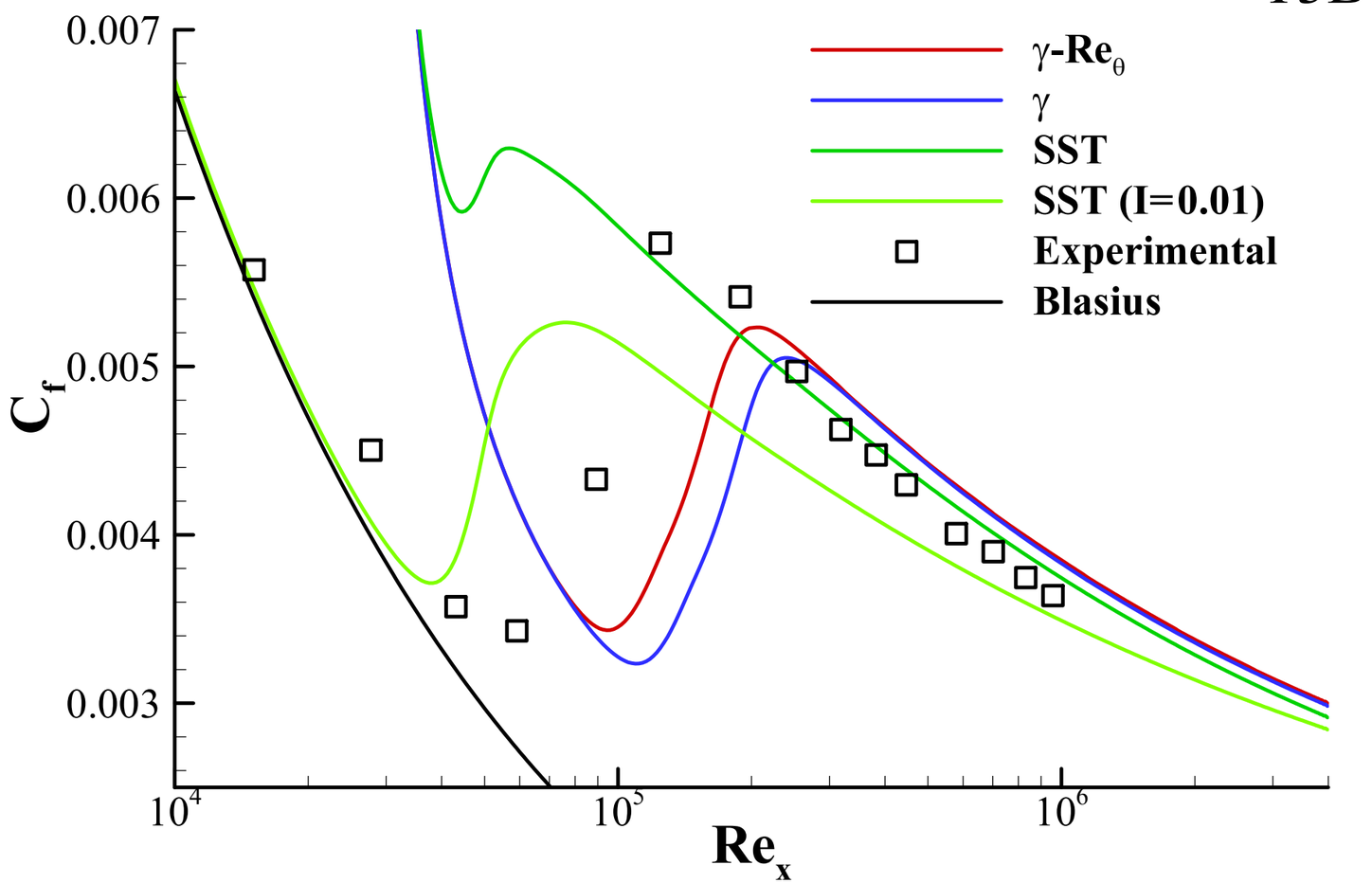

1st AIAA Transition Workshop

Case 2 – NLF(1)-0416 airfoil

Mach number	0.1
Angle of attack	Case 2A: 0° and 5° Case 2B and 2C: [-4°,8°] in 2° increments
Reynolds number	4 million (based on chord length)
Reference temperature	540 R
Freestream turb. Intensity	0.15% (or N_{crit} = 7.2)
Gridding guidelines	Recommended medium-grid spacings: LE spacing: 0.0010 chords TE spacing: 0.0005 chords $\Delta y = 3.5 \times 10^{-6}$ chords Growth rates < 1.2 normal to wall Far-field boundaries at least 1000 chords from surface

L. Eça, 9 and 12 April 2021

1st AIAA Transition Workshop

Case 2 – NLF(1)-0416 airfoil

Study of size of the computational domain

$\lambda = 1536c/L_y = 2304c/L_x$

Selected domain

$\lambda = 16$

$L_x = 144\text{c}, L_y = 96c$

- V_∞ aligned with x;
- Free slip at top and bottom boundaries;
- Pressure imposed at the outlet.

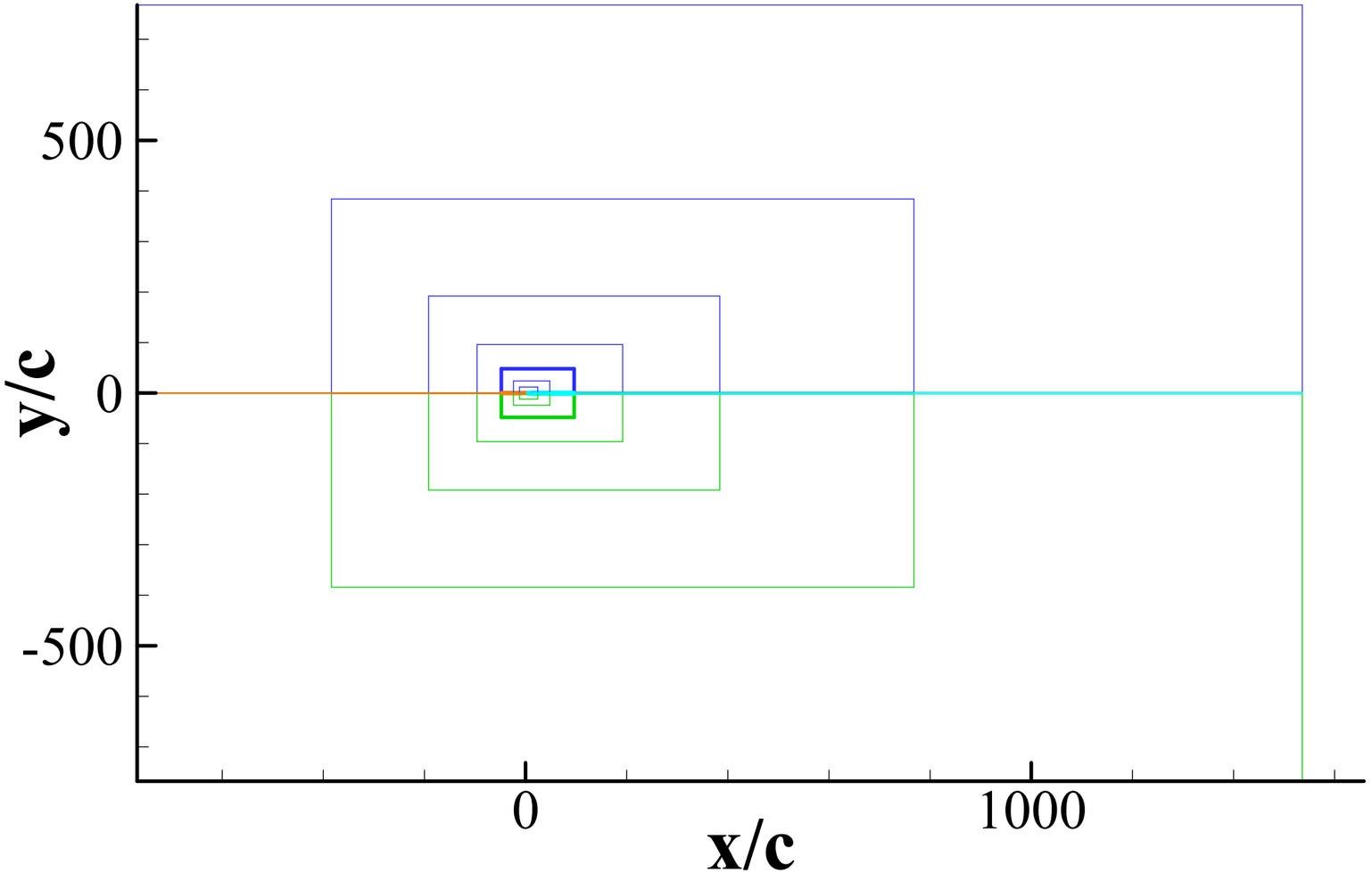

1st AIAA Transition Workshop

Case 2 – NLF(1)-0416 airfoil

Study of size of the computational domain
$\lambda = 1536c/L_y = 2304c/L_x$

Selected domain
$\lambda = 16$
$L_x = 144\text{c}, L_y = 96c$

- V_∞ aligned with x;
- Free slip at top and bottom boundaries;
- Pressure imposed at the outlet.

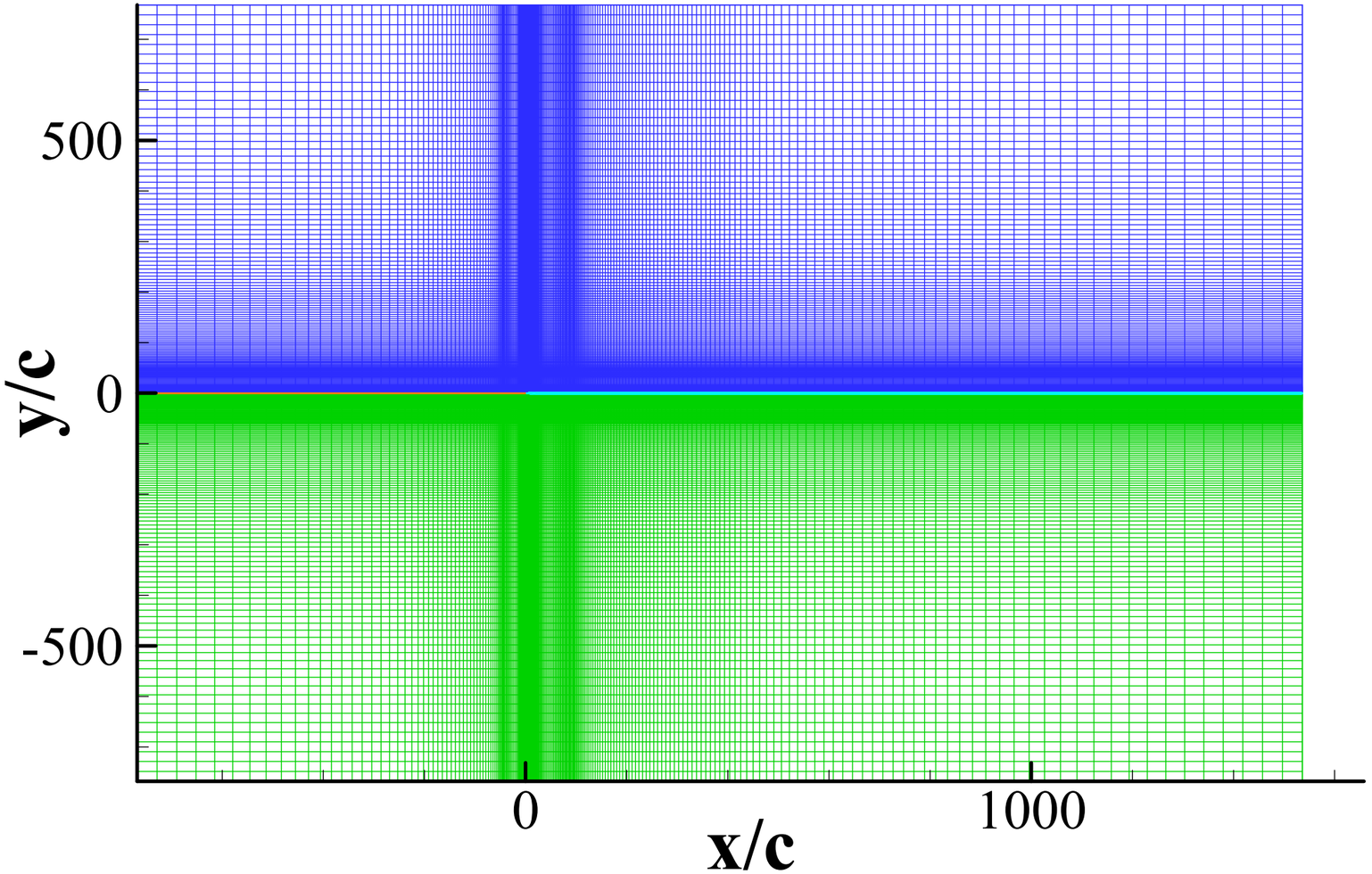

1st AIAA Transition Workshop

Case 2 – NLF(1)-0416 airfoil

Computational domain for $\lambda = 16 \Rightarrow L_x = 72c \wedge L_y = 48c$

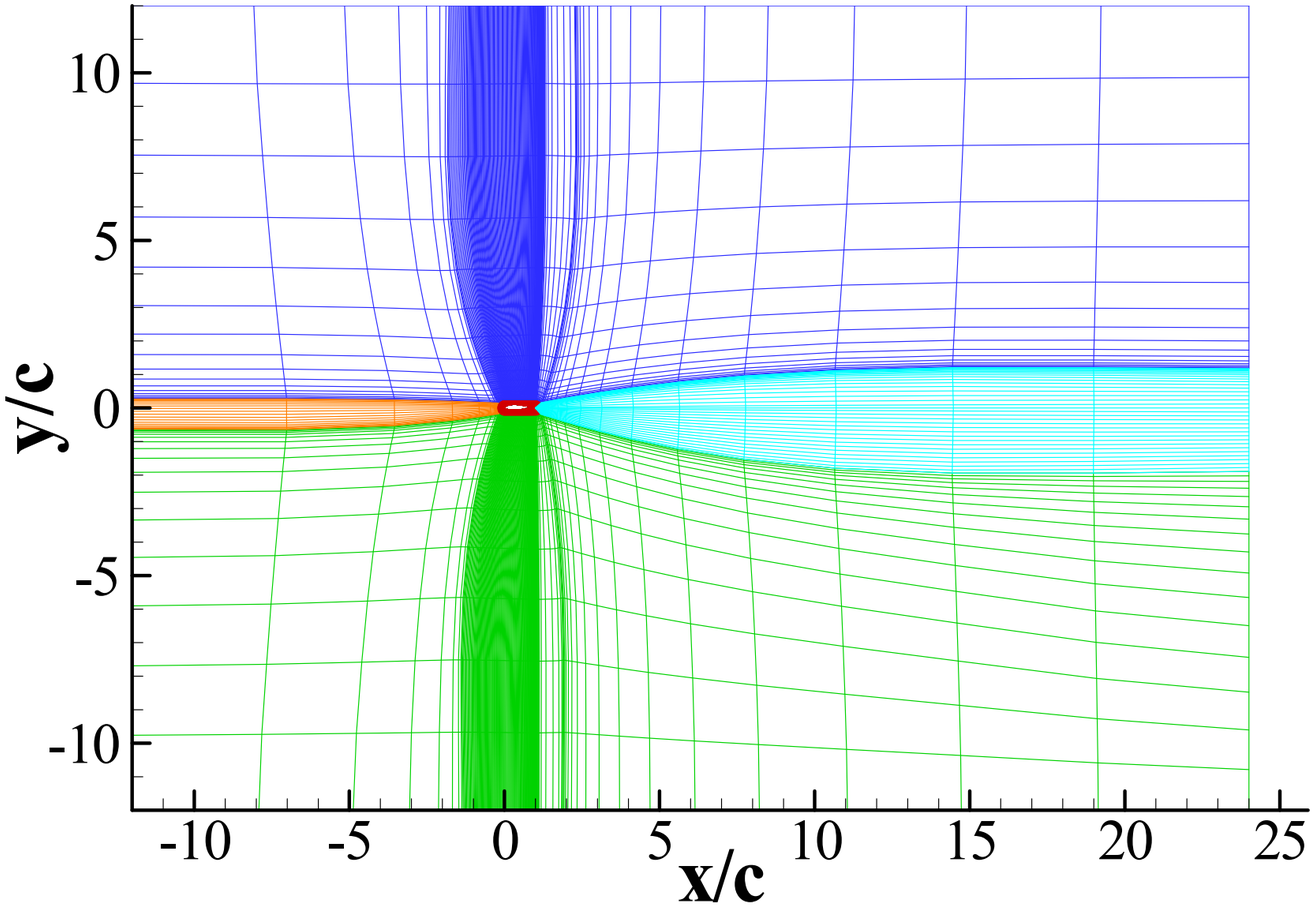

L. Eça, 9 and 12 April 2021

1st AIAA Transition Workshop

Case 2 – NLF(1)-0416 airfoil

Computational domain for $\lambda = 16 \Rightarrow L_x = 72c \wedge L_y = 48c$

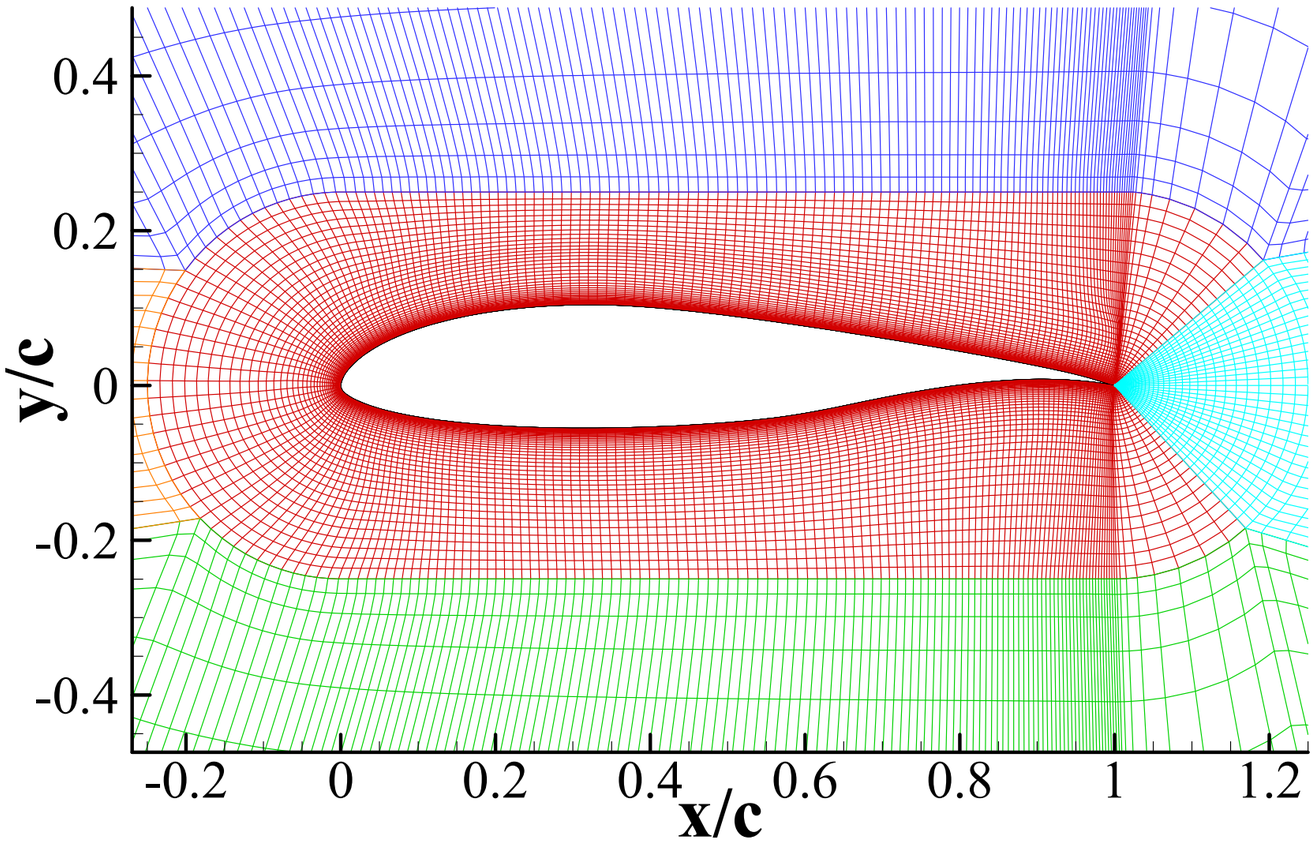

L. Eça, 9 and 12 April 2021

1st AIAA Transition Workshop

Case 2 – NLF(1)-0416 airfoil

Computational domain for $\lambda = 16 \Rightarrow L_x = 72c \wedge L_y = 48c$

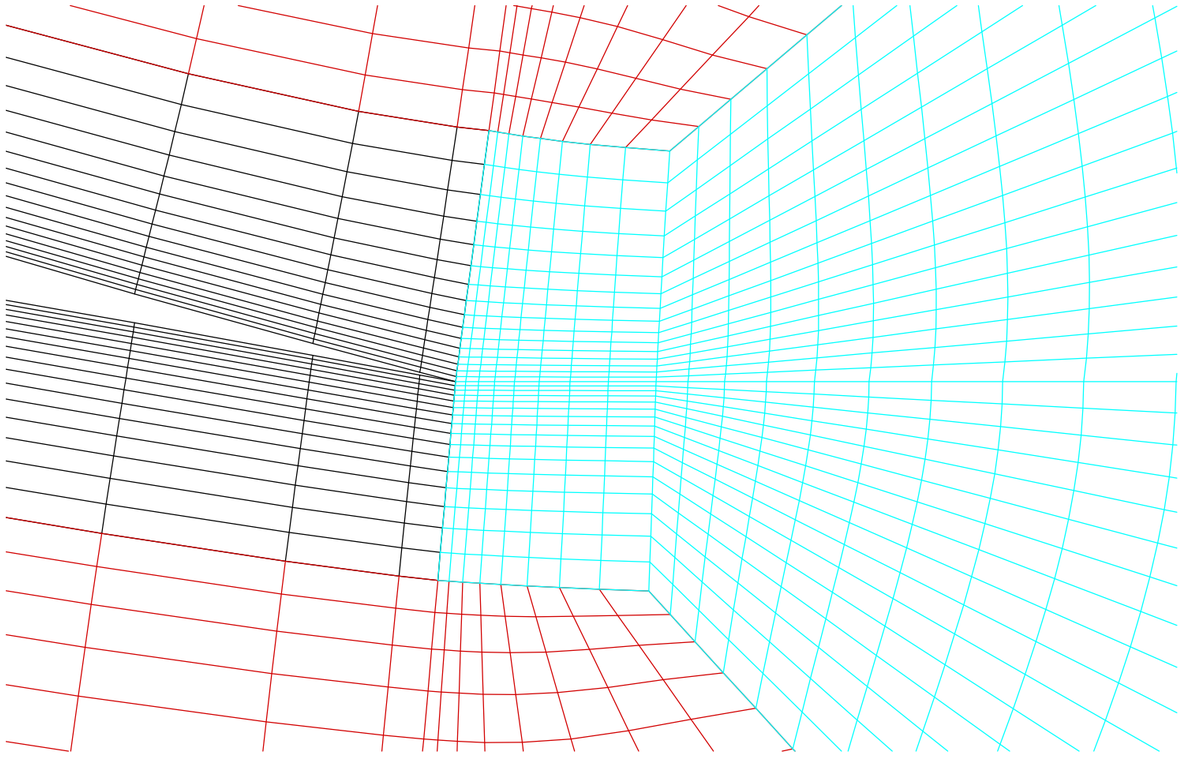

L. Eça, 9 and 12 April 2021

1st AIAA Transition Workshop

Case 2 – NLF(1)-0416 airfoil

Simulation of the flow at $\alpha = 0^o$ for $\lambda = 64,32,16,8,4,2,1$

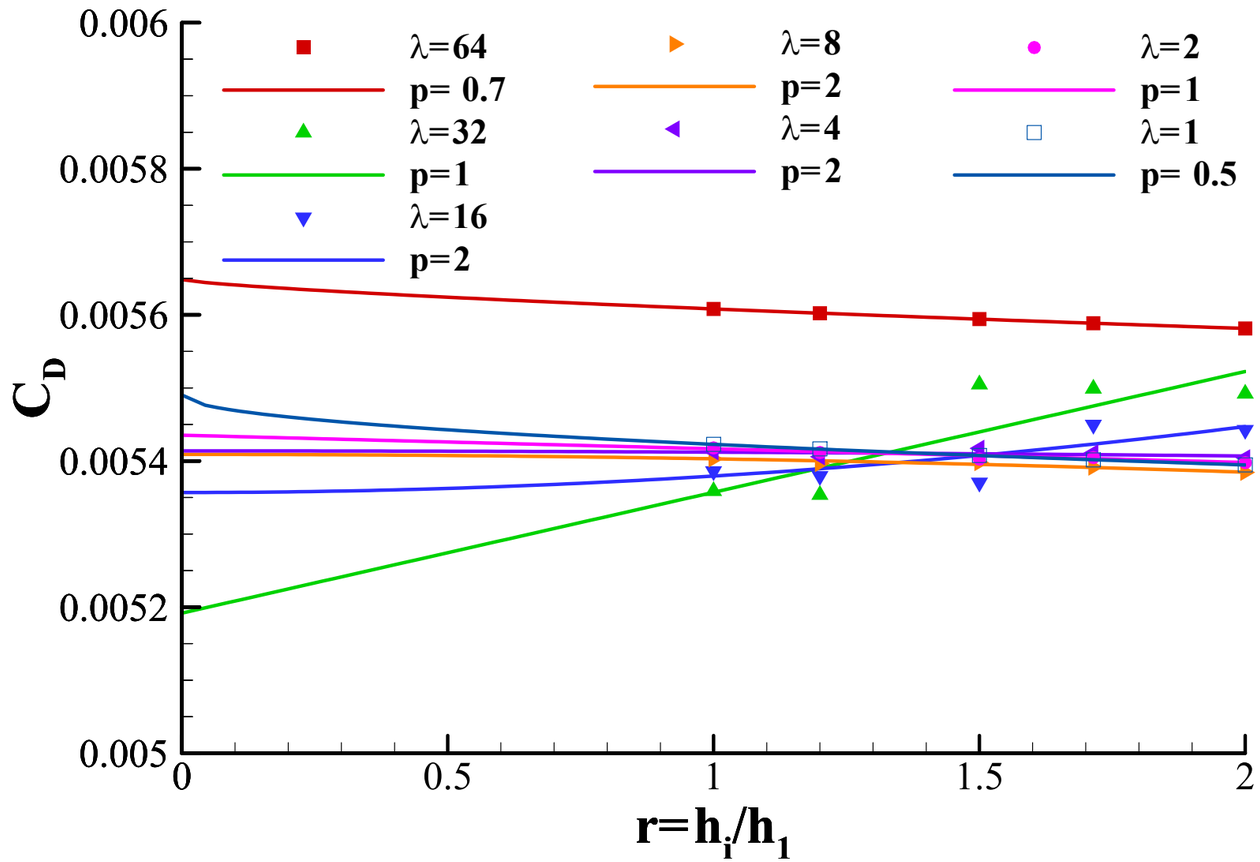

L. Eça, 9 and 12 April 2021

1st AIAA Transition Workshop

Case 2 – NLF(1)-0416 airfoil

Simulation of the flow at $\alpha = 0^o$ for $\lambda = 64,32,16,8,4,2,1$

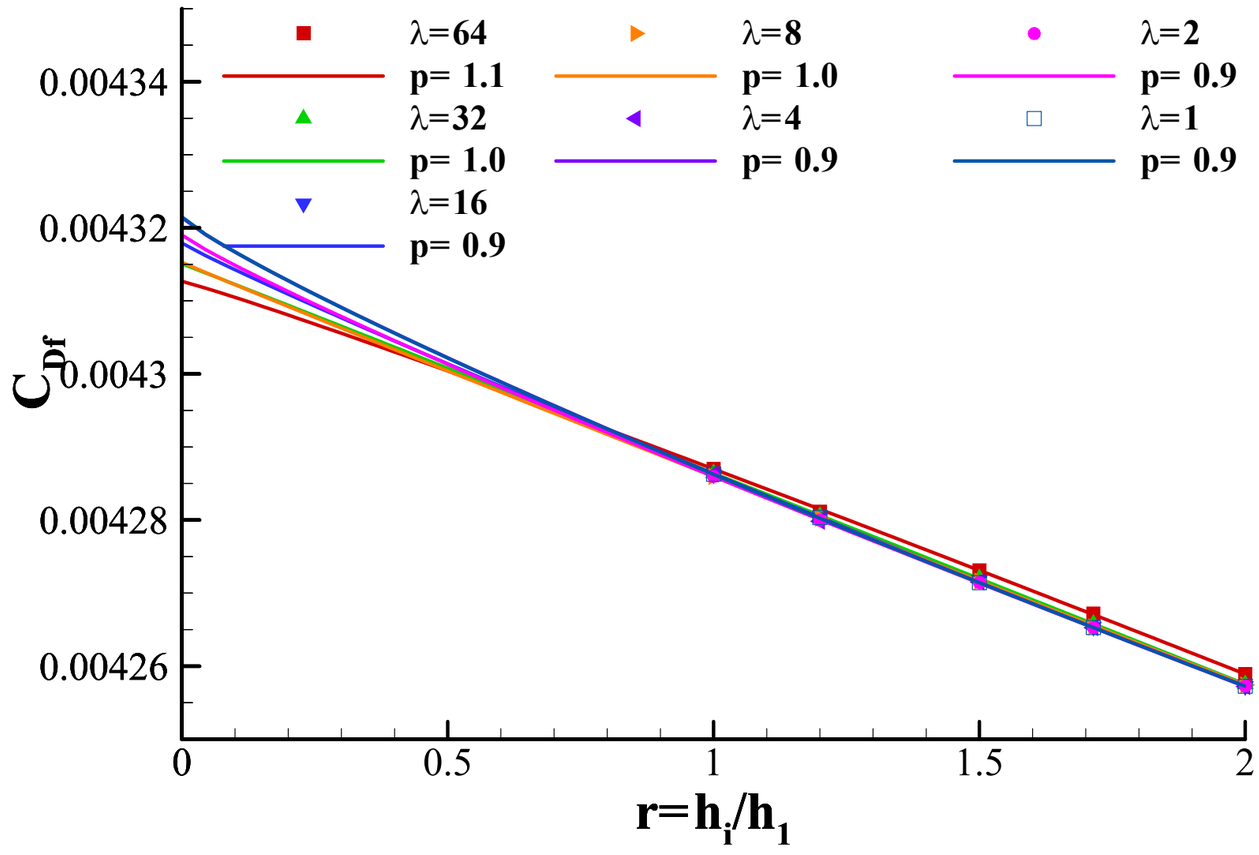

L. Eça, 9 and 12 April 2021

1st AIAA Transition Workshop

Case 2 – NLF(1)-0416 airfoil

Simulation of the flow at $\alpha = 0^o$ for $\lambda = 64,32,16,8,4,2,1$

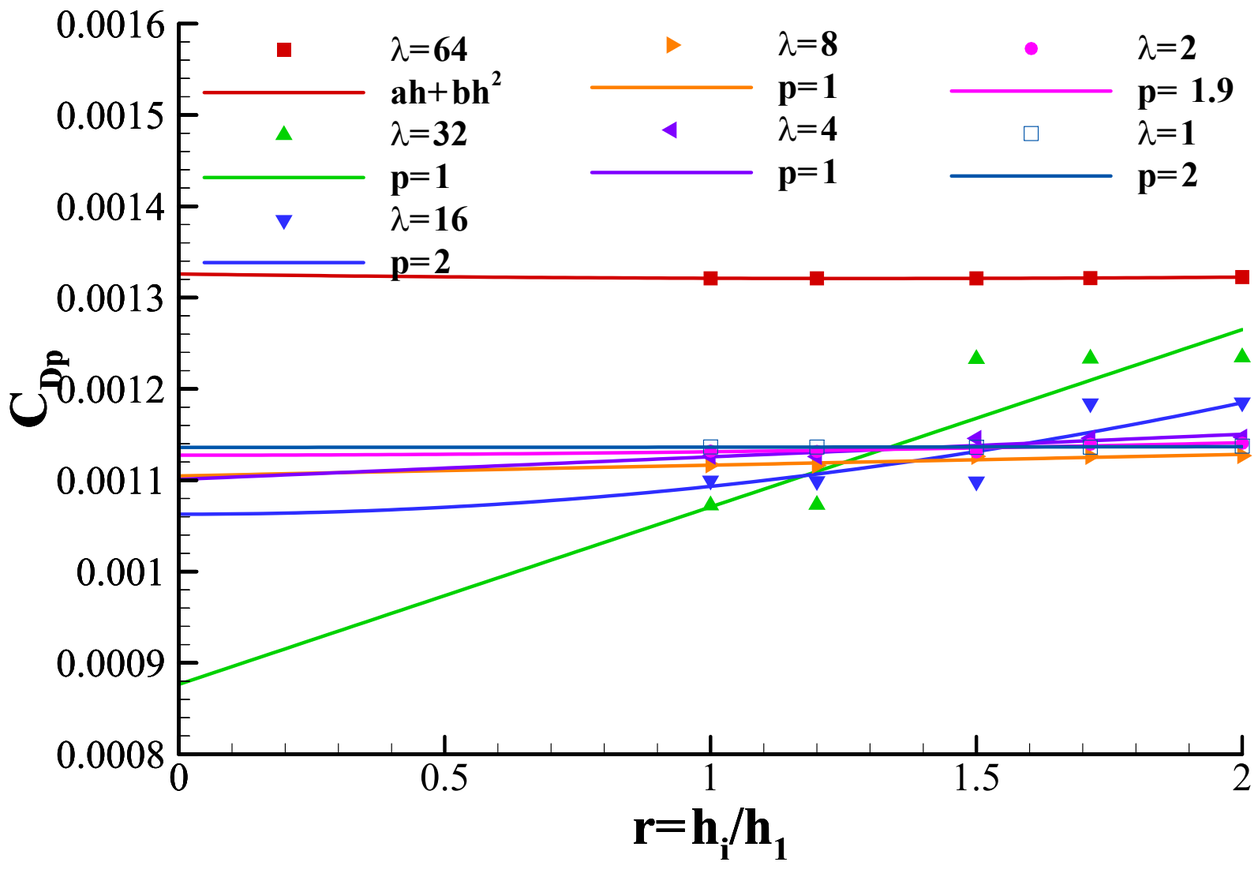

L. Eça, 9 and 12 April 2021

1st AIAA Transition Workshop

Case 2 – NLF(1)-0416 airfoil

Simulation of the flow at $\alpha = 0^o$ for $\lambda = 64,32,16,8,4,2,1$

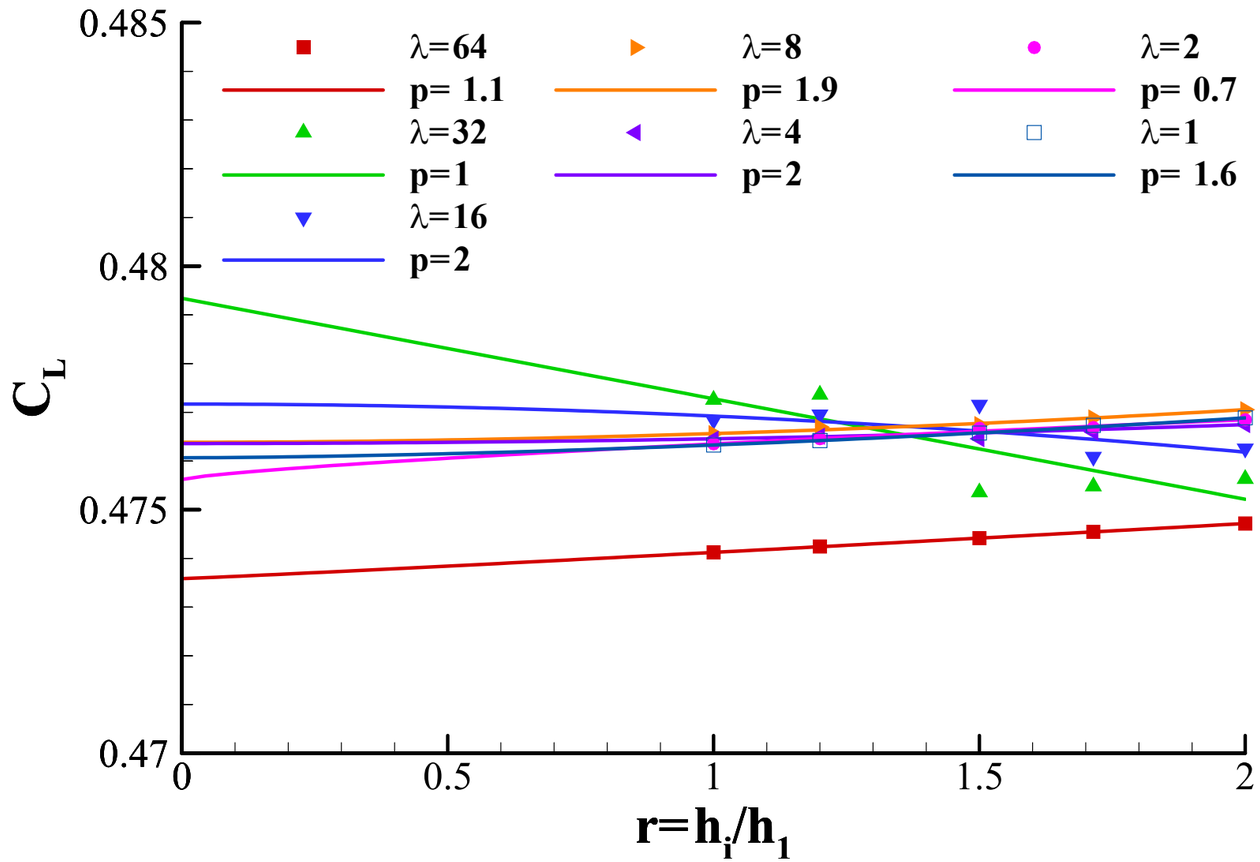

L. Eça, 9 and 12 April 2021

1st AIAA Transition Workshop

Case 2 – NLF(1)-0416 airfoil

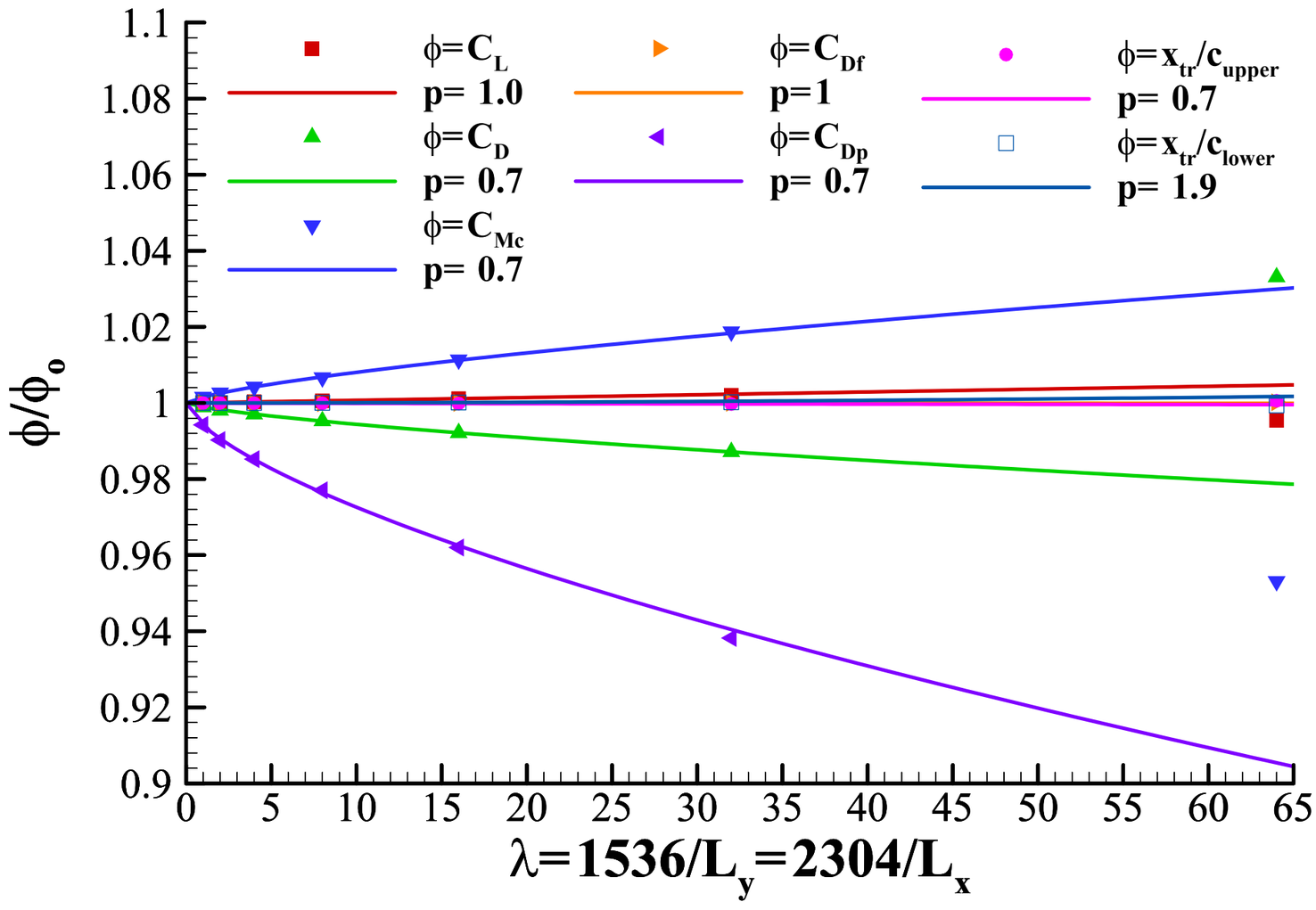

1st AIAA Transition Workshop

Case 2 – NLF(1)-0416 airfoil

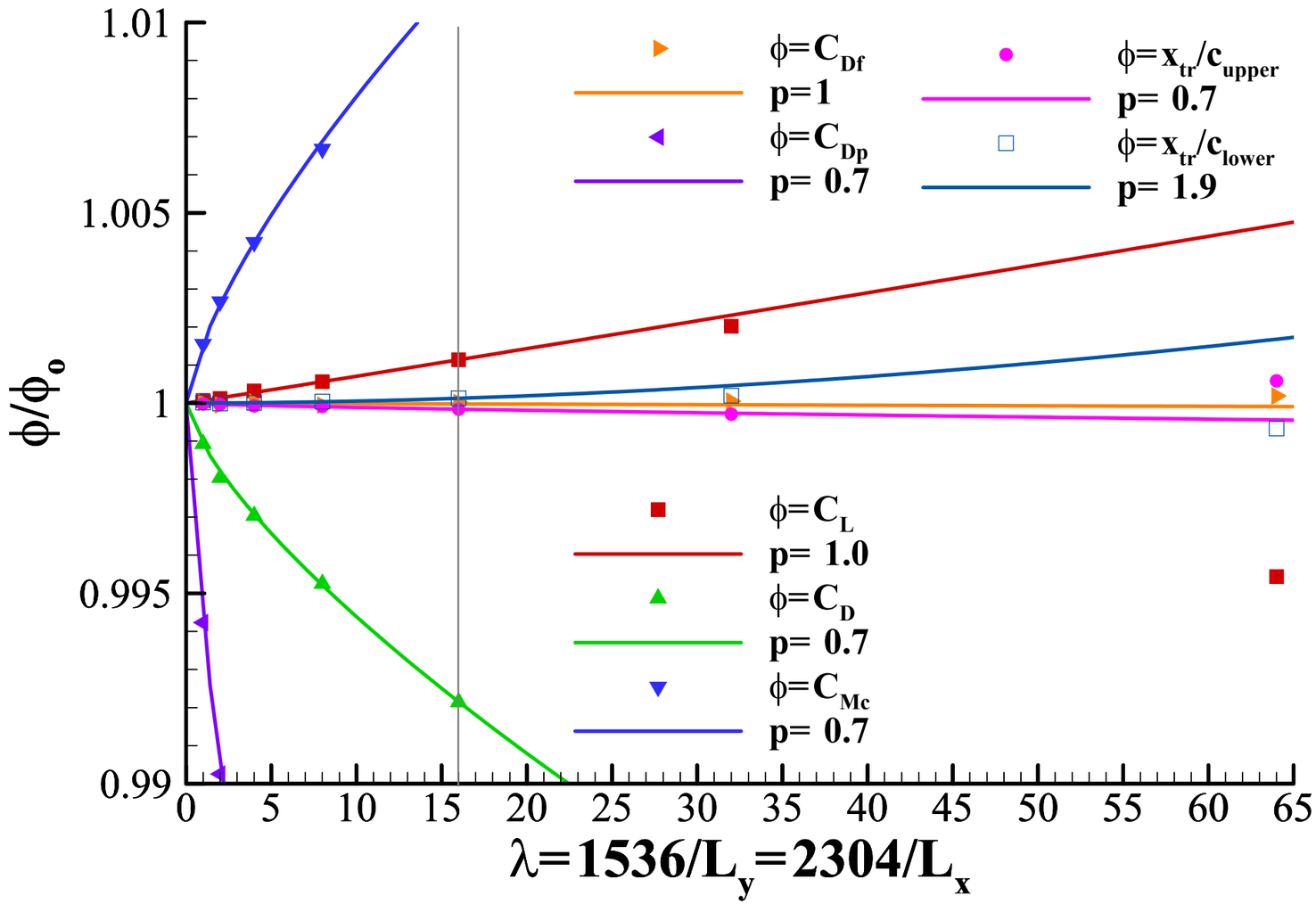

L. Eça, 9 and 12 April 2021

Transition from Laminar to Turbulent Flow

1st AIAA Transition Workshop

Case 2 – NLF(1)-0416 airfoil

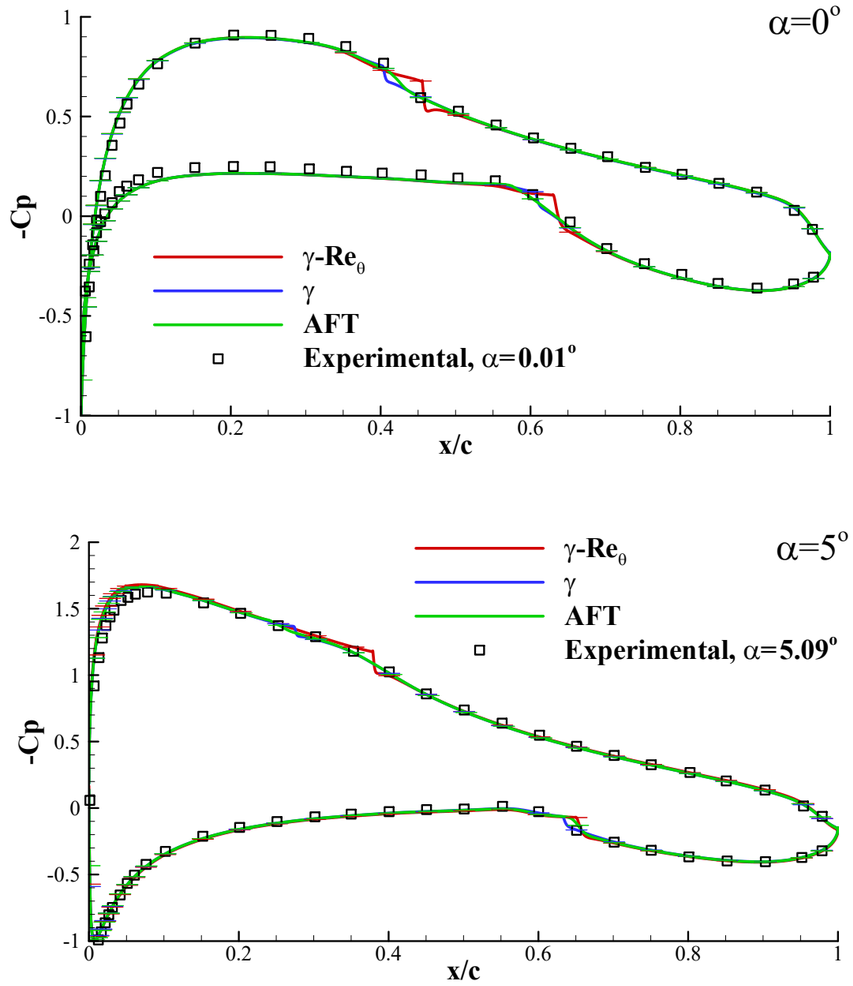

Upper surface

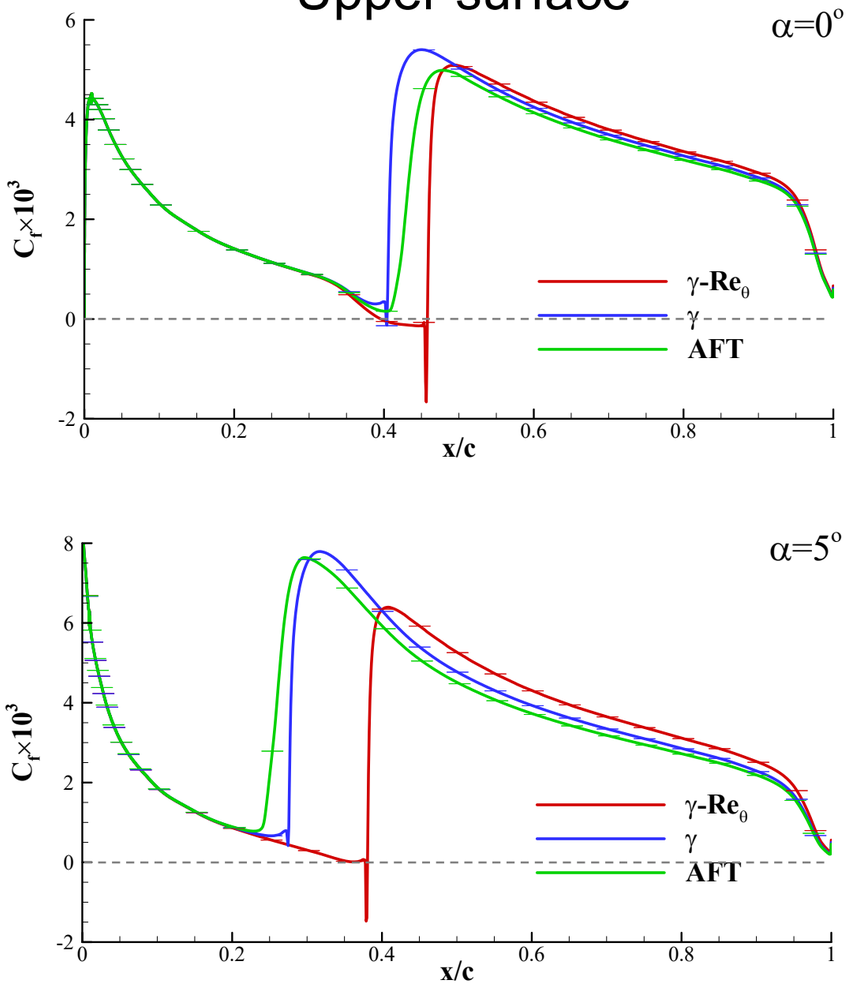

Lower surface

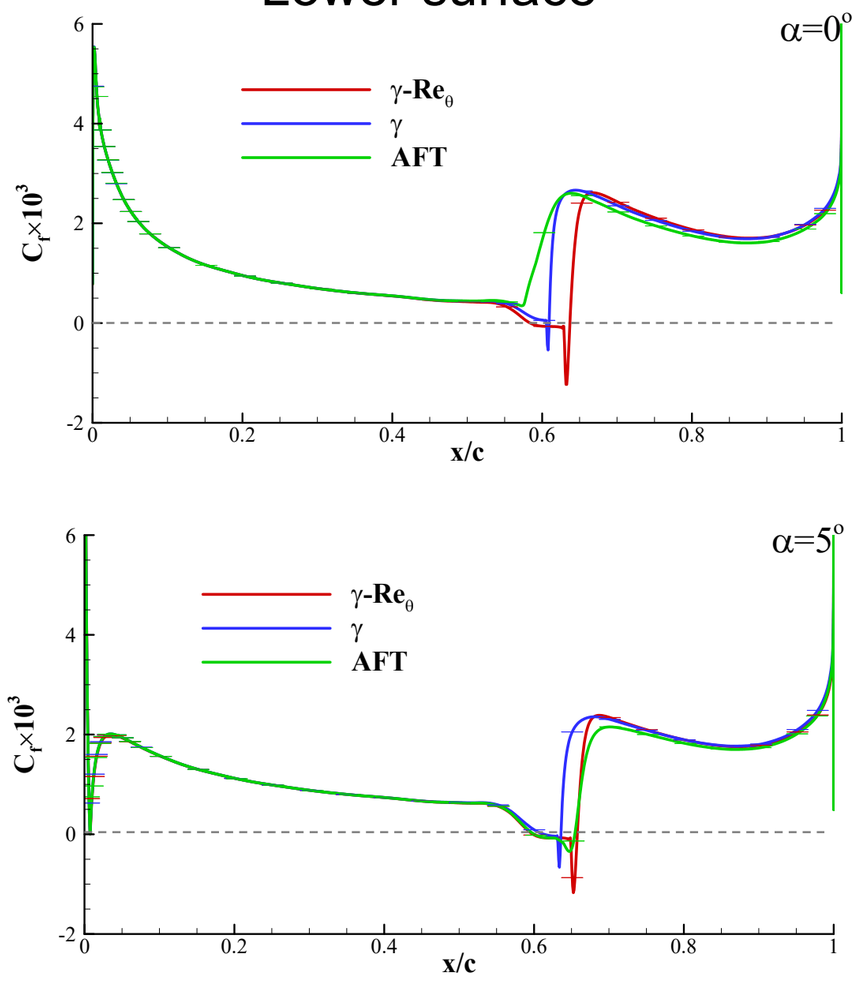

L. Eça, 9 and 12 April 2021

1st AIAA Transition Workshop

Case 2 – NLF(1)-0416 airfoil

Lower surface, $\alpha = 0^o$

Num
Numerical Uncertainty

AFT Num γ Num γ-Re_θ Num

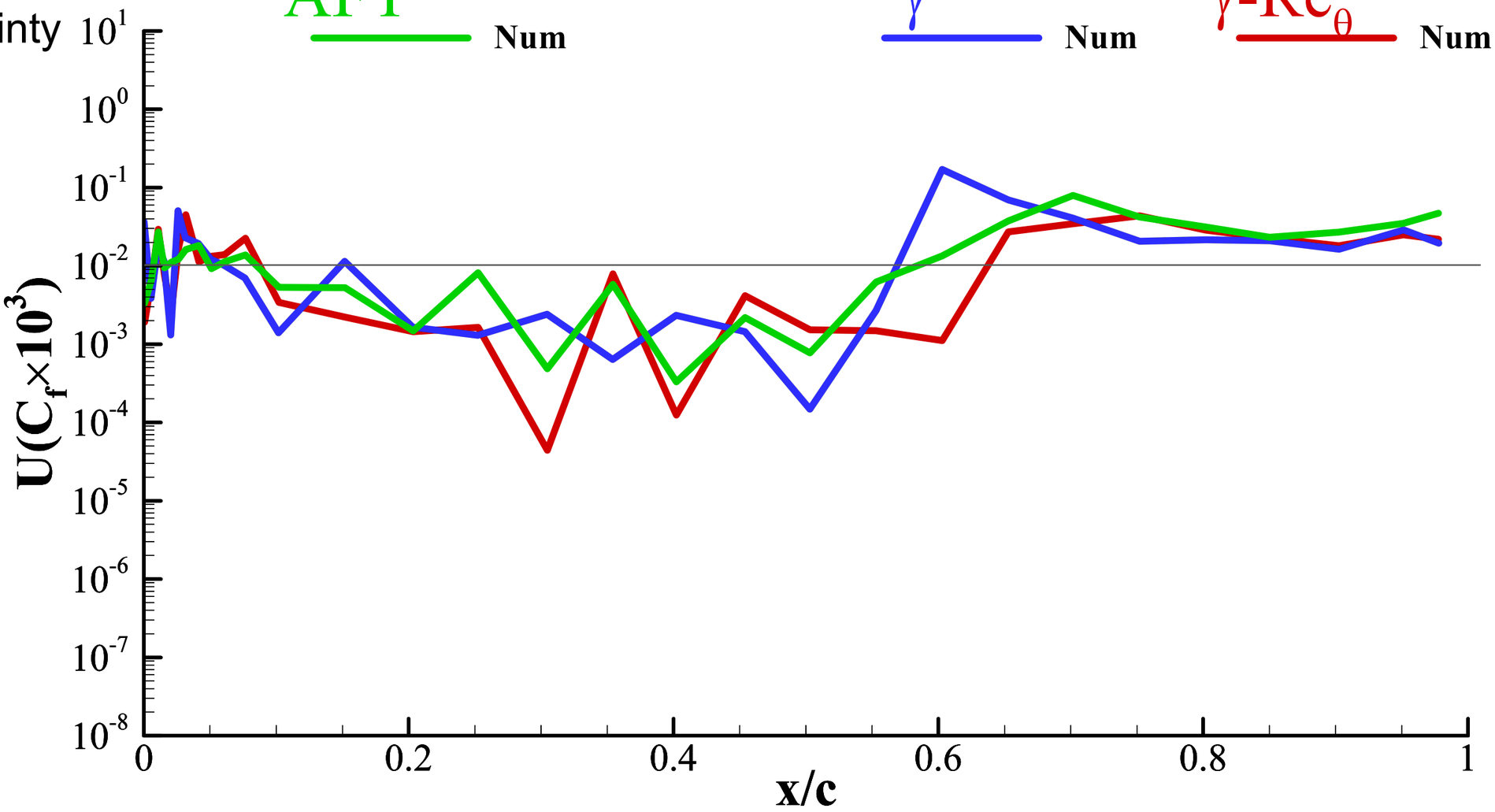

1st AIAA Transition Workshop

Case 2 – NLF(1)-0416 airfoil

Lower surface, $\alpha = 0^o$

Num
Numerical uncertainty.

In(I)
Input uncertainty from 5% uncertainty in I at the inlet.

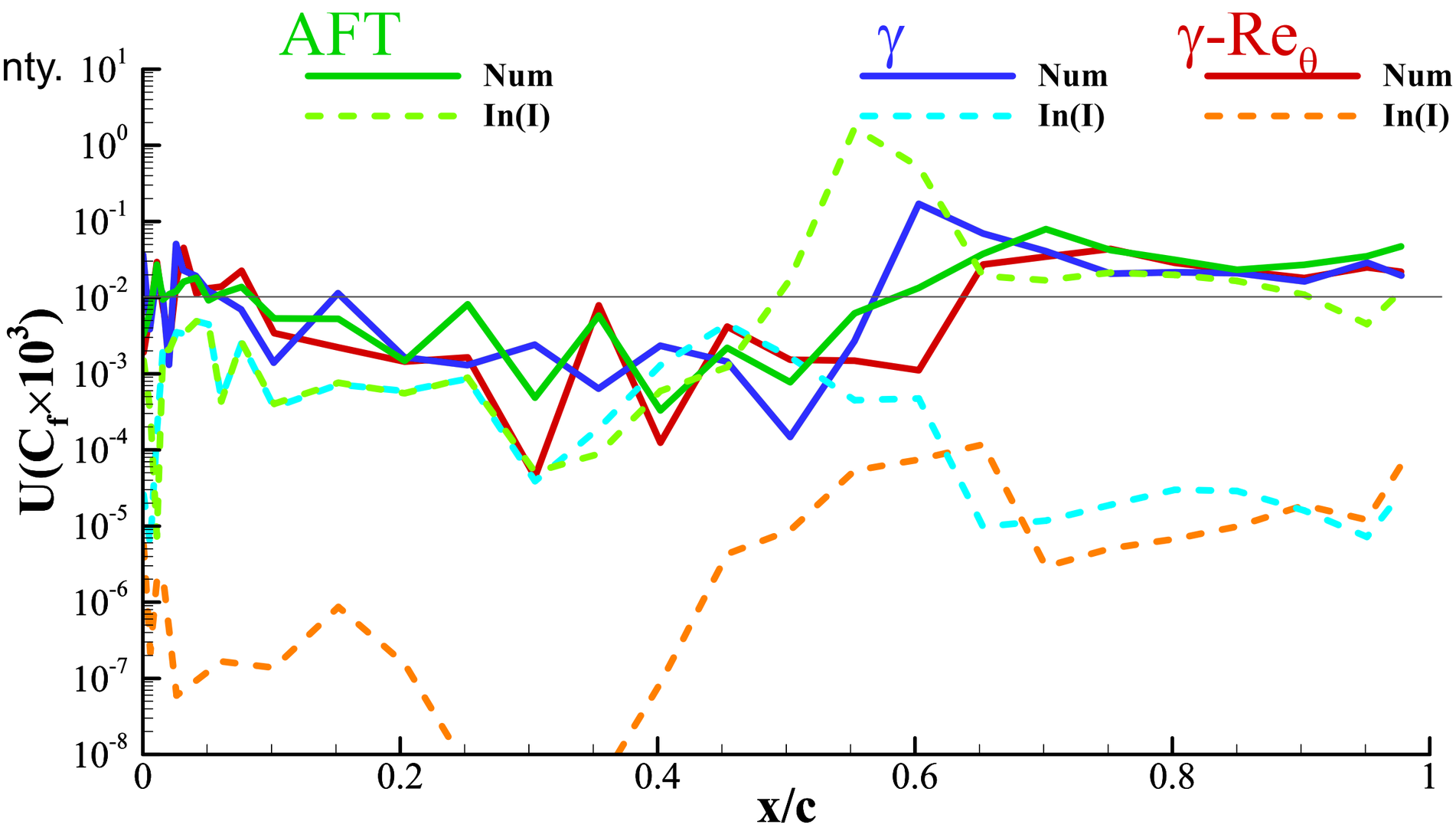

Transition from Laminar to Turbulent Flow

1st AIAA Transition Workshop

Case 2 – NLF(1)-0416 airfoil

Lower surface, $\alpha = 0^o$

Num
Numerical uncertainty.

In(I)
Input uncertainty from 5% uncertainty in I at the inlet.

In(ν_t)
Input uncertainty from 5% uncertainty in ν_t at the inlet.

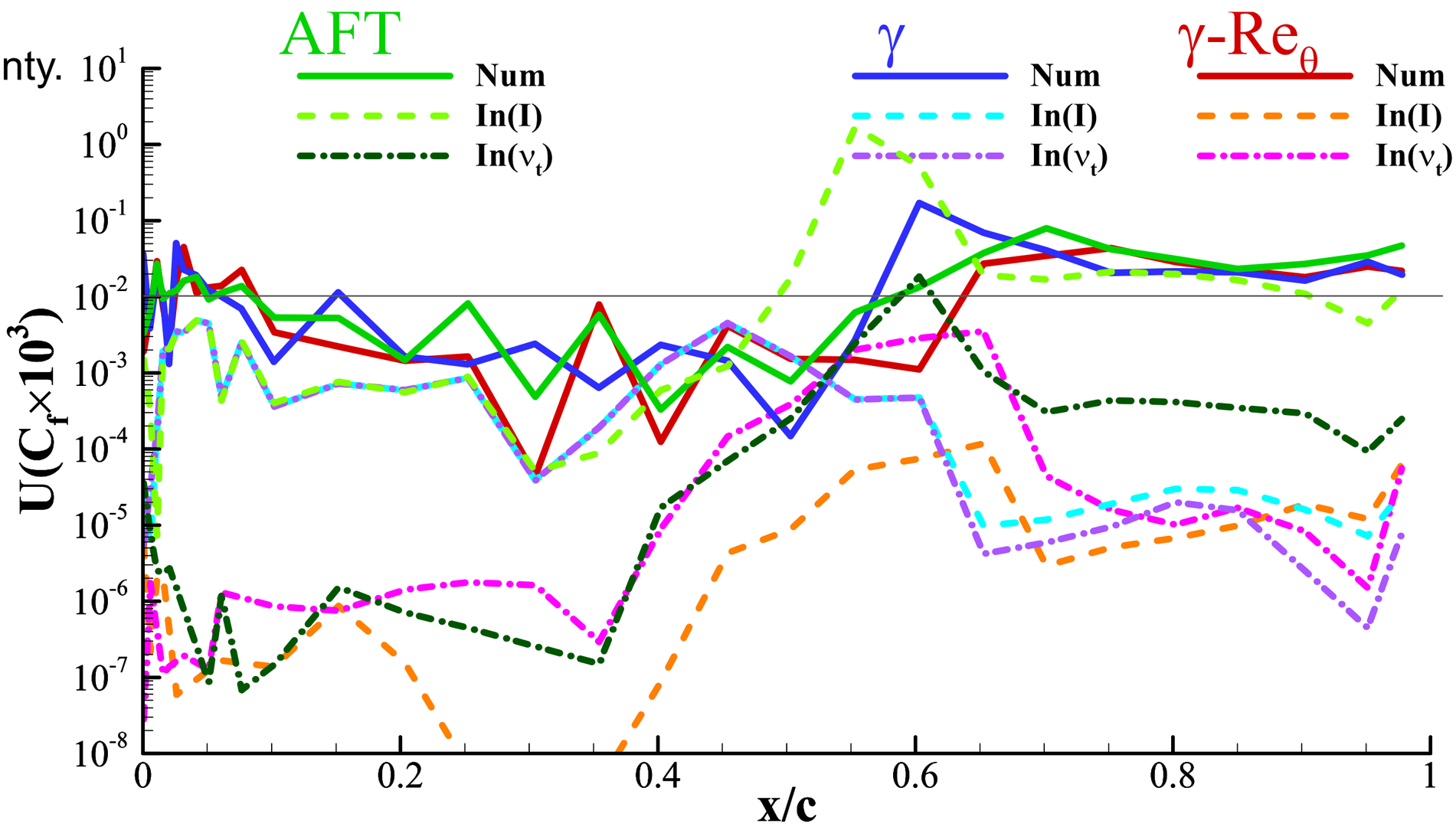

1st AIAA Transition Workshop

Case 2 – NLF(1)-0416 airfoil

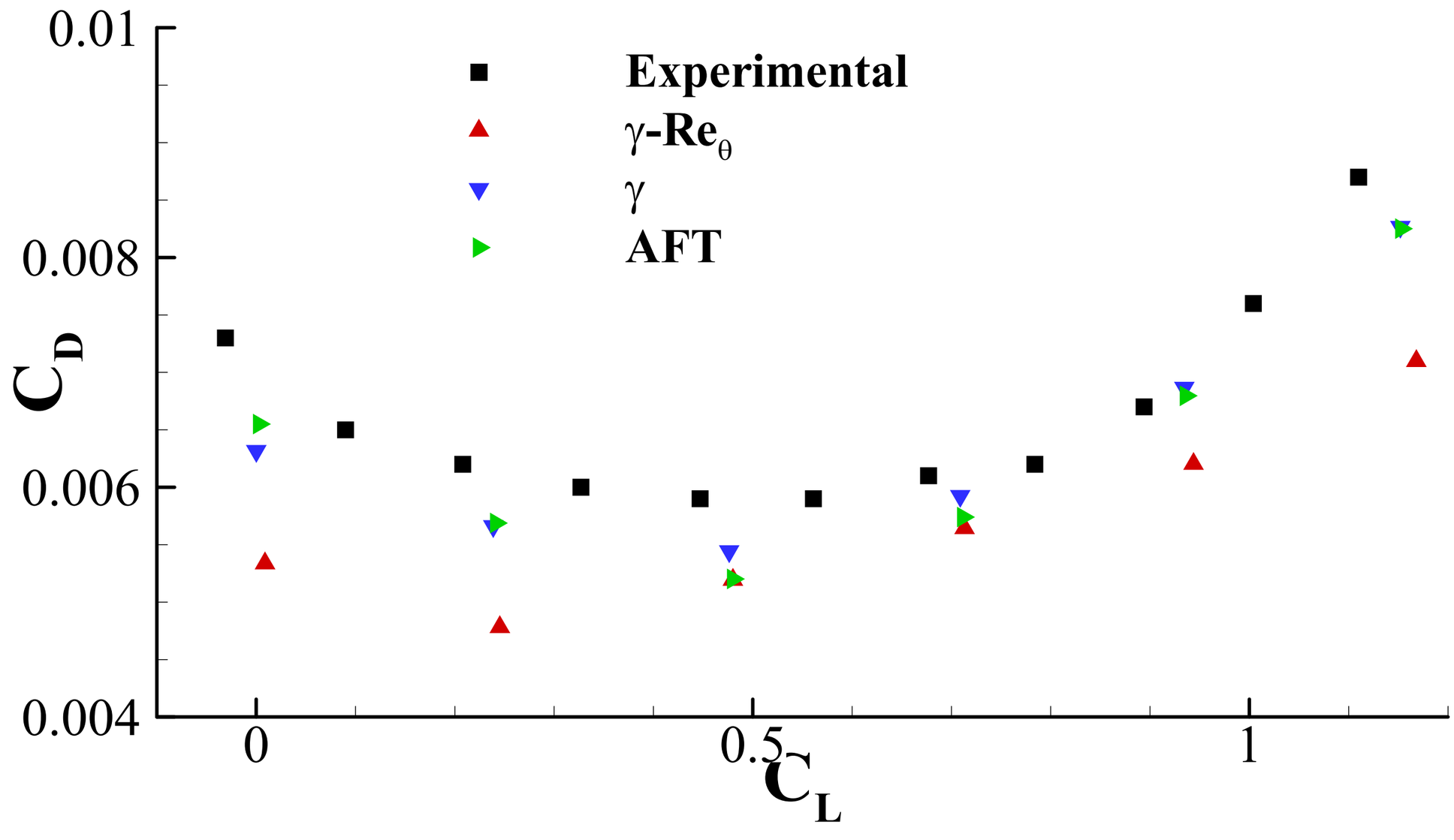

2-D Test Cases

Geometry	Re	Flow condition	Experimental Data	Transition Model	
				$\gamma - Re_\theta$	γ
Flat Plate	10^7	$I = 1.0\%$ (T3AM)	C_f, V_x	6	3
		$I = 5.4\%$ (T3A)	C_f, V_x	5	3
Eppler 387 Foil	3×10^5	$\alpha = 1^o$	C_p both sides	7	4
		$\alpha = 7^o$	C_p both sides	6	3
NACA 0015 Foil	1.8×10^5	$\alpha = 5^o$	C_f upper	5	3
		$\alpha = 10^o$	C_f upper	4	2

AVT-313 Transition Workshop

Flow over a Flat Plate

- Two-dimensional rectangular domain

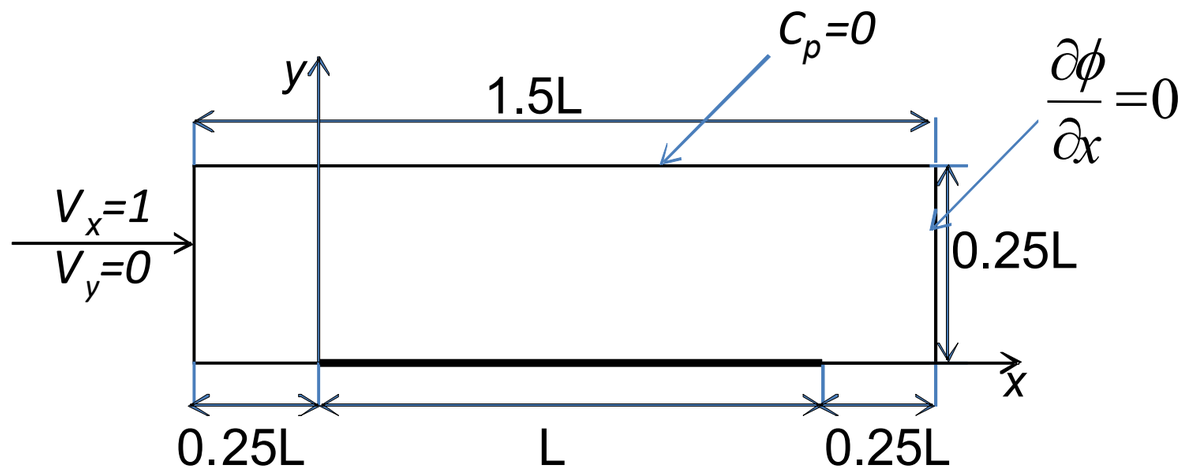

with L as the plate length, V_∞ as the incoming velocity. Incompressible fluid. Reynolds number $Re = \frac{V_\infty L}{\nu} = 10^7$. Experimental data from ERCOFTAC Classic Database

AVT-313 Transition Workshop

Flow over a Flat Plate

- Three sets of five geometrically similar grids using
  $L = 1\text{m}$ ($V_\infty = 1\text{m/s} \Rightarrow \nu = 10^{-7}\text{m}^2/\text{s}$)

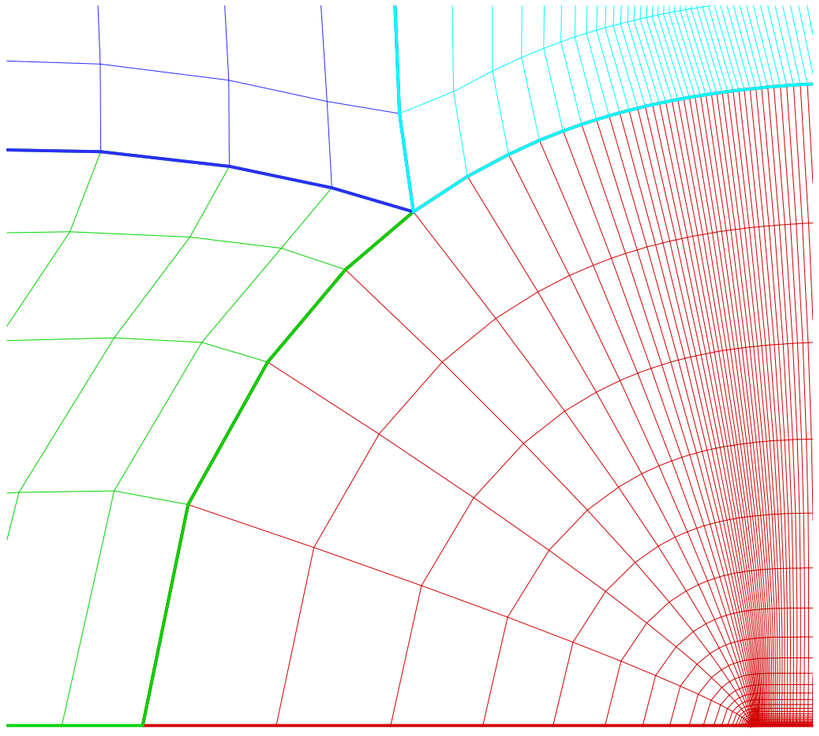

“O grids”

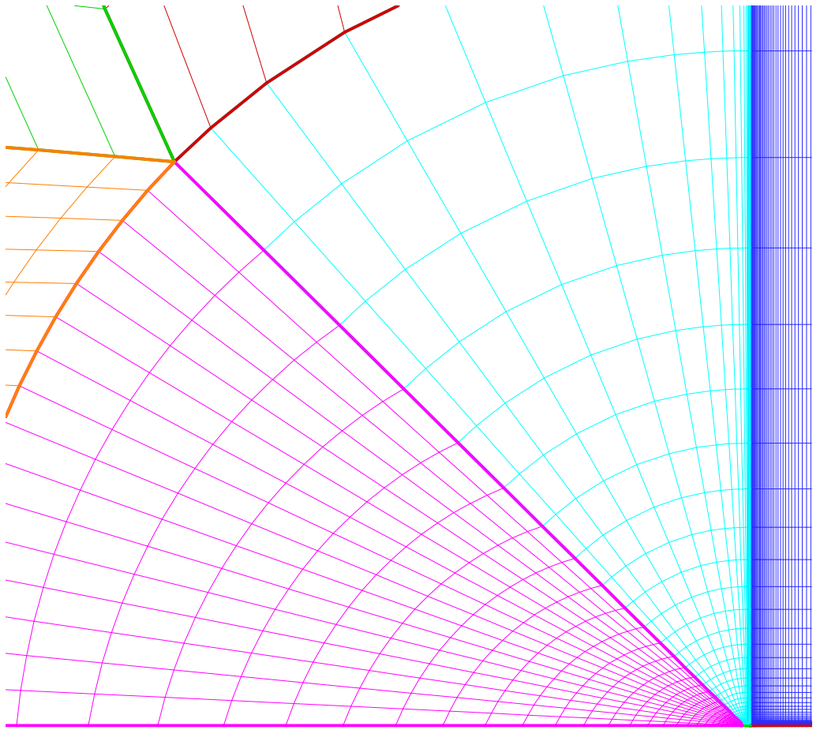

“HO grids”

AVT-313 Transition Workshop

Flow over a Flat Plate

- Three sets of five geometrically similar grids using
  $L = 1\text{m}$ ($V_\infty = 1\text{m/s} \Rightarrow \nu = 10^{-7}\text{m}^2/\text{s}$)

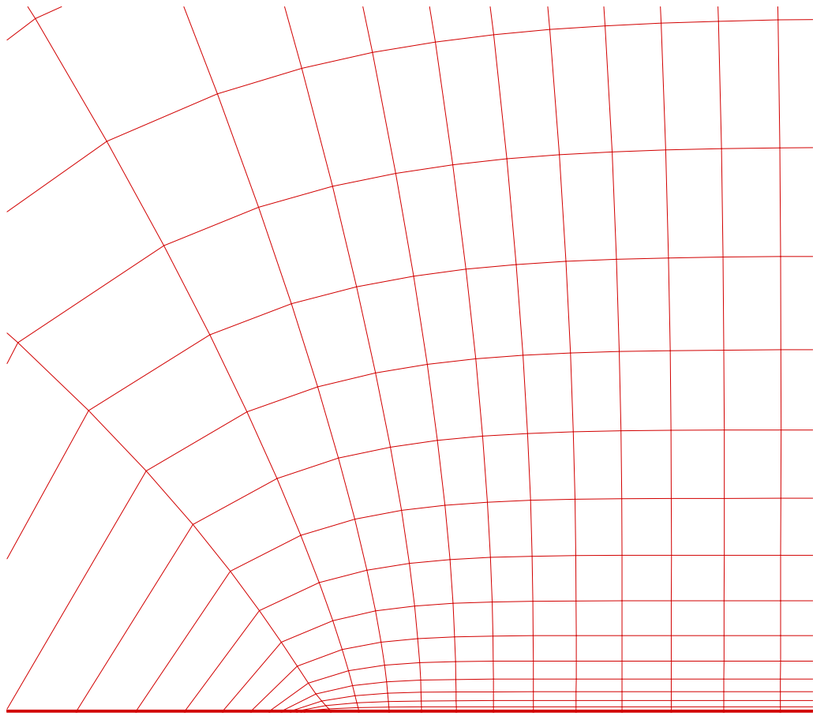

“O grids”

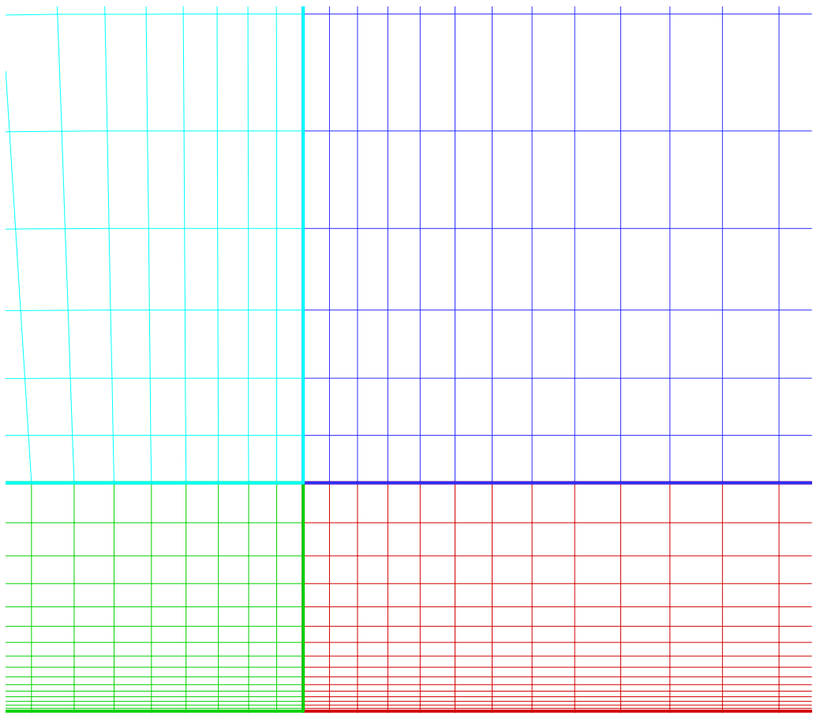

“HO grids”

AVT-313 Transition Workshop

Flow over a Flat Plate (T3AM)

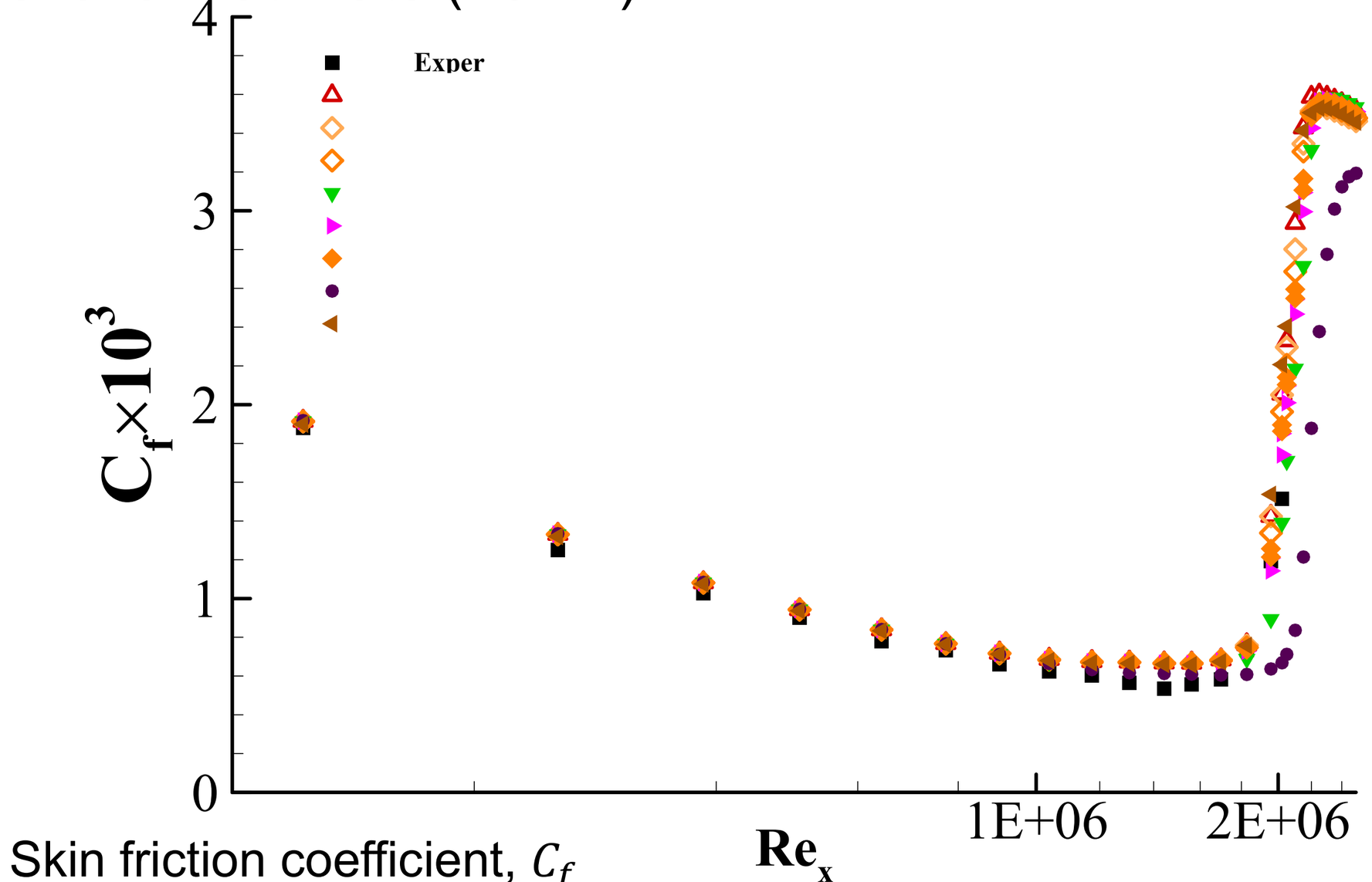

Skin friction coefficient, C_f

$\gamma - Re_\theta$

Transition from Laminar to Turbulent Flow

AVT-313 Transition Workshop

Flow over a Flat Plate (T3AM)

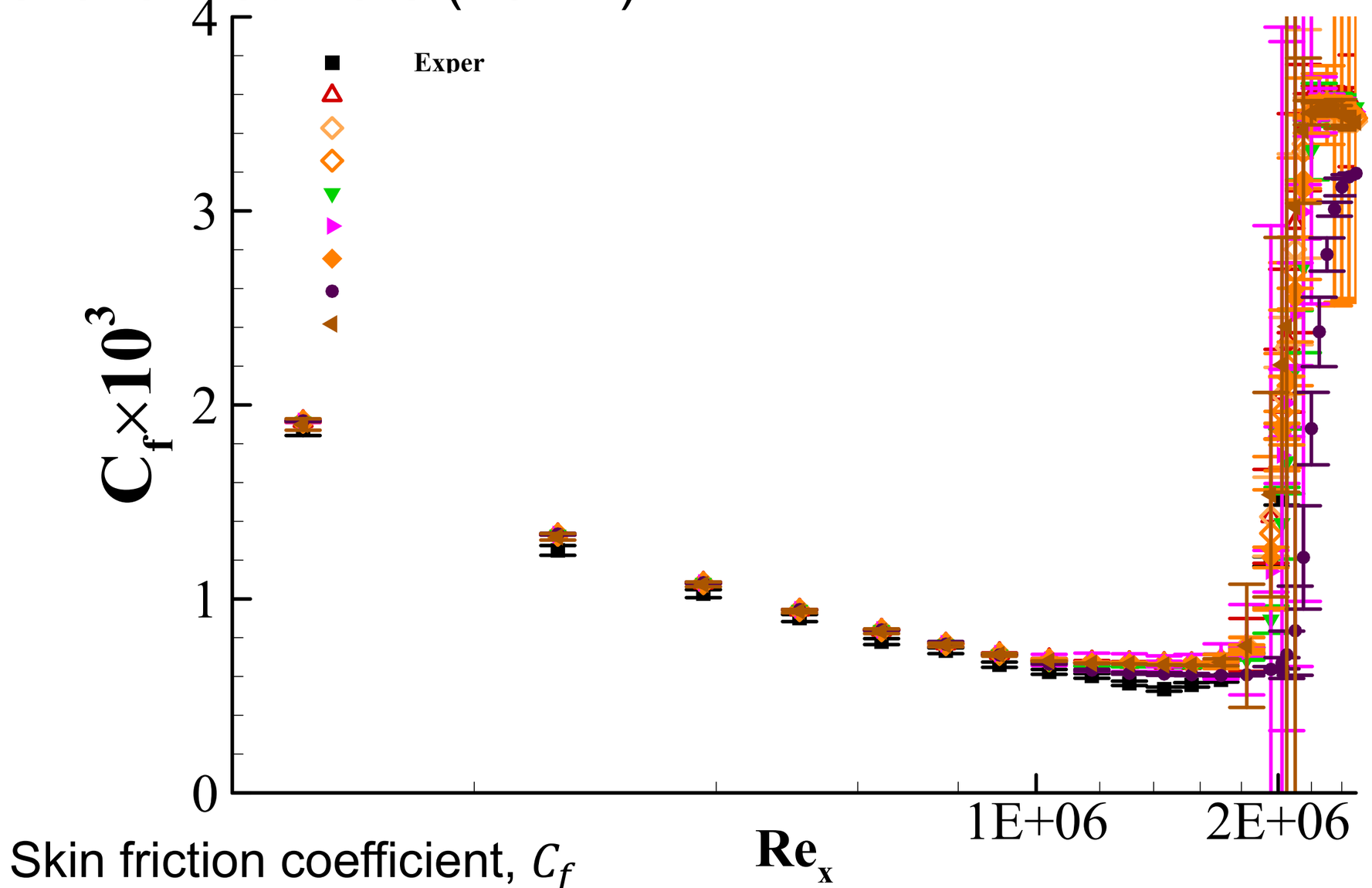

Skin friction coefficient, C_f

$\gamma - Re_\theta$

AVT-313 Transition Workshop

Flow over a Flat Plate (T3AM)

$\gamma - Re_\theta$

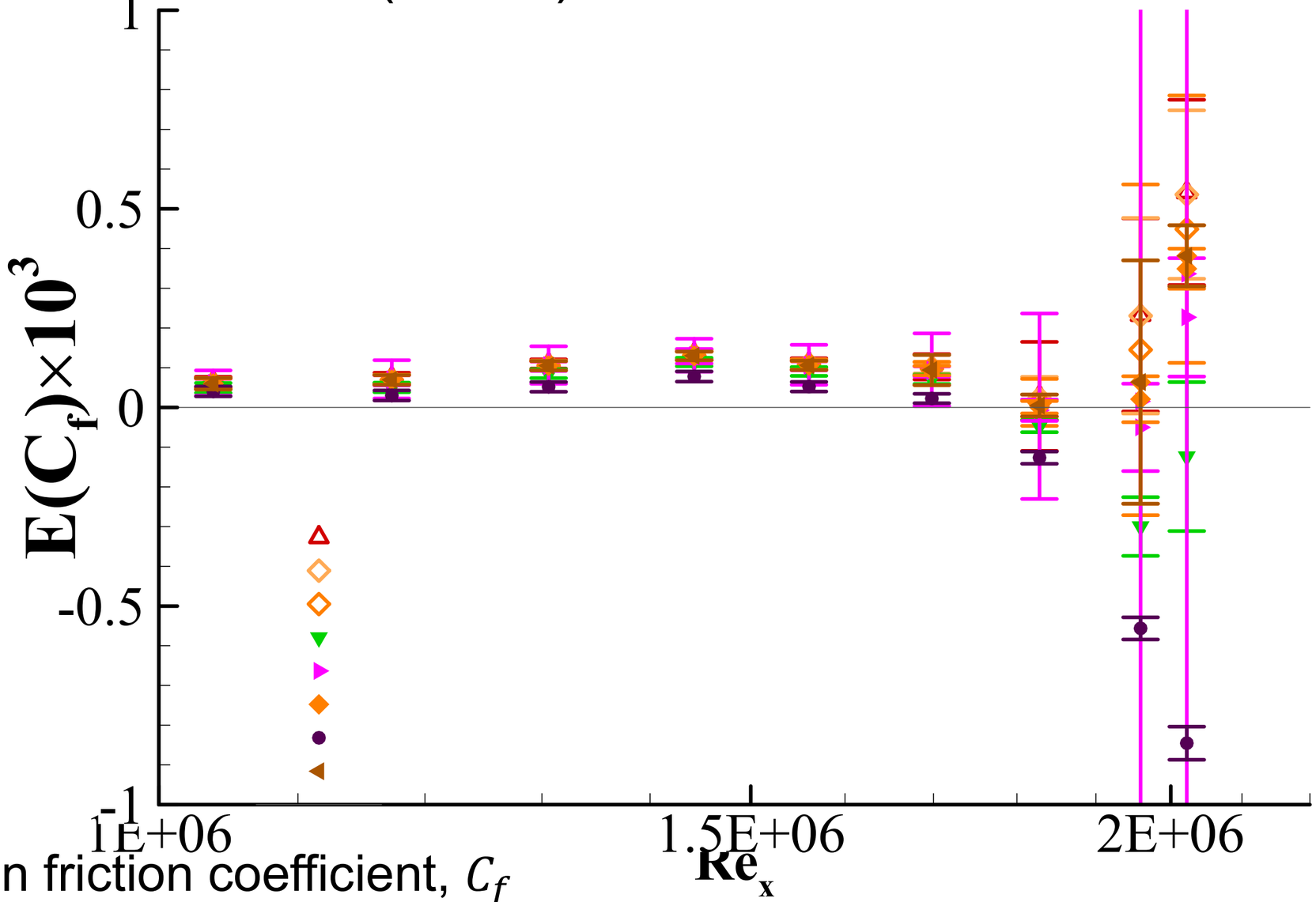

Skin friction coefficient, C_f

AVT-313 Transition Workshop

Flow over a Flat Plate (T3AM)

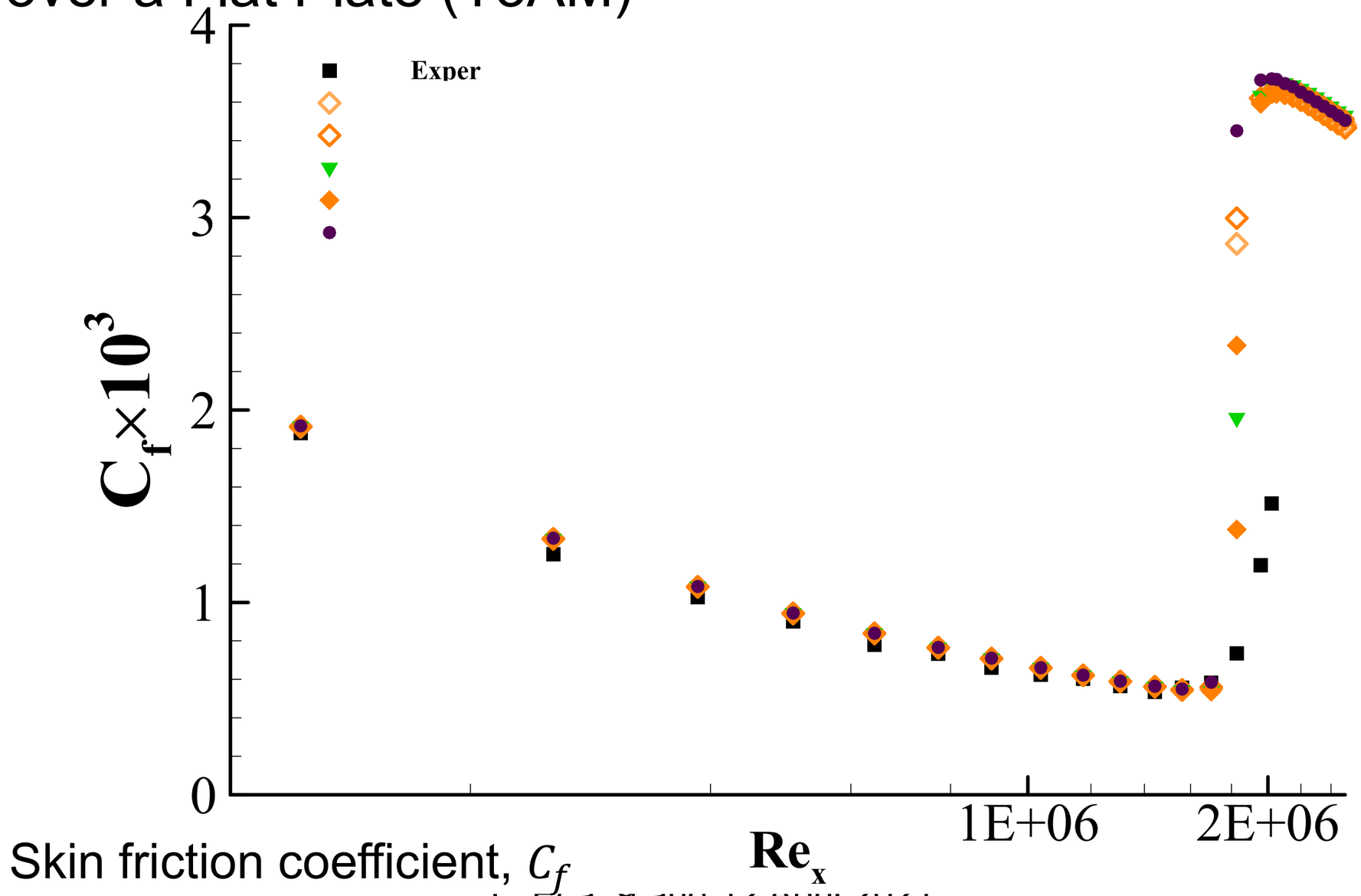

Skin friction coefficient, C_f

Transition from Laminar to Turbulent Flow

AVT-313 Transition Workshop

γ

Flow over a Flat Plate (T3AM)

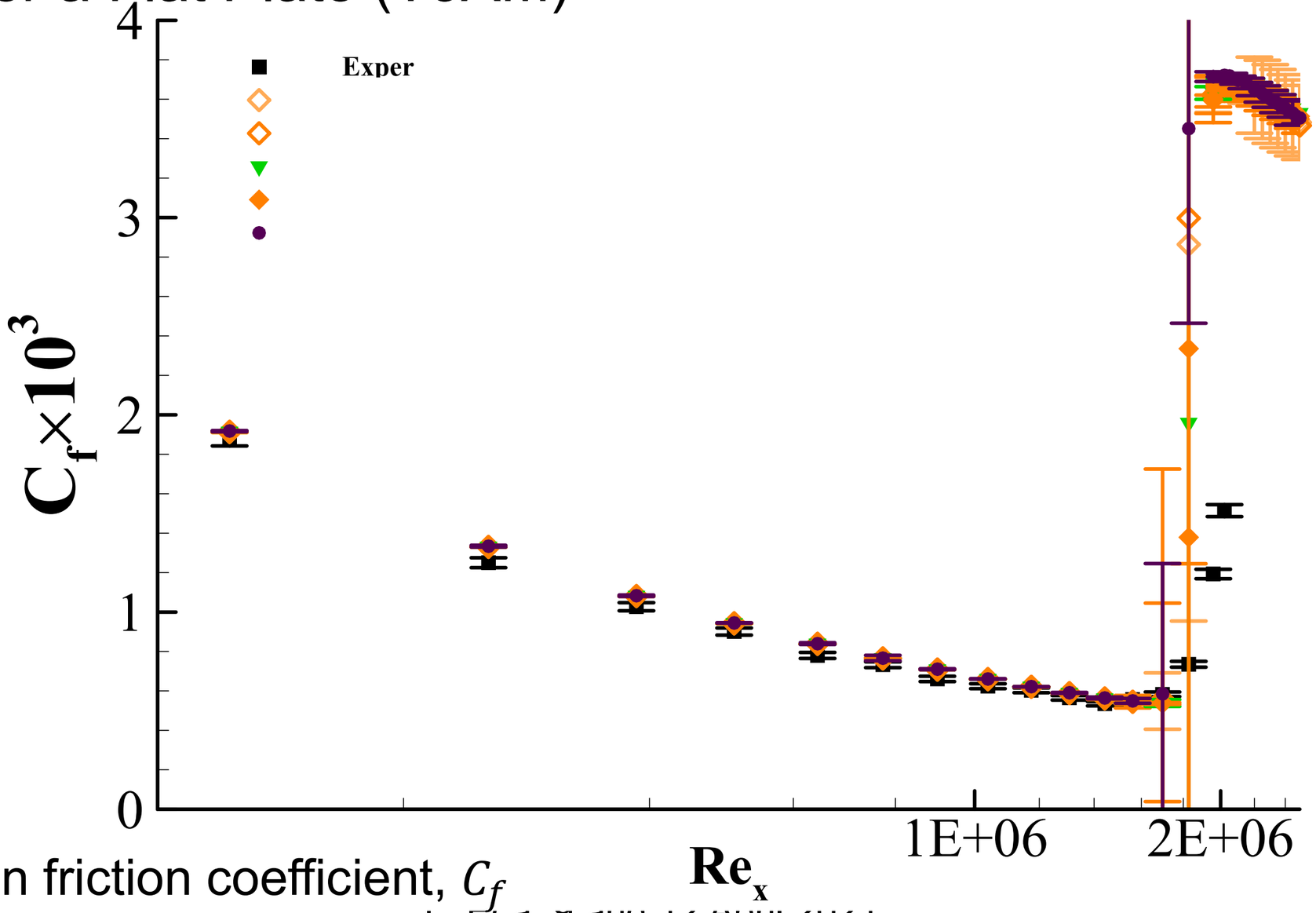

Skin friction coefficient, C_f

γ

Flow over a Flat Plate (T3AM)

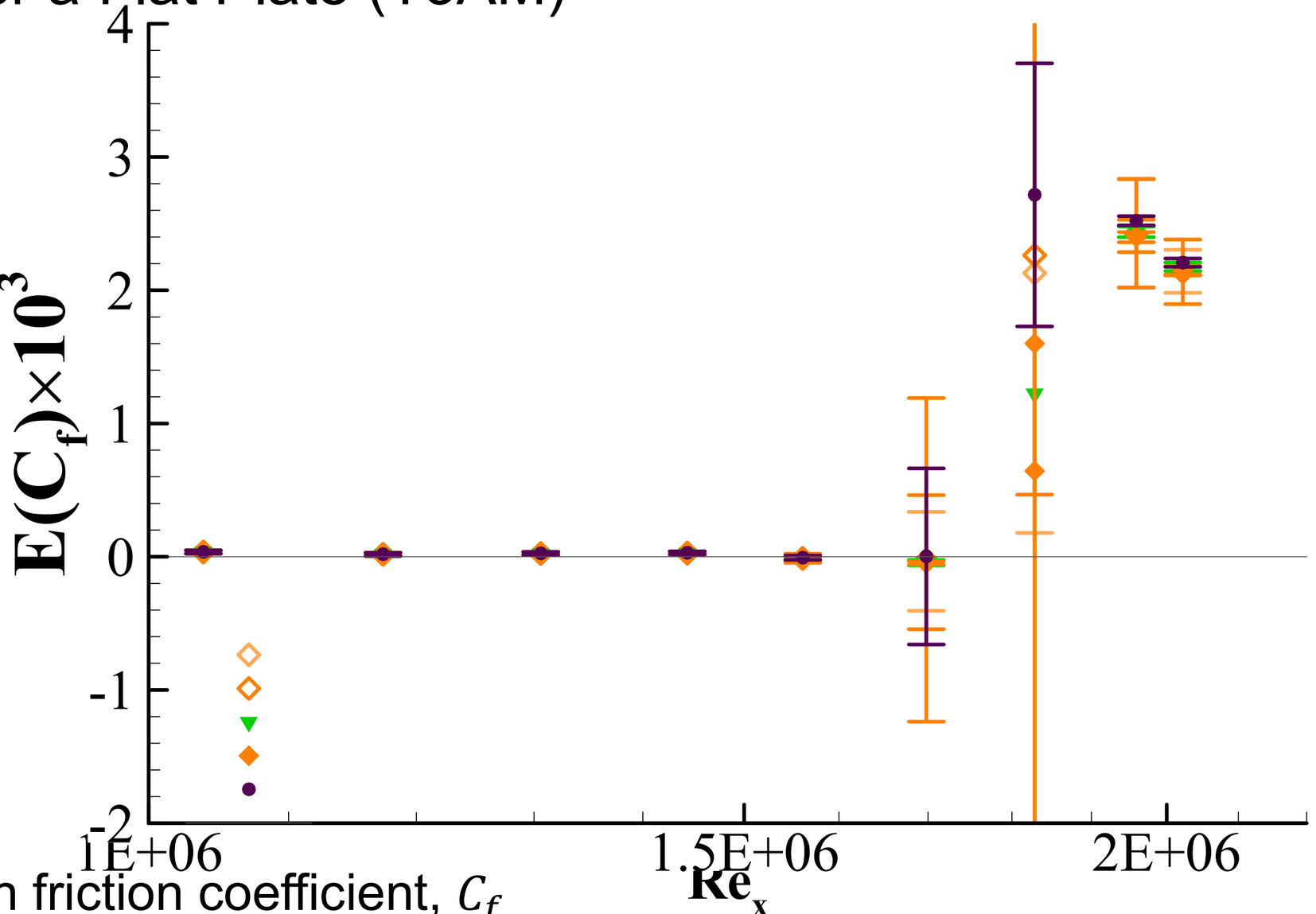

Skin friction coefficient, C_f

Transition from Laminar to Turbulent Flow

AVT-313 Transition Workshop

$\gamma - Re_\theta$

Flow over a Flat Plate (T3A)

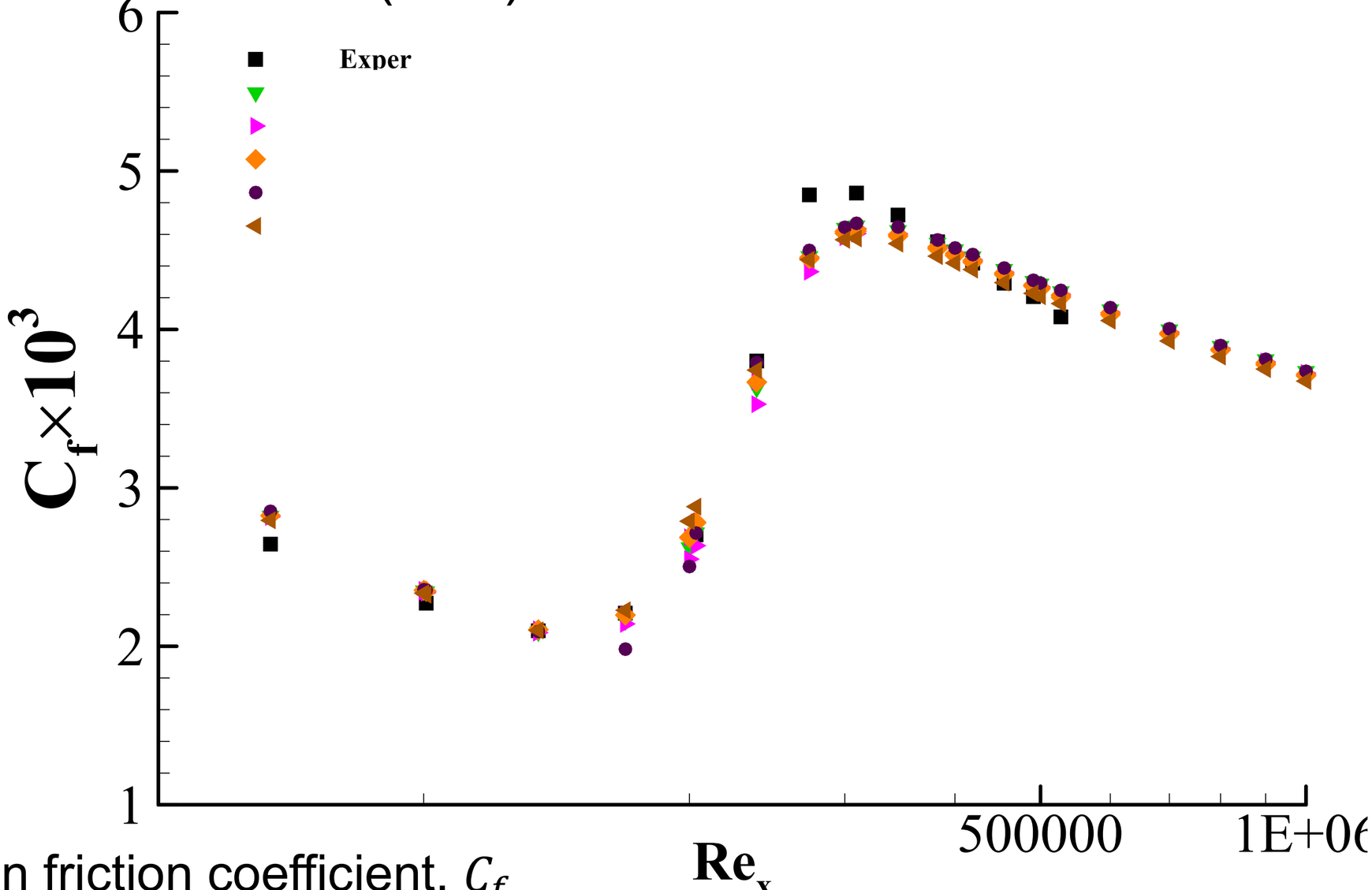

Skin friction coefficient, C_f

AVT-313 Transition Workshop

$\gamma - Re_\theta$

Flow over a Flat Plate (T3A)

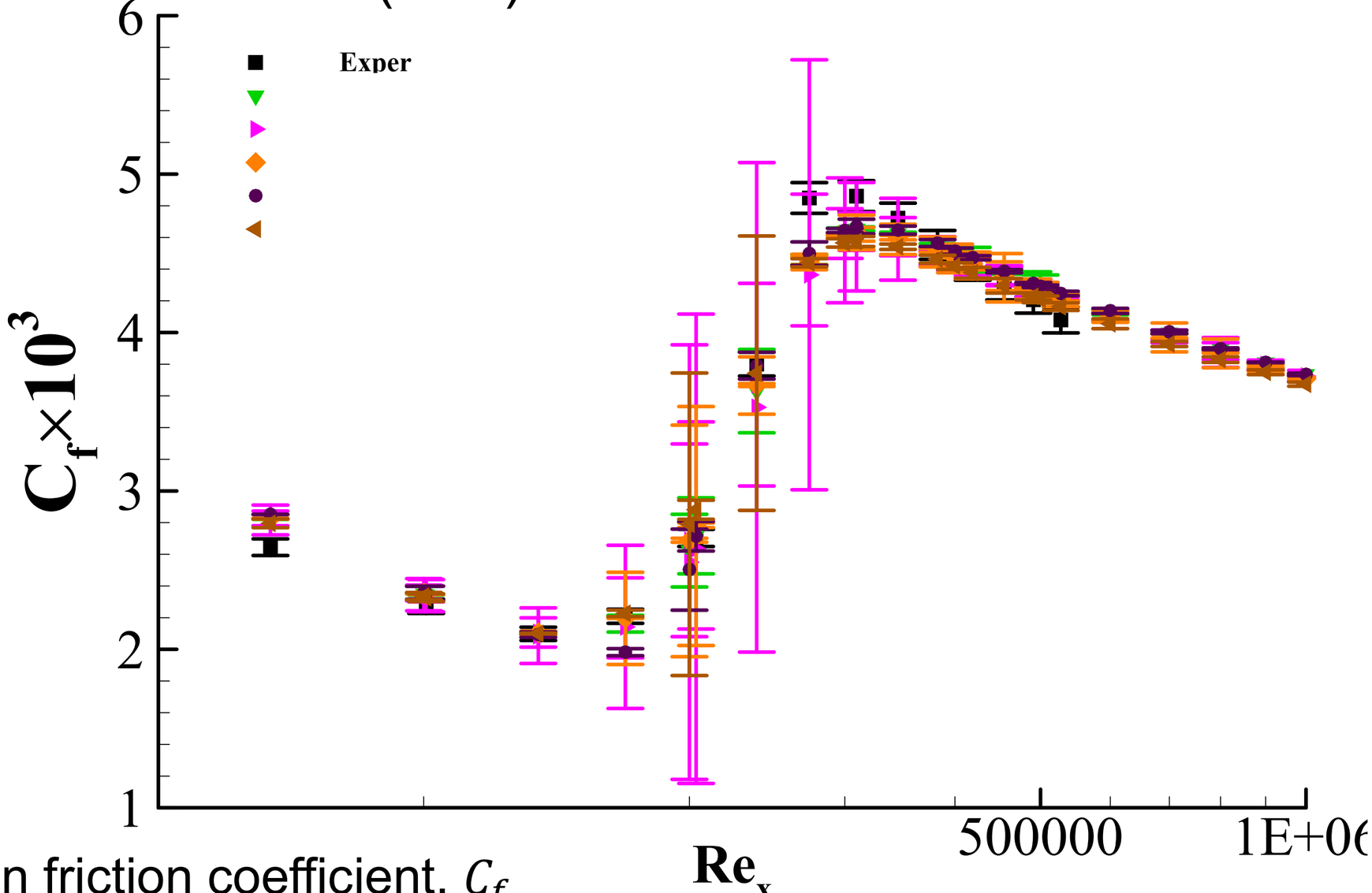

Skin friction coefficient, C_f

Transition from Laminar to Turbulent Flow

AVT-313 Transition Workshop

$\gamma - Re_\theta$

Flow over a Flat Plate (T3A)

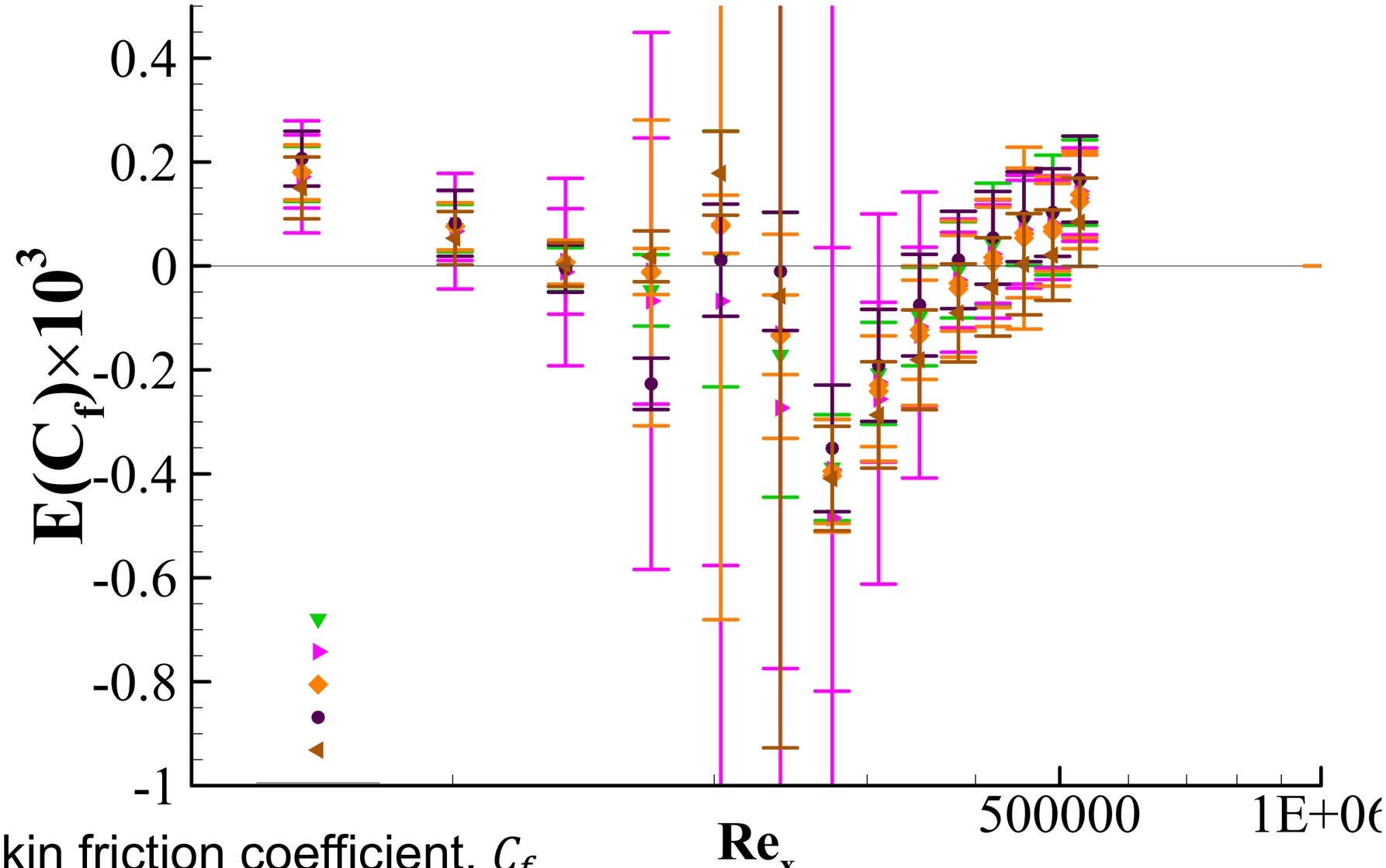

Skin friction coefficient, C_f

Transition from Laminar to Turbulent Flow

AVT-313 Transition Workshop

γ

Flow over a Flat Plate (T3A)

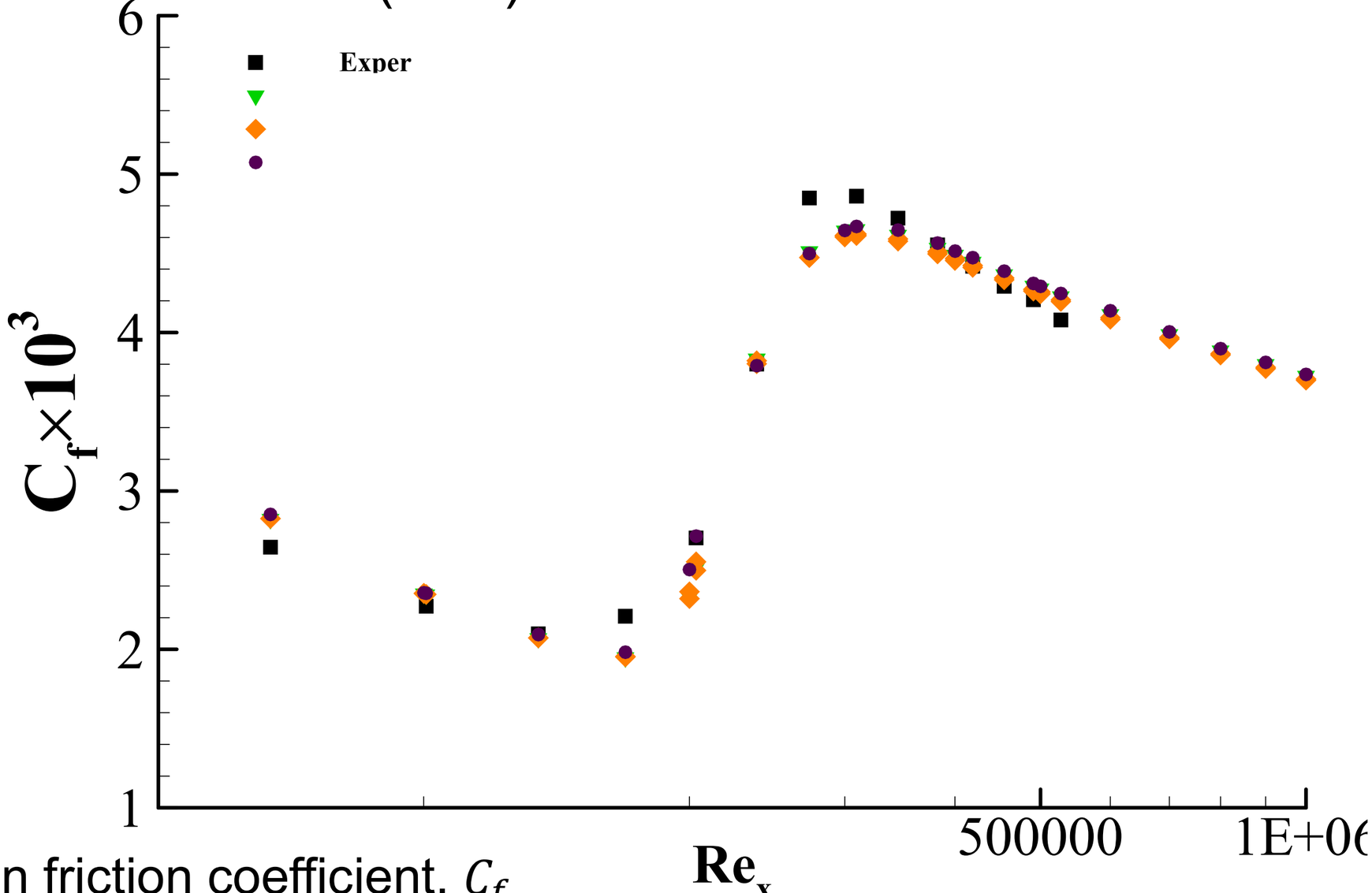

Skin friction coefficient, C_f

Transition from Laminar to Turbulent Flow

AVT-313 Transition Workshop

γ

Flow over a Flat Plate (T3A)

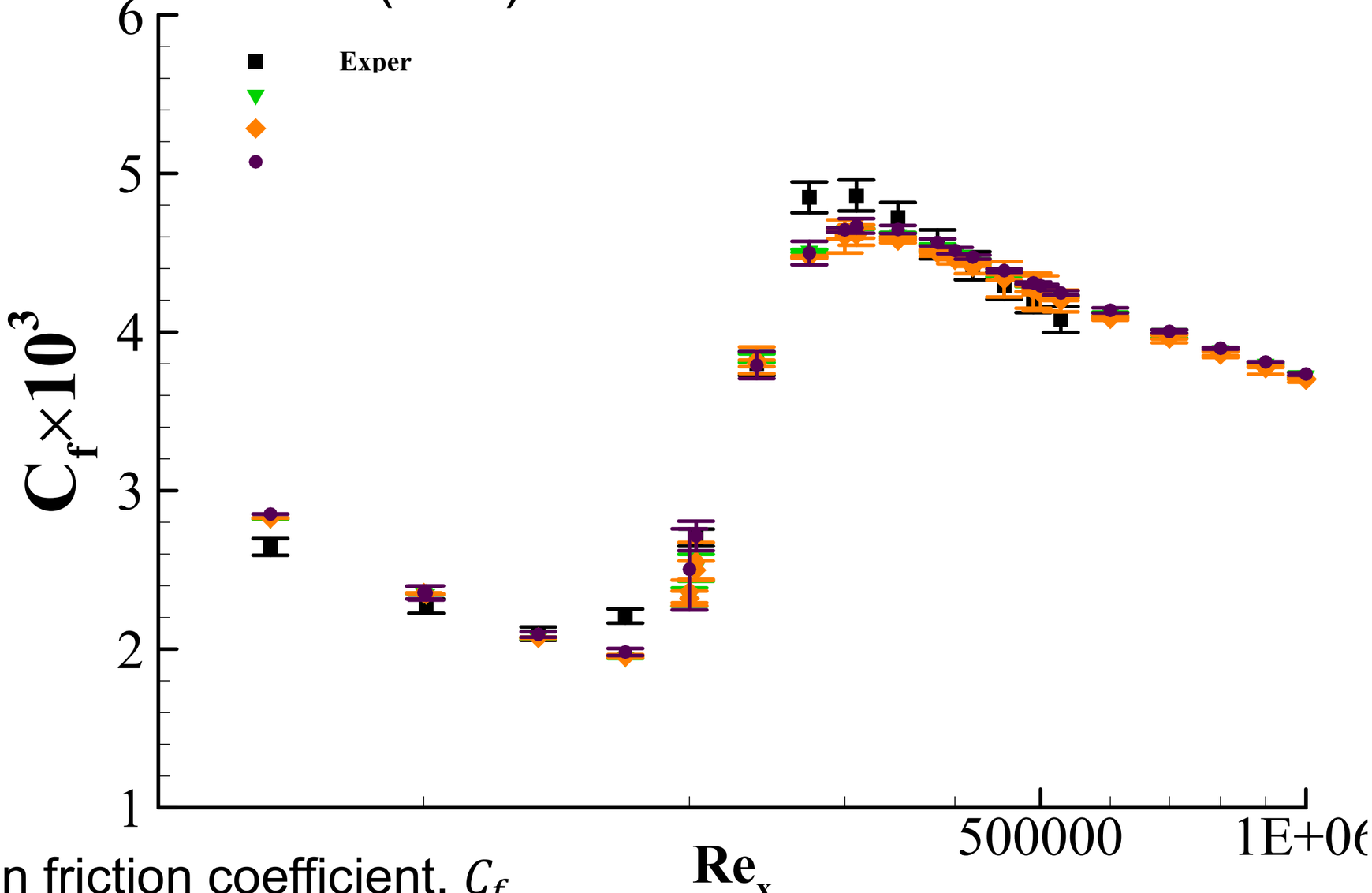

Skin friction coefficient, C_f

Transition from Laminar to Turbulent Flow

AVT-313 Transition Workshop

γ

Flow over a Flat Plate (T3A)

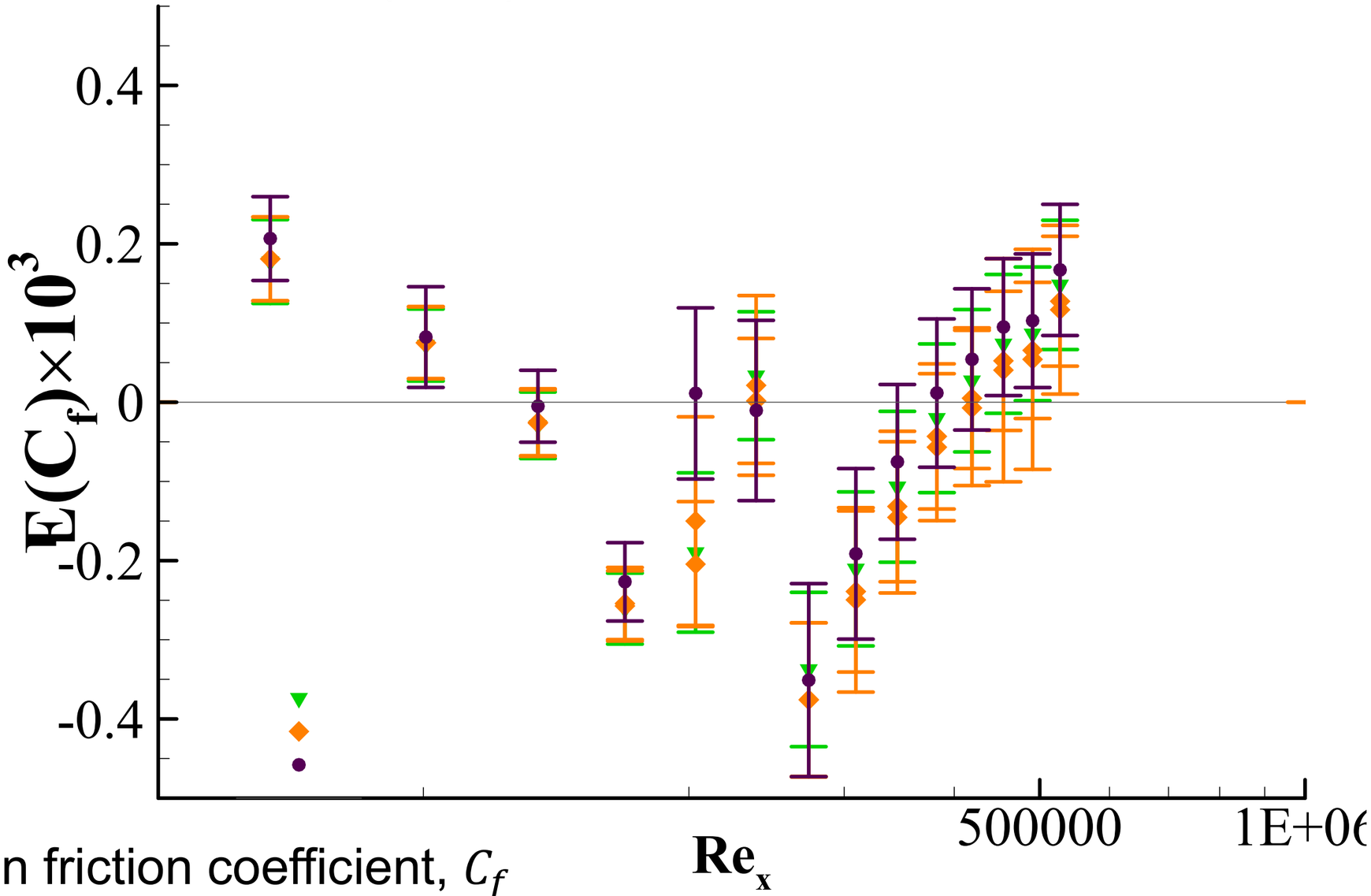

Skin friction coefficient, C_f

AVT-313 Transition Workshop

Flow over a Flat Plate

- General Remarks

- One outlier for the T3AM simulations with the $\gamma - Re_\theta$ model. Same submission with the γ model consistent with the others;
- No outliers for T3A and better overall agreement between the different codes than in the T3AM;
- Grid dependency significantly dependent on flow solver (iterative convergence, discretization schemes are not equal);
- Same flow solver with different grid topologies showed consistency for all quantities of interest.

L. Eça, 9 and 12 April 2021

AVT-313 Transition Workshop

Flow around the Eppler 387 foil

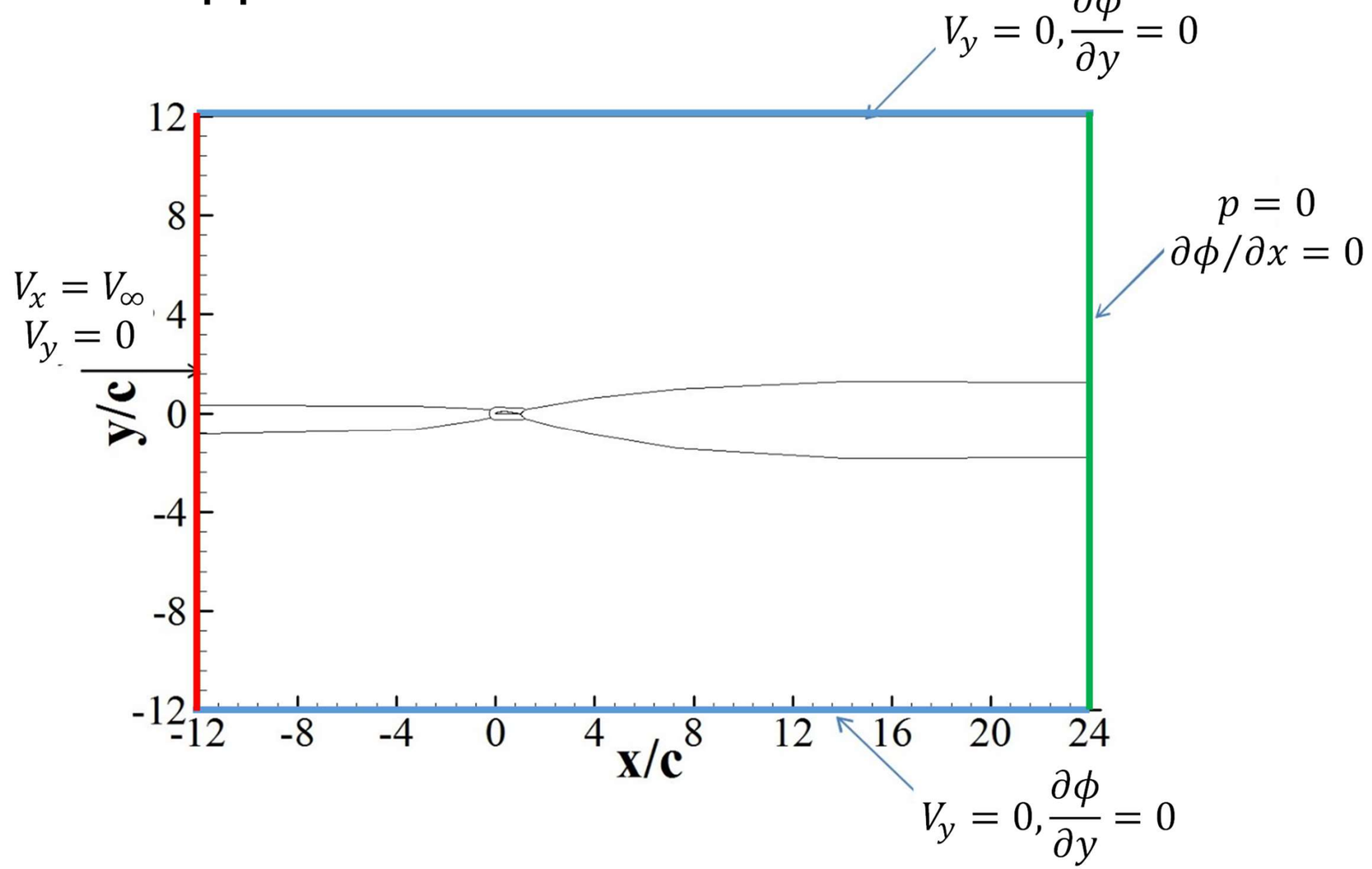

L. Eça, 9 and 12 April 2021

AVT-313 Transition Workshop

Flow around the Eppler 387 foil

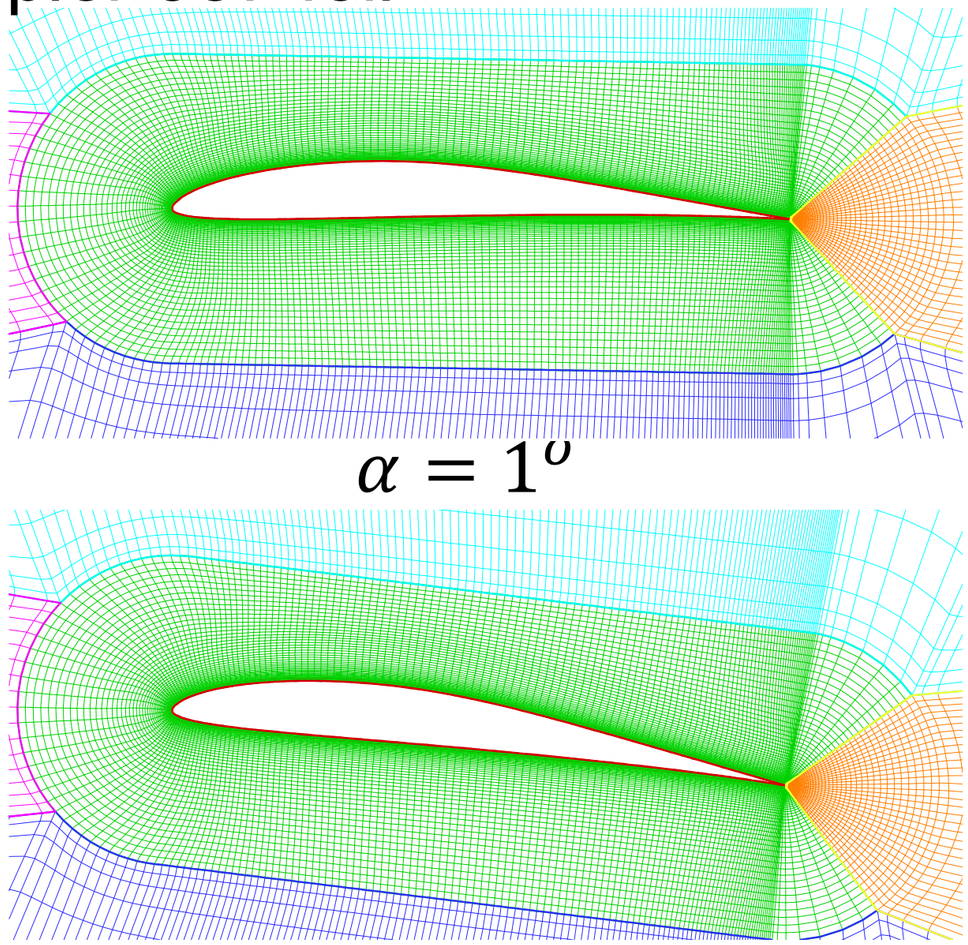

$\alpha = 1^o$

$\alpha = 7^o$

- Trailing edge at $\frac{x}{c} = \cos(\alpha), \frac{y}{c} = -\sin(\alpha)$.

AVT-313 Transition Workshop

Flow around the Eppler 387 foil

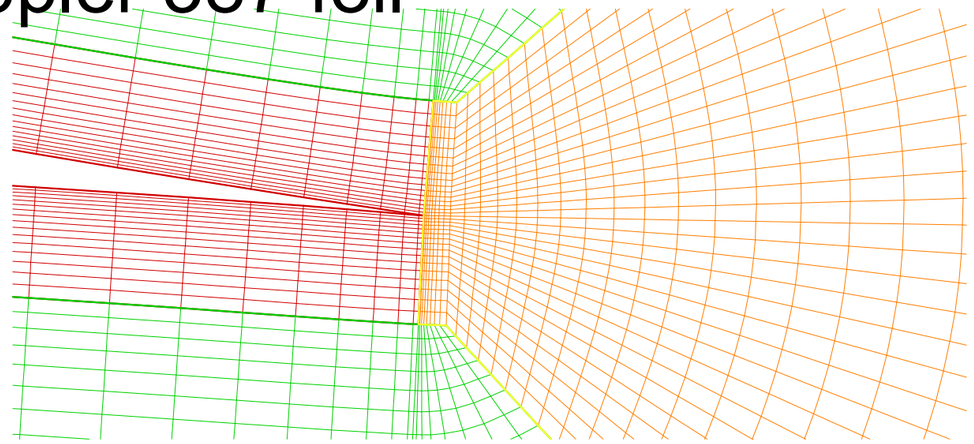

$\alpha = 1^o$

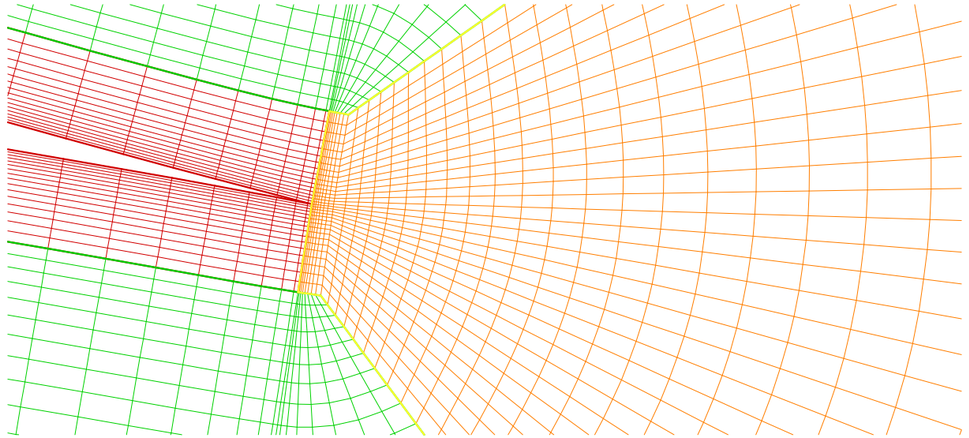

$\alpha = 7^o$

- Trailing edge at $\frac{x}{c} = \cos(\alpha), \frac{y}{c} = -\sin(\alpha)$.

Transition from Laminar to Turbulent Flow

AVT-313 Transition Workshop

Flow around the Eppler 387 foil

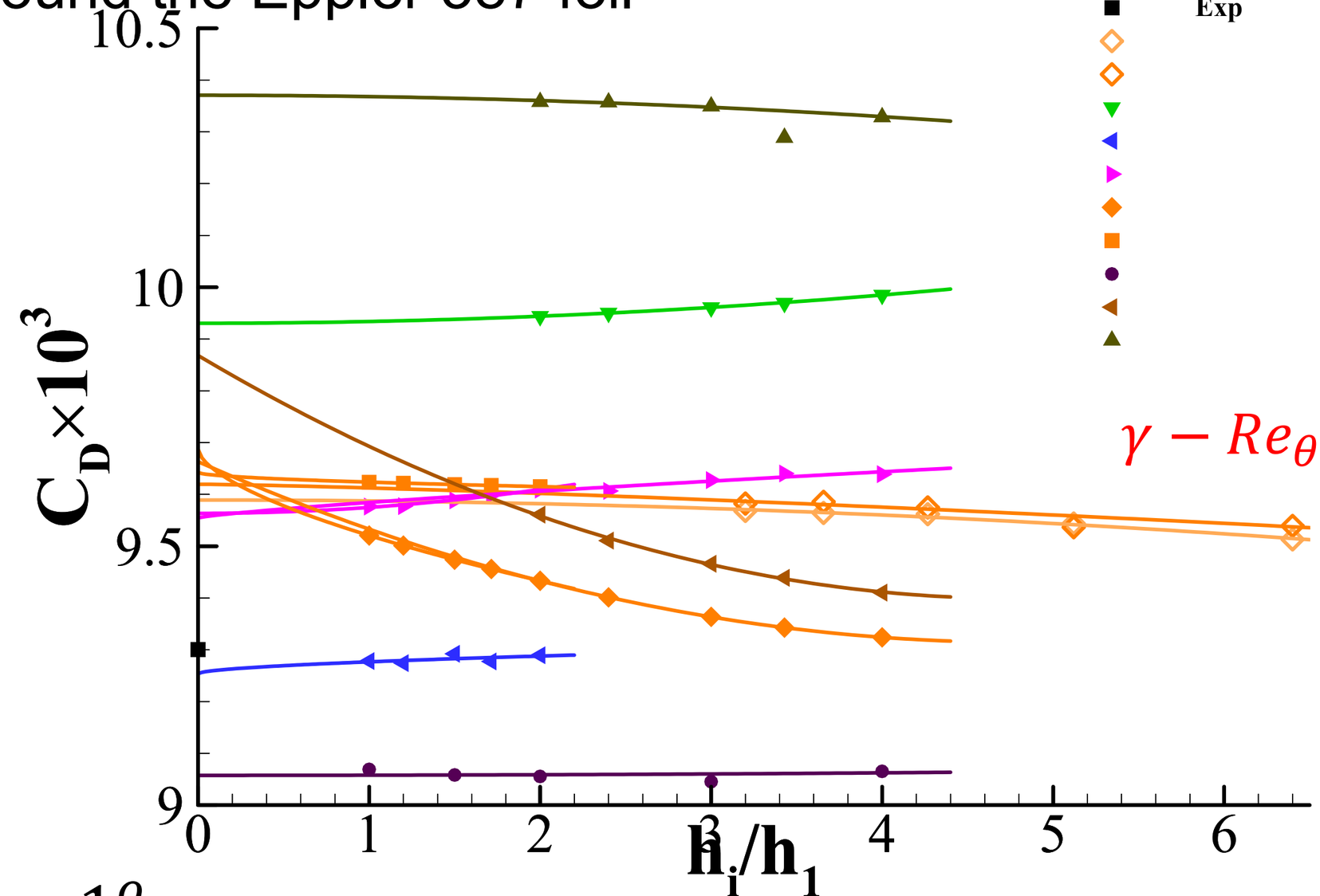

$\alpha = 1^o$

 Resistance coefficient, C_D

AVT-313 Transition Workshop

γ

Flow around the Eppler 387 foil

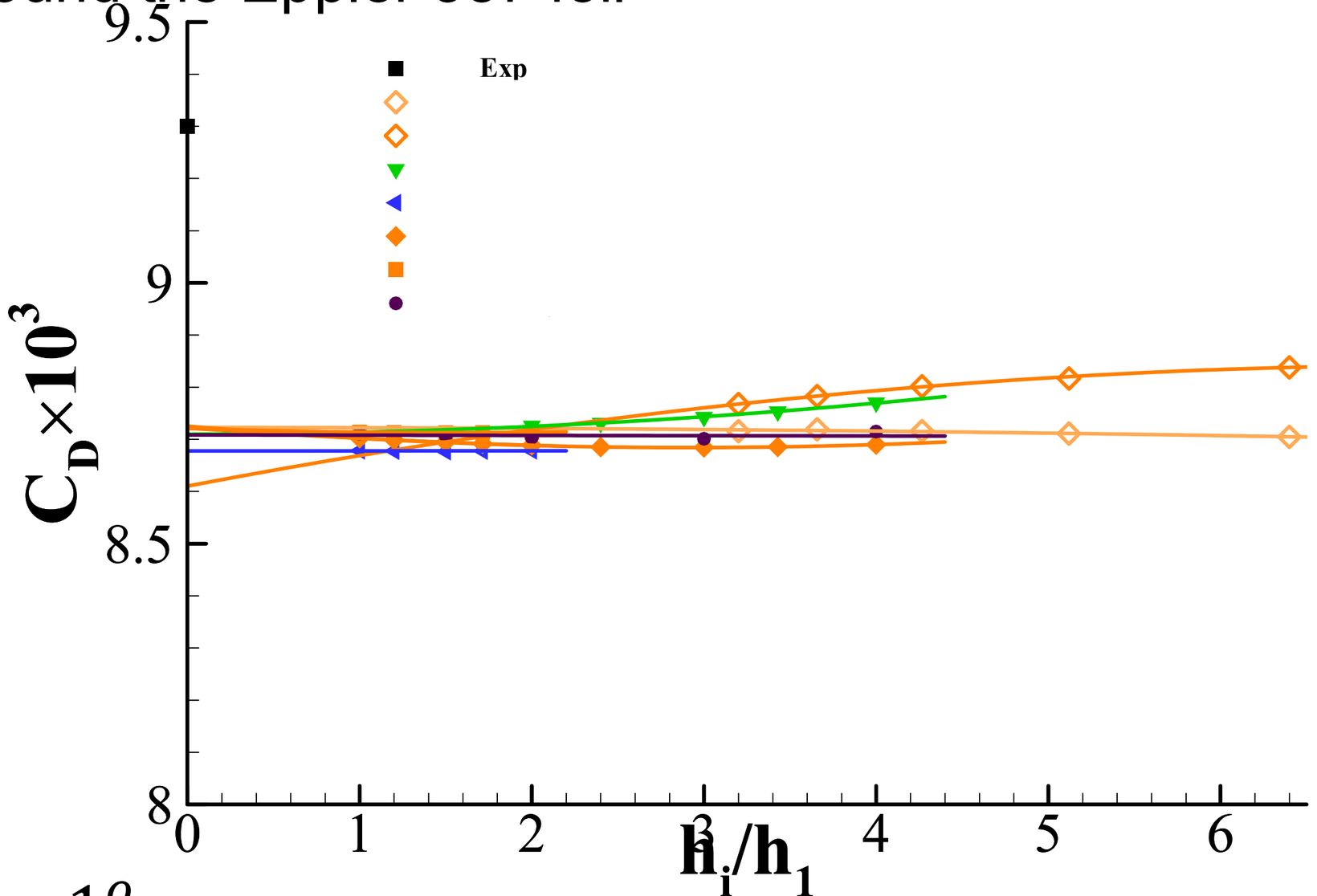

$\alpha = 1^o$

Resistance coefficient, C_D

Transition from Laminar to Turbulent Flow

AVT-313 Transition Workshop

Flow around the Eppler 387 foil

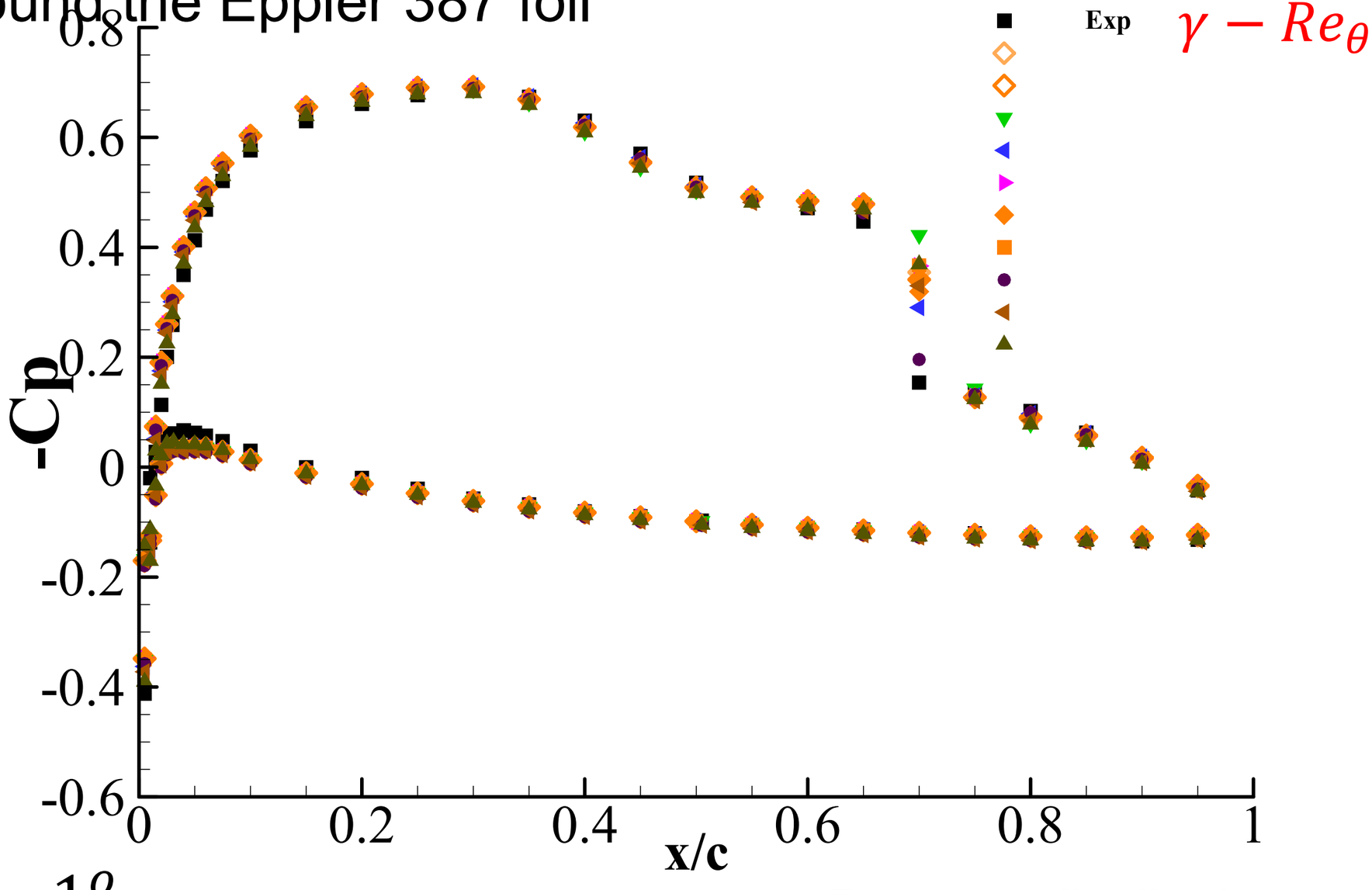

$\alpha = 1^o$

Pressure distribution, C_p

Transition from Laminar to Turbulent Flow

AVT-313 Transition Workshop

Flow around the Eppler 387 foil

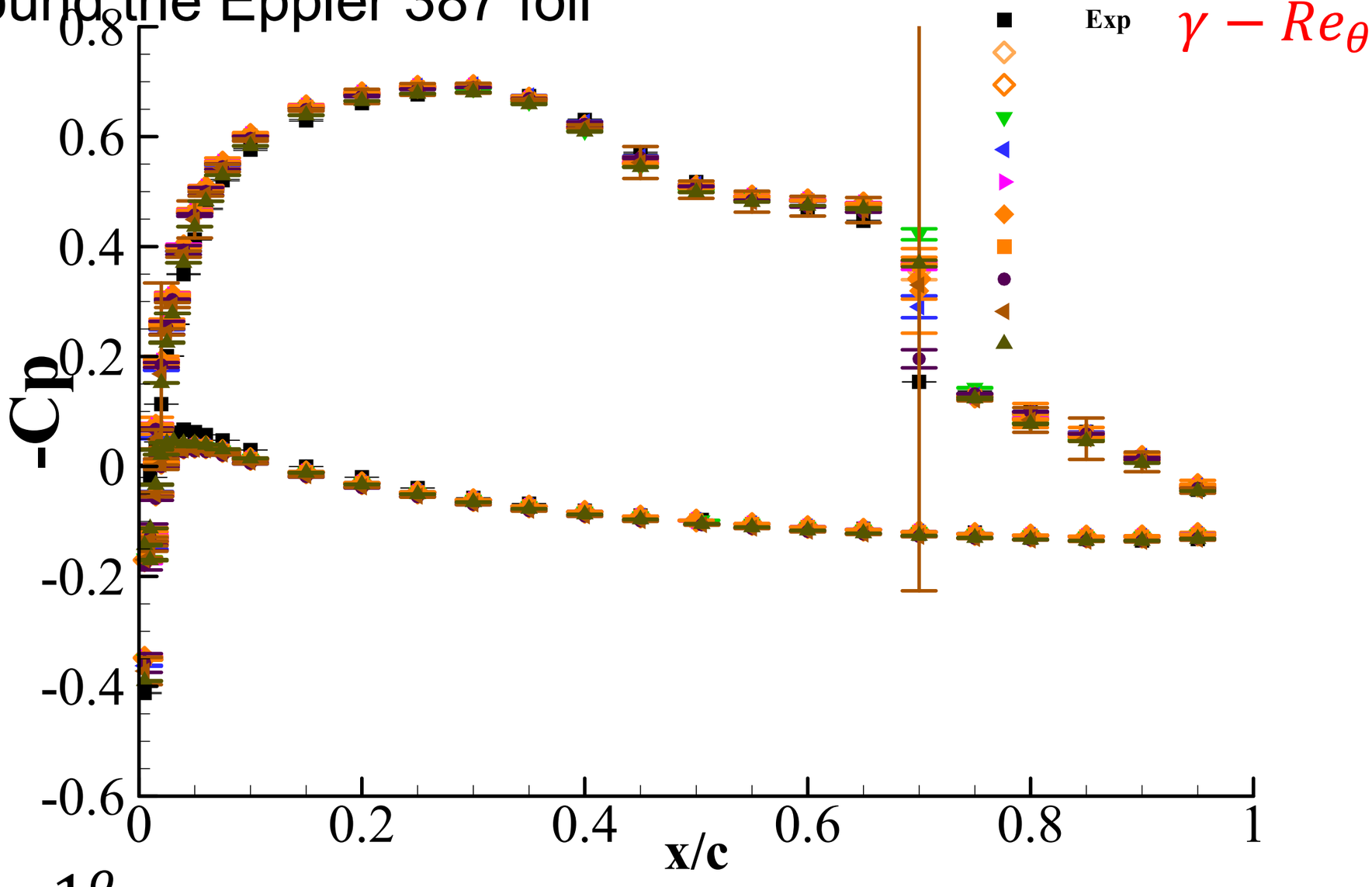

$\alpha = 1^o$

Pressure distribution, C_p

Transition from Laminar to Turbulent Flow

AVT-313 Transition Workshop

γ

Flow around the Eppler 387 foil

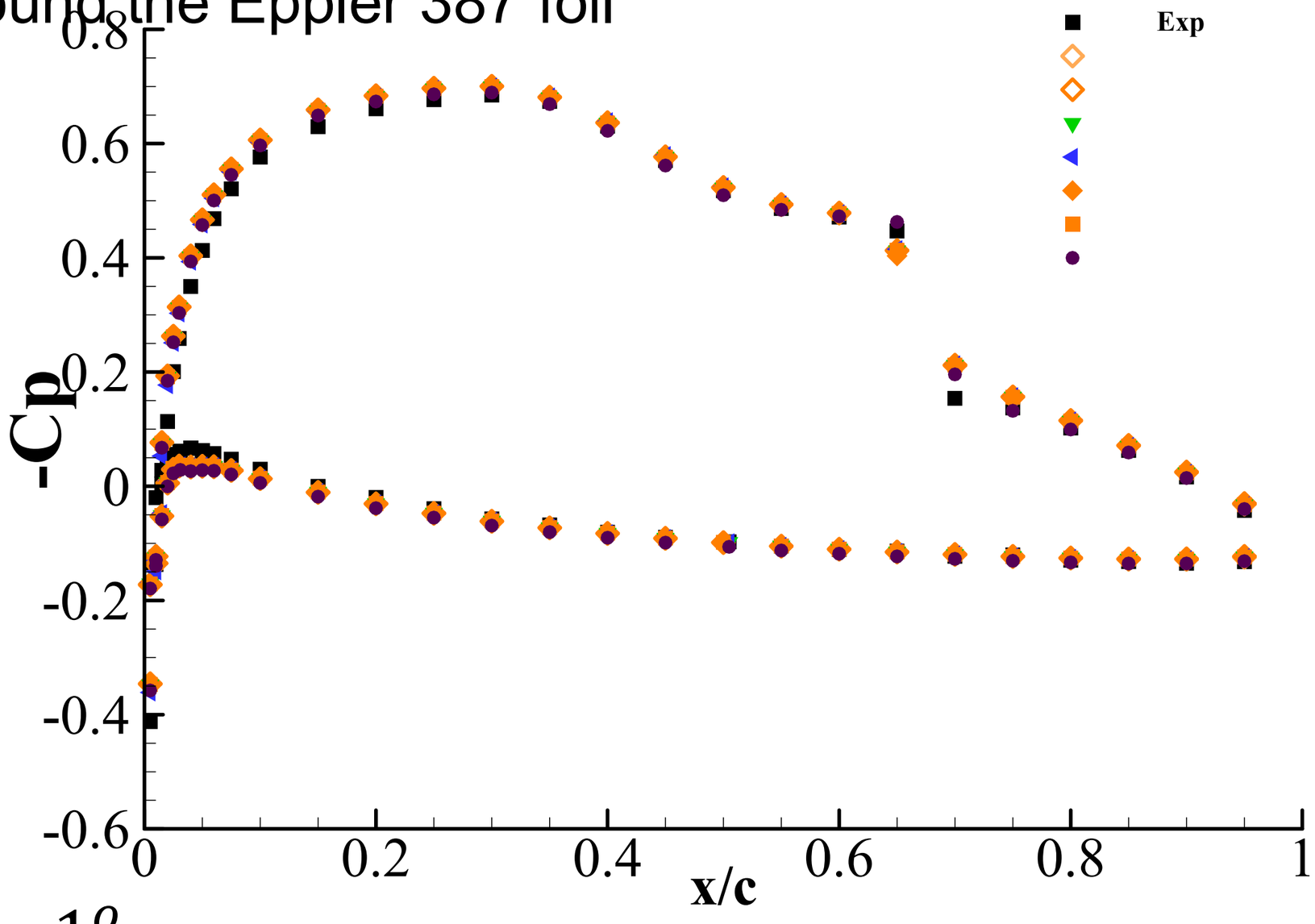

$\alpha = 1^o$

L. Eça, 9 and 12 April 20 Pressure distribution, C_p

γ

Flow around the Eppler 387 foil

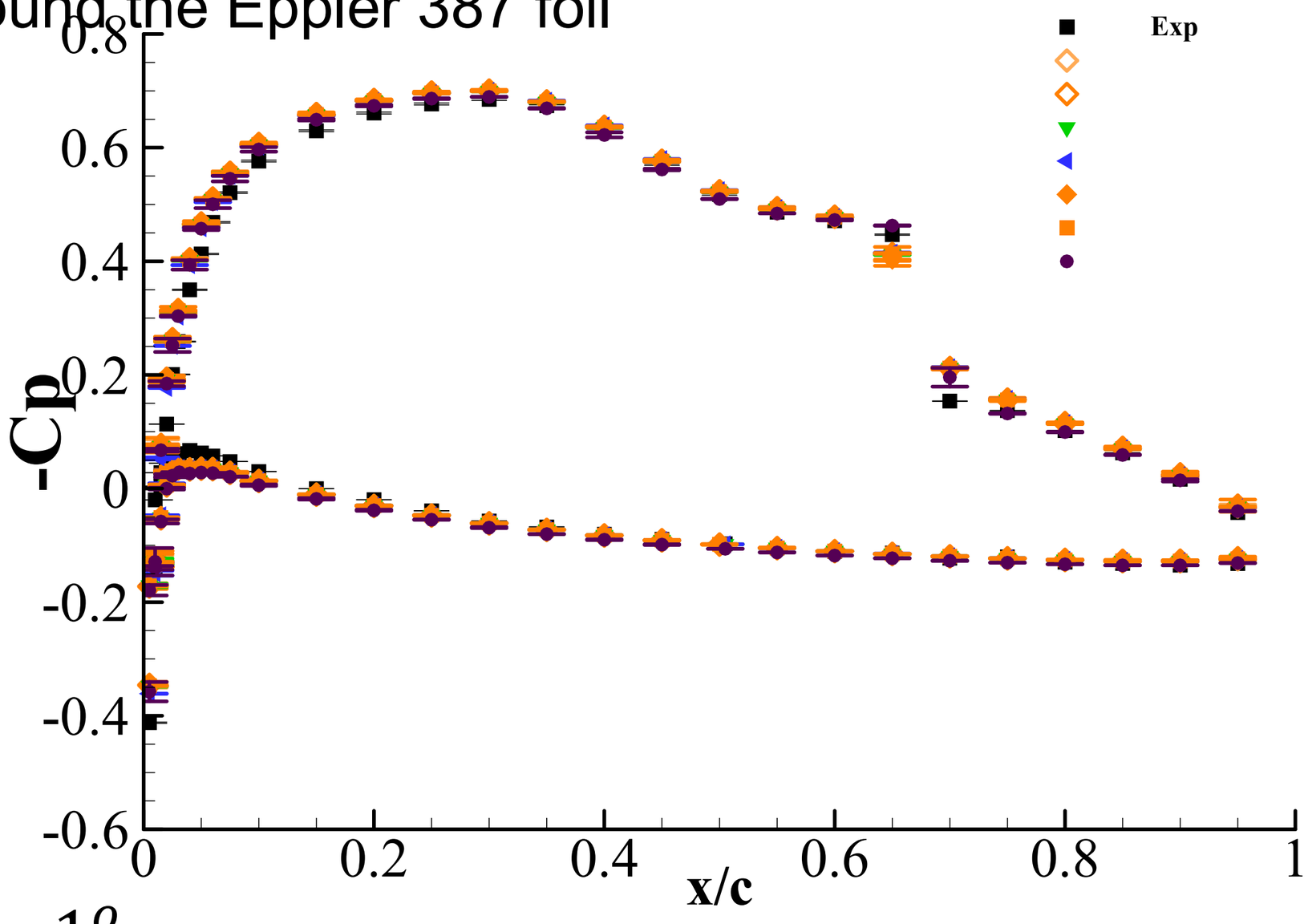

$\alpha = 1^o$

Pressure distribution, C_p

AVT-313 Transition Workshop

Flow around the Eppler 387 foil

- General Remarks

  - Pressure force exhibits less consistency between the different submissions than the friction force;

  - Skin friction coefficient exhibits a remarkable agreement between all simulations;

  - Largest comparison errors (Simulations-Experiments) obtained at the laminar separation bubbles;

  - Grid dependency significantly dependent on flow solver;

    - Same code with different grid topologies showed consistency for all quantities of interest.

AVT-313 Transition Workshop

Flow around the NACA 0015 foil

- c is the chord length and U_∞ is the incoming velocity.
- Incompressible fluid.
- Reynolds number $Re = \frac{U_\infty c}{\nu} = 1.8 \times 10^5$.
- Angles of attack of $\alpha = 5^o$ and $\alpha = 10^o$.
- Experimental data obtained from

  Miozzi, Di Felice, Klein, Costantini:
  "Taylor hypothesis applied to direct measurement of skin friction using data from Temperature Sensitive Paint", Experimental Thermal and Fluid Science, Volume 110, 2020, 10991
  https://doi.org/10.1016/j.expthermflusci.2019.109913

Transition from Laminar to Turbulent Flow

AVT-313 Transition Workshop

Flow around the NACA 0015 foil

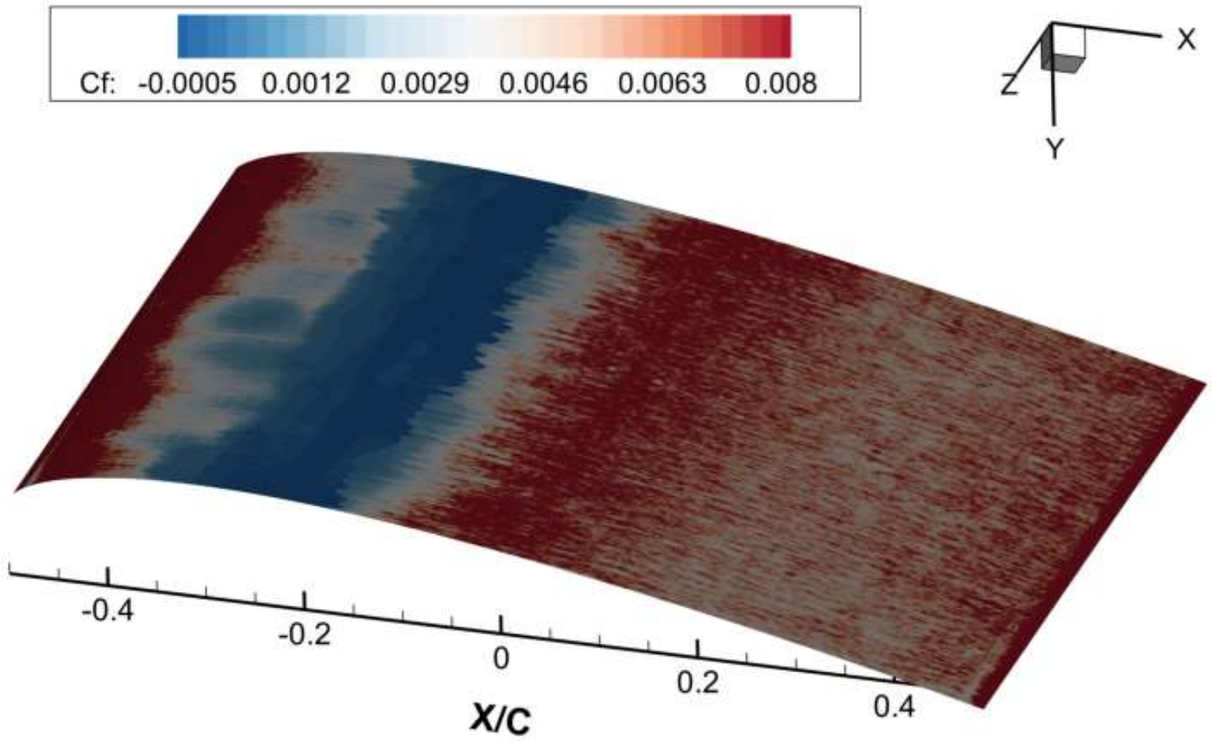

$\alpha = 5^o$

L. Eça, 9 and 12 April 2021

AVT-313 Transition Workshop

Flow around the NACA 0015 foil

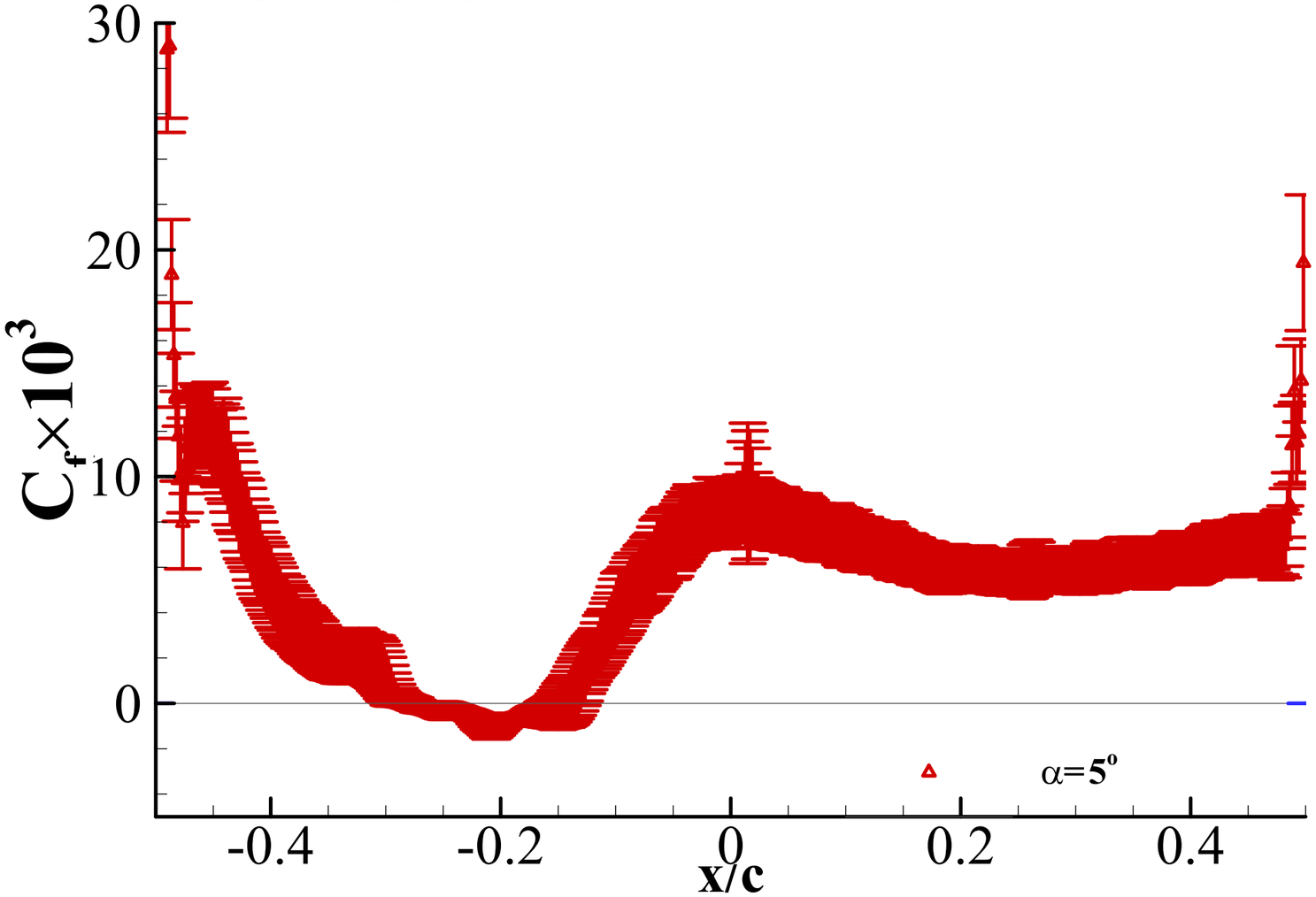

$\alpha = 5^o$

L. Eça, 9 and 12 April 2021

AVT-313 Transition Workshop

Flow around the NACA 0015 foil

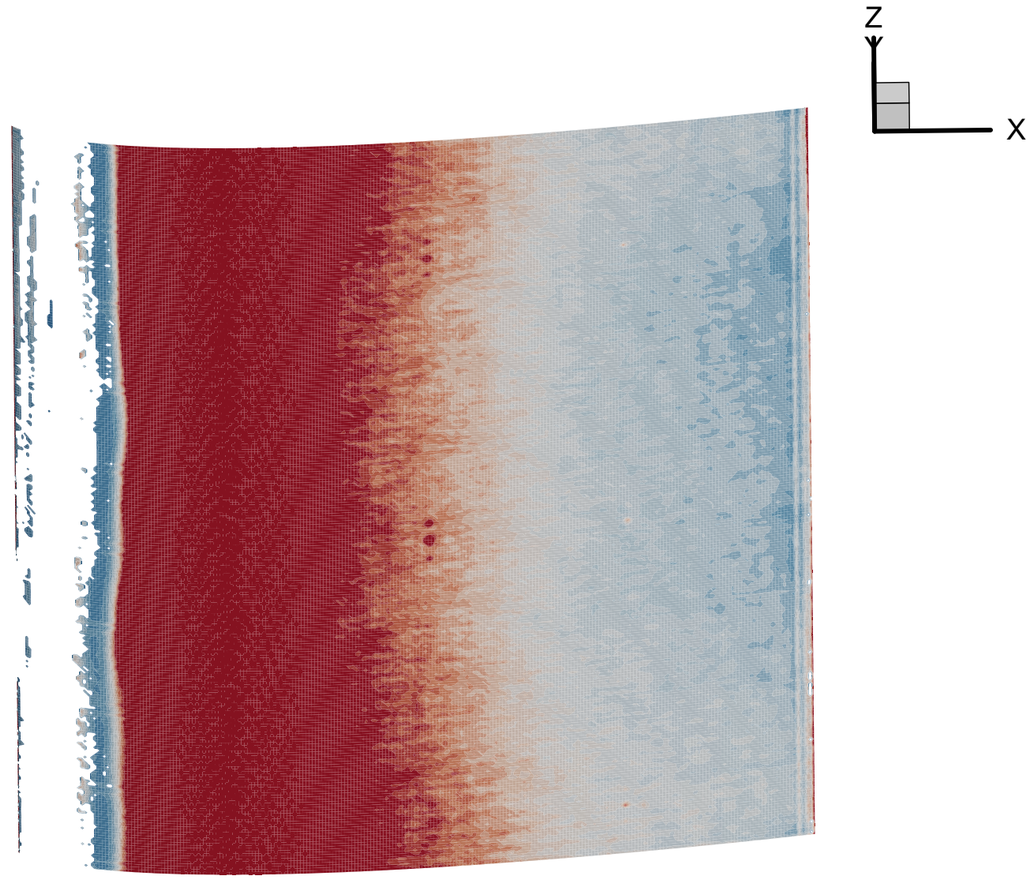

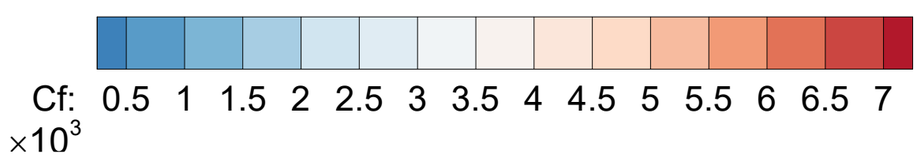

$\alpha = 10^c$

L. Eça, 9 and 12 April 2021

AVT-313 Transition Workshop

Flow around the NACA 0015 foil

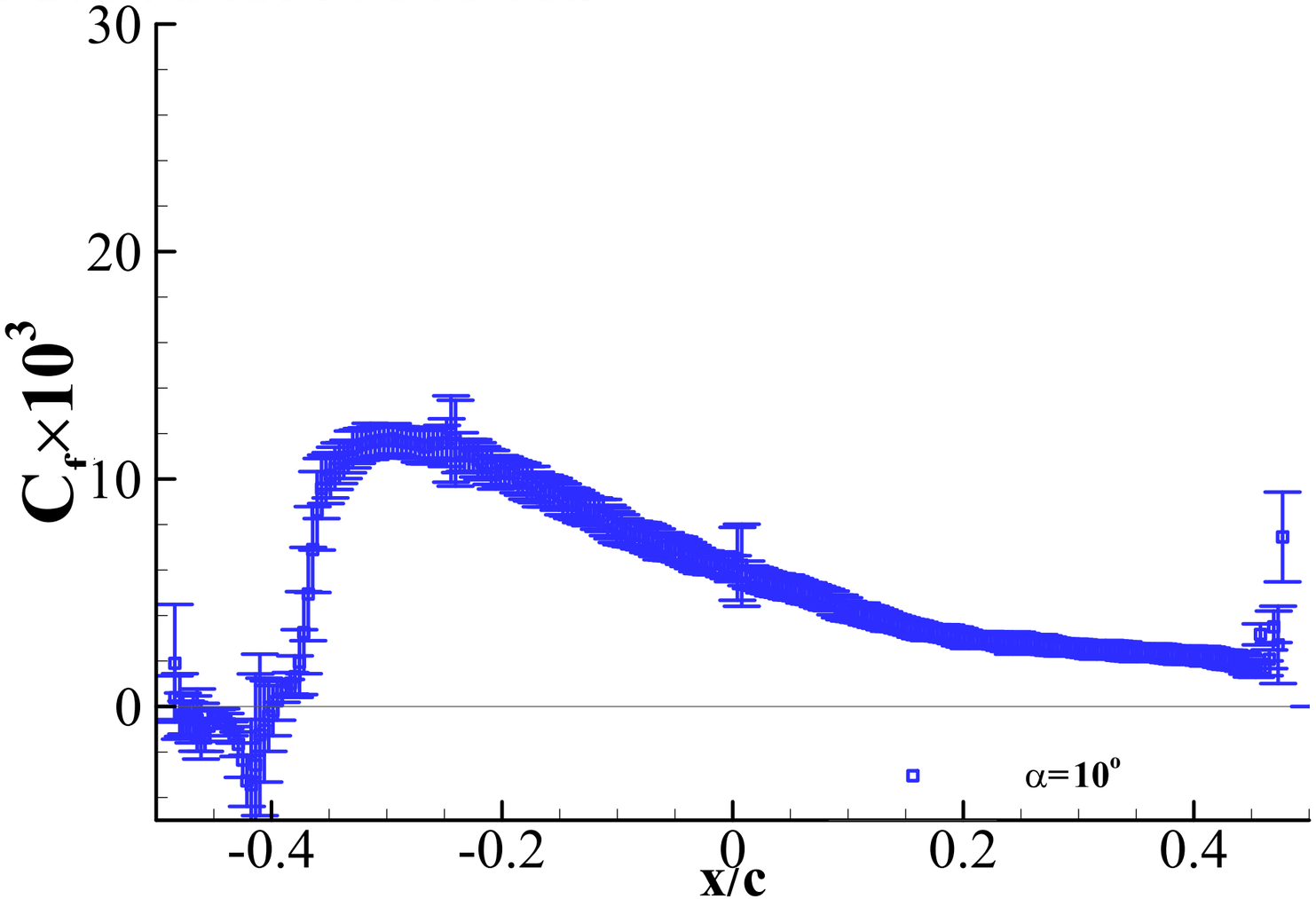

$\alpha = 10^o$

L. Eça, 9 and 12 April 2021

AVT-313 Transition Workshop

Flow around the NACA 0015 foil

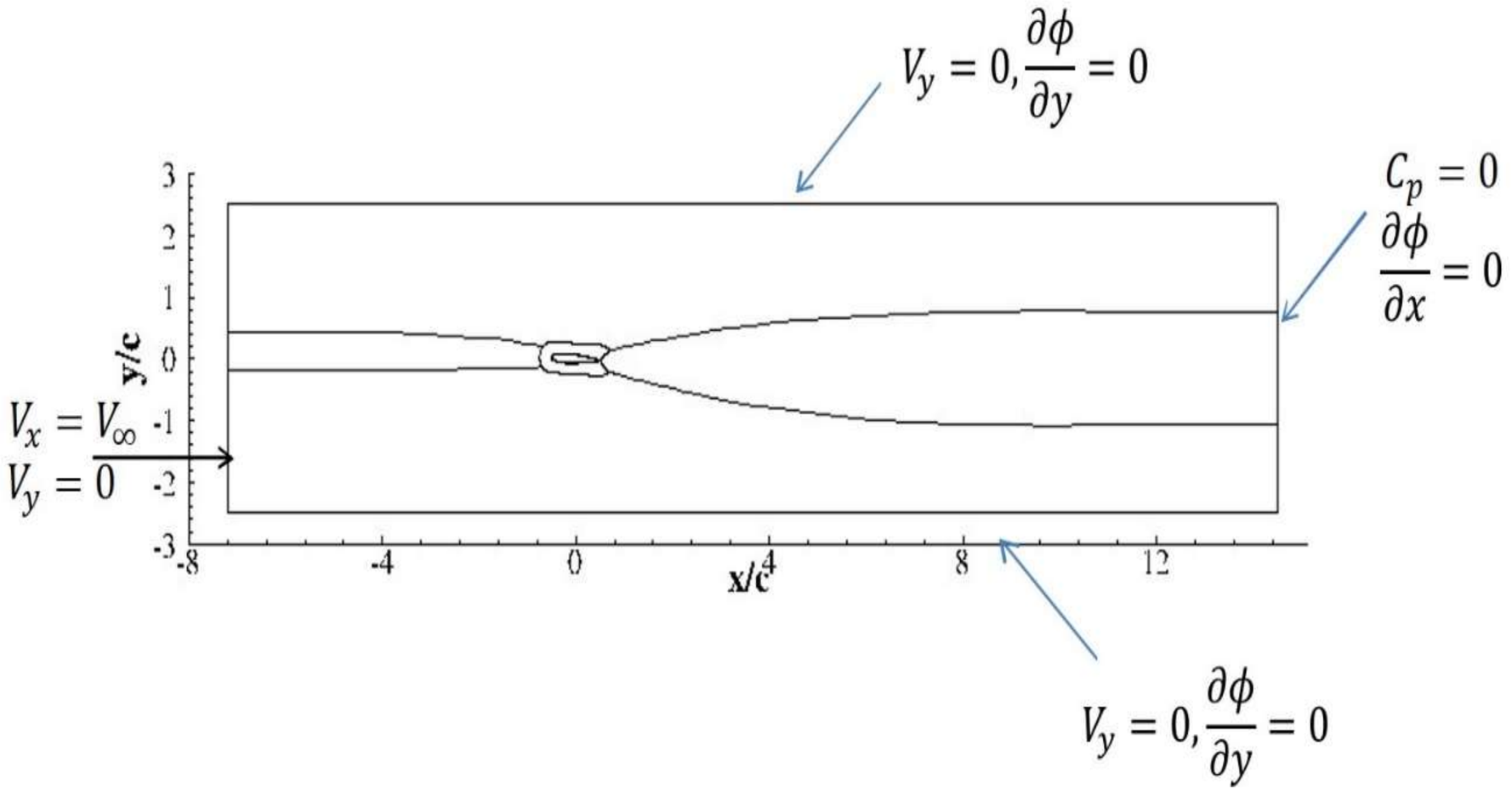

L. Eça, 9 and 12 April 2021

AVT-313 Transition Workshop

Flow around the NACA 0015 foil

- Two-dimensional rectangular domain

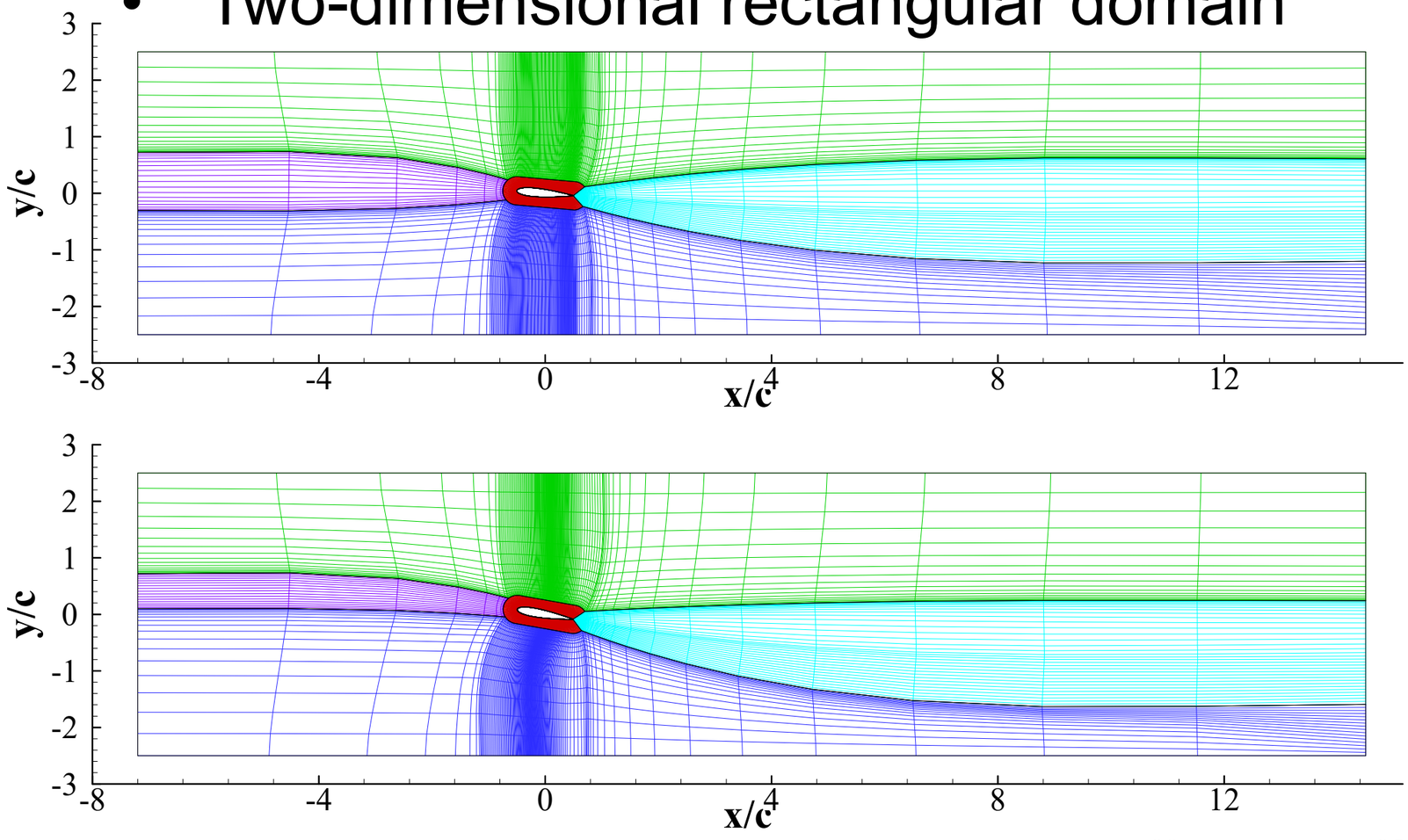

- Centre of the airfoil at the origin $\frac{x}{c} = 0.5, \frac{y}{c} = 0.$

AVT-313 Transition Workshop

Flow around the NACA 0015 foil

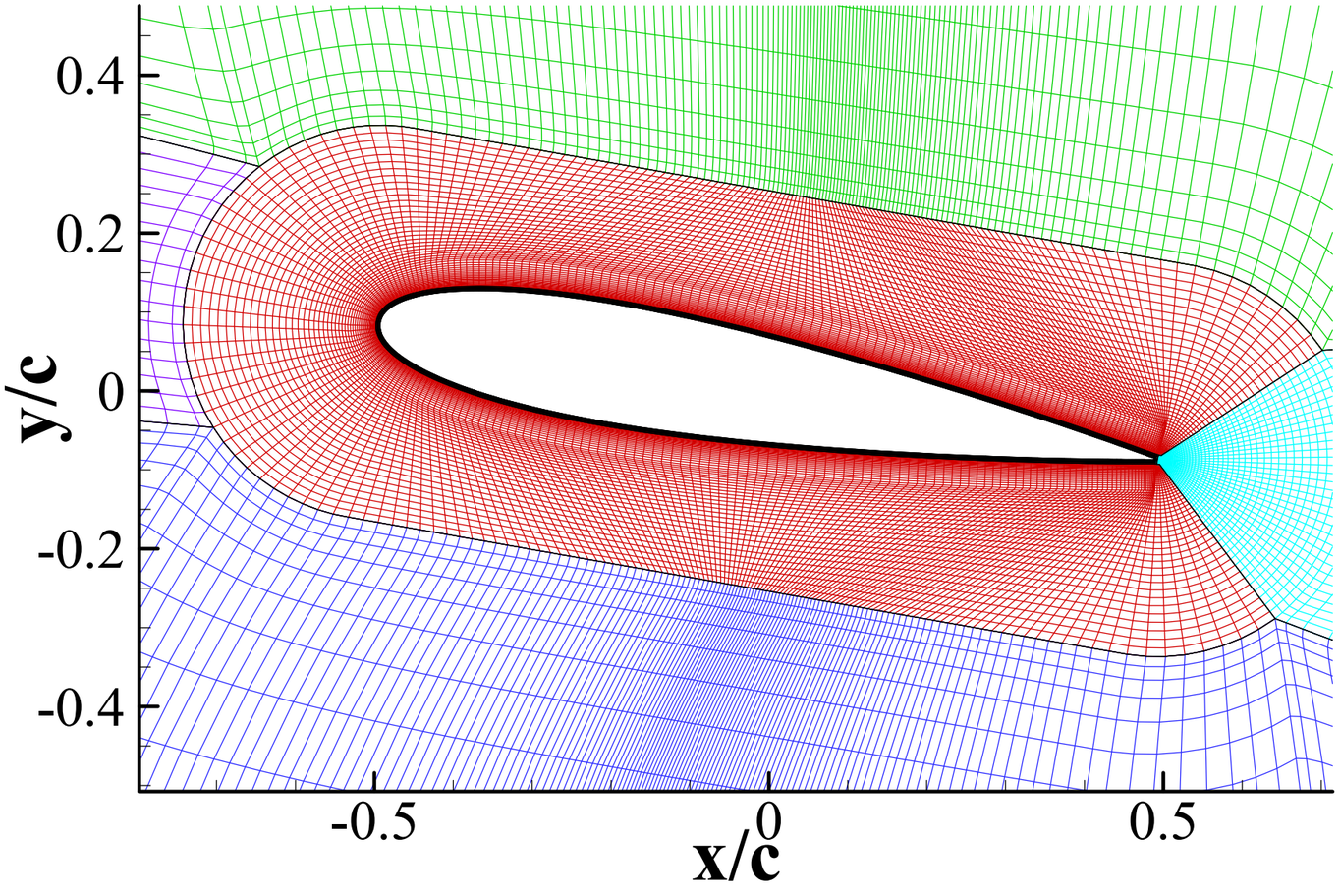

$$\alpha = 10^o$$

$\alpha = 10^o$ Leading edge at $\frac{x}{c} = -0.5\cos(\alpha)$, $\frac{y}{c} = 0.5\sin(\alpha)$.

L. Eça, 9 and 12 April 2021

Transition from Laminar to Turbulent Flow

AVT-313 Transition Workshop

Flow around the NACA 0015 foil

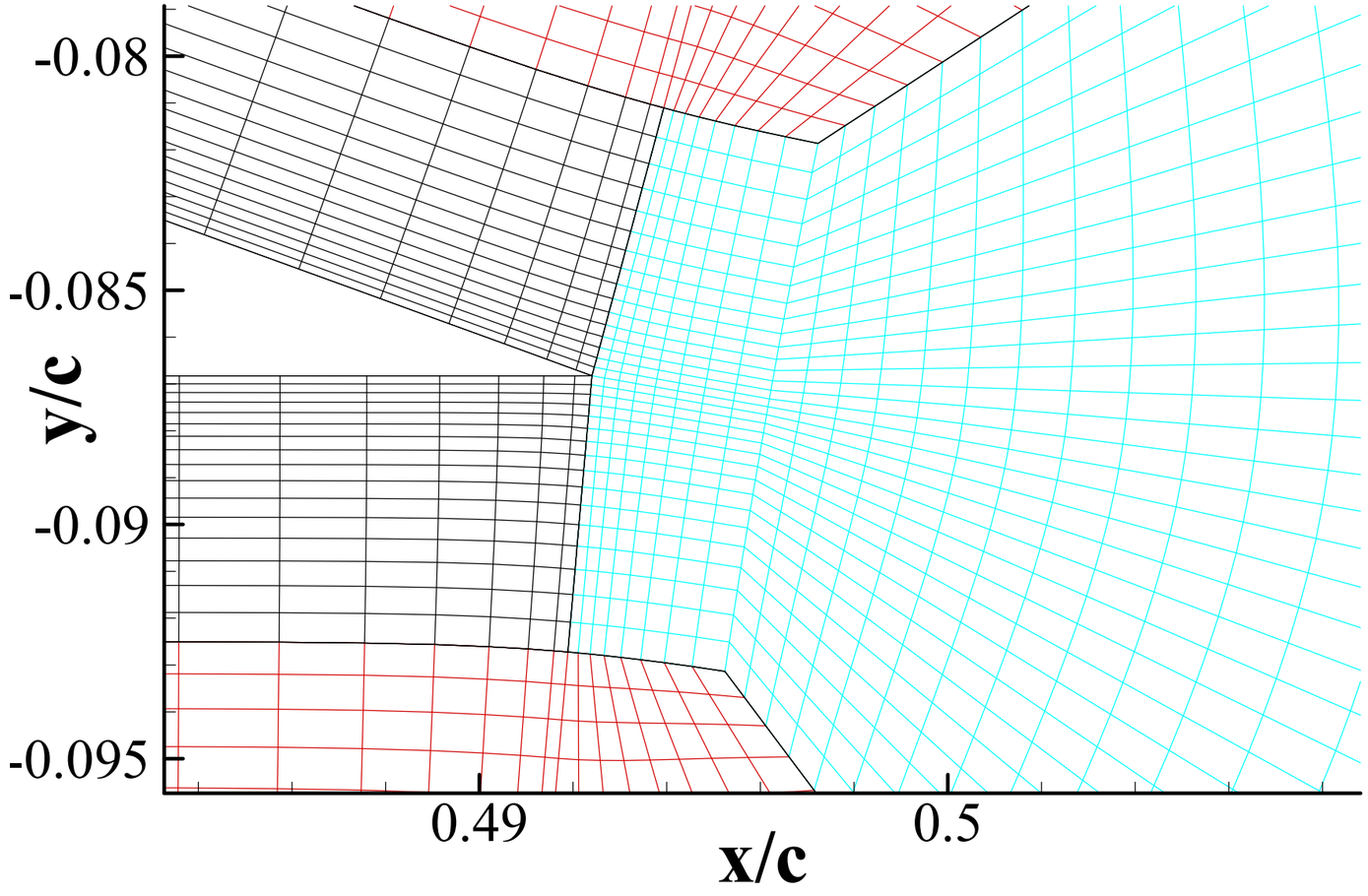

$\alpha = 10^o$

$\alpha = 10^o$ Trailing edge at $\frac{x}{c} = 0.5\cos(\alpha)\,, \frac{y}{c} = -0.5\sin(\alpha).$

L. Eça, 9 and 12 April 2021

Transition from Laminar to Turbulent Flow

AVT-313 Transition Workshop

Flow around the NACA 0015 foil

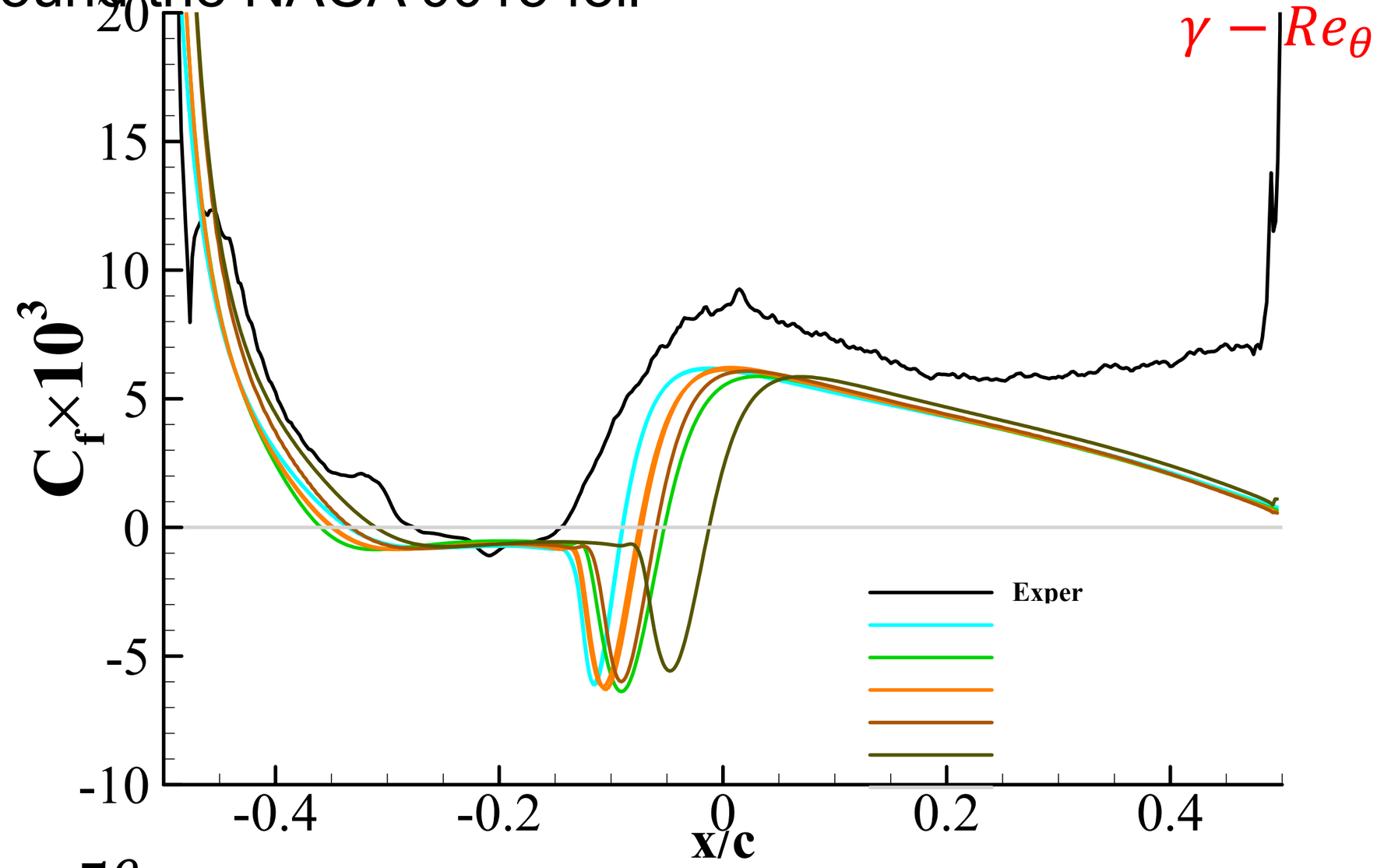

$\alpha = 5^o$

L. Eça, 9 and 12 / Upper surface, Skin friction c_f

AVT-313 Transition Workshop

Flow around the NACA 0015 foil

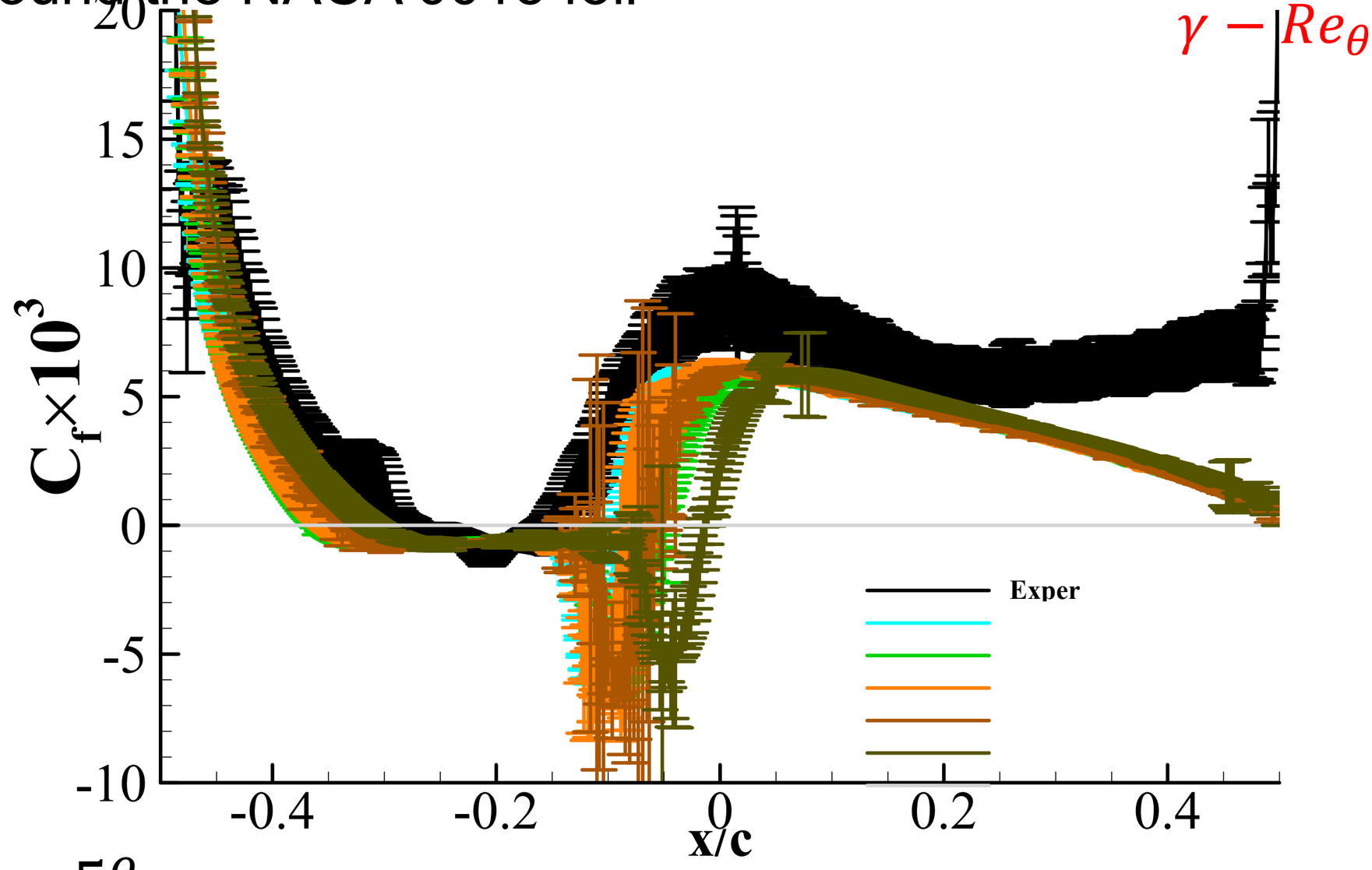

$\alpha = 5^o$

L. Eça, 9 and 12 / Upper surface, Skin friction C_f

Transition from Laminar to Turbulent Flow

AVT-313 Transition Workshop

γ

Flow around the NACA 0015 foil

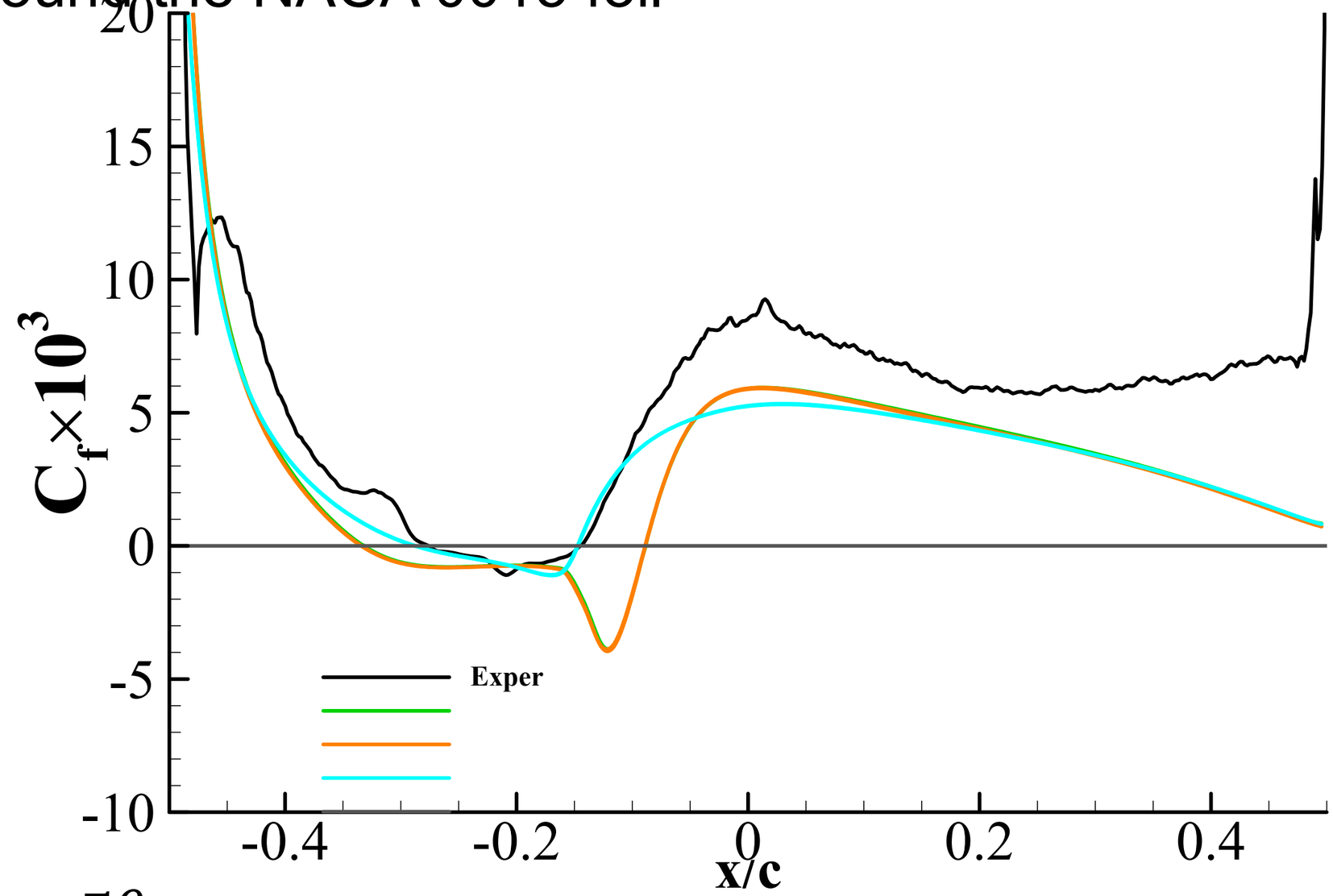

$\alpha = 5^o$

L. Eça, 9 and 12 , Upper surface, Skin friction c_f

Transition from Laminar to Turbulent Flow

AVT-313 Transition Workshop

γ

Flow around the NACA 0015 foil

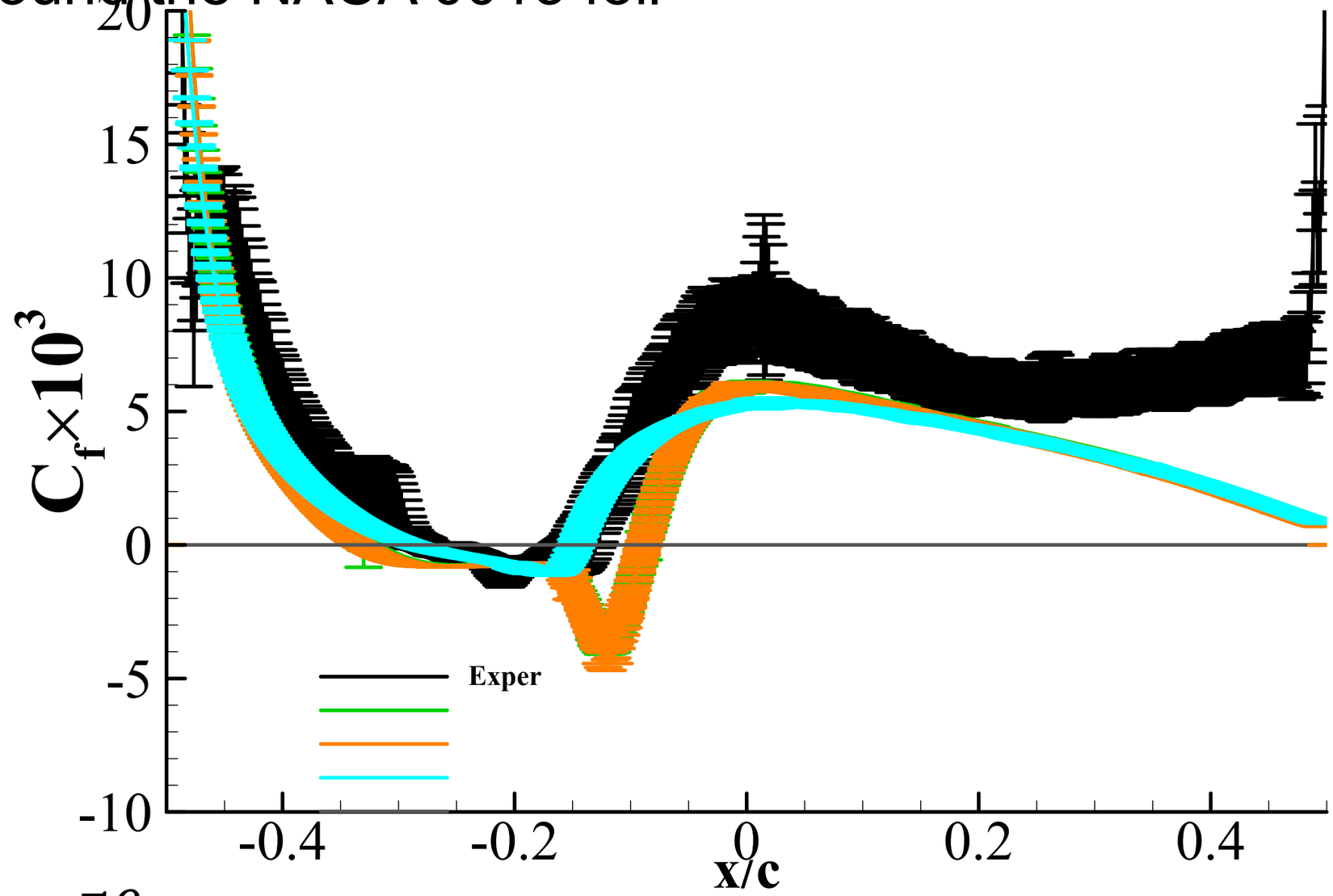

$\alpha = 5^o$

L. Eça, 9 and 12 / Upper surface, Skin friction C_f

Transition from Laminar to Turbulent Flow

AVT-313 Transition Workshop

Flow around the NACA 0015 foil

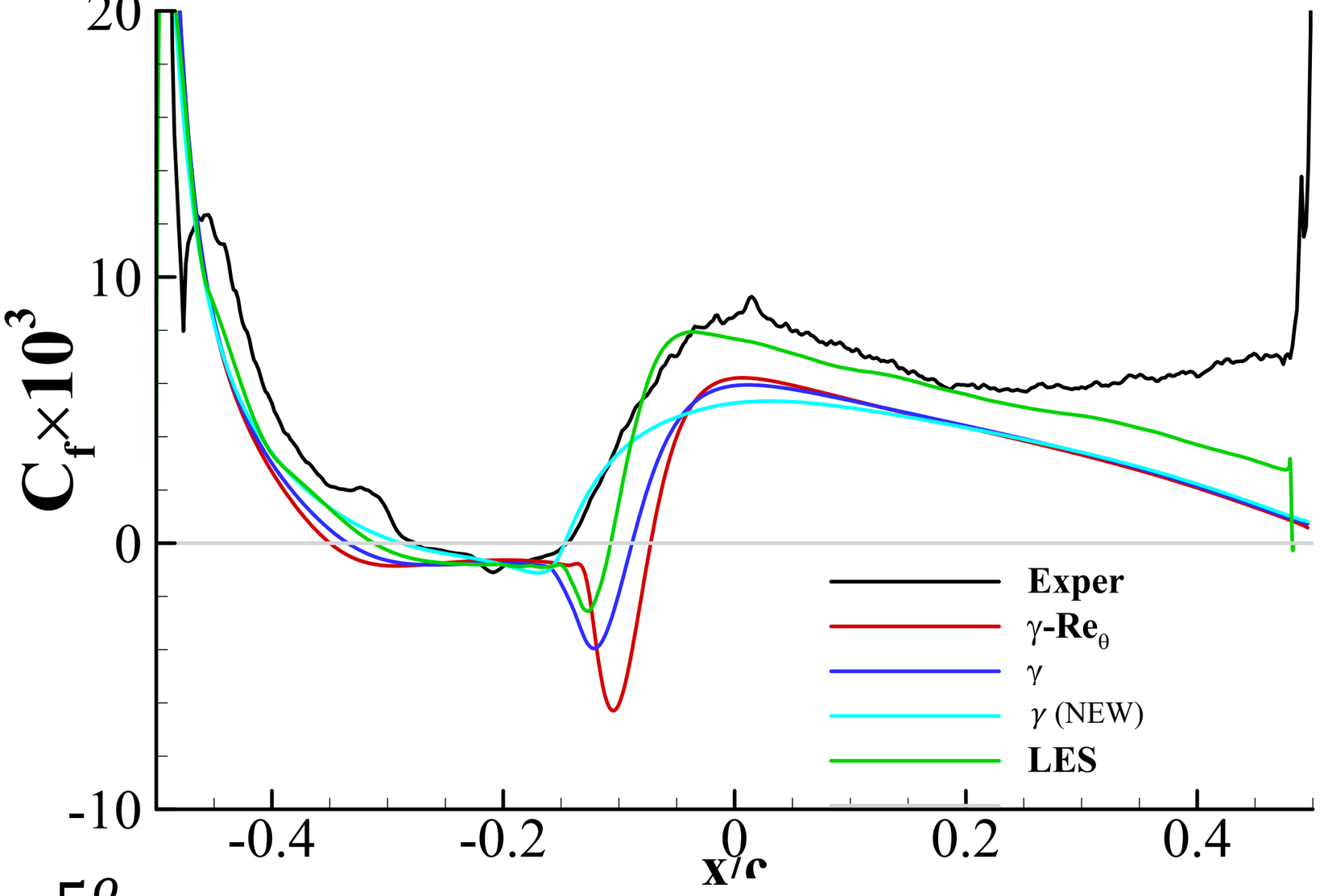

$\alpha = 5^o$

L. Eça, 9 and 12 / Upper surface, Skin friction C_f

Transition from Laminar to Turbulent Flow

AVT-313 Transition Workshop

Flow around the NACA 0015 foil

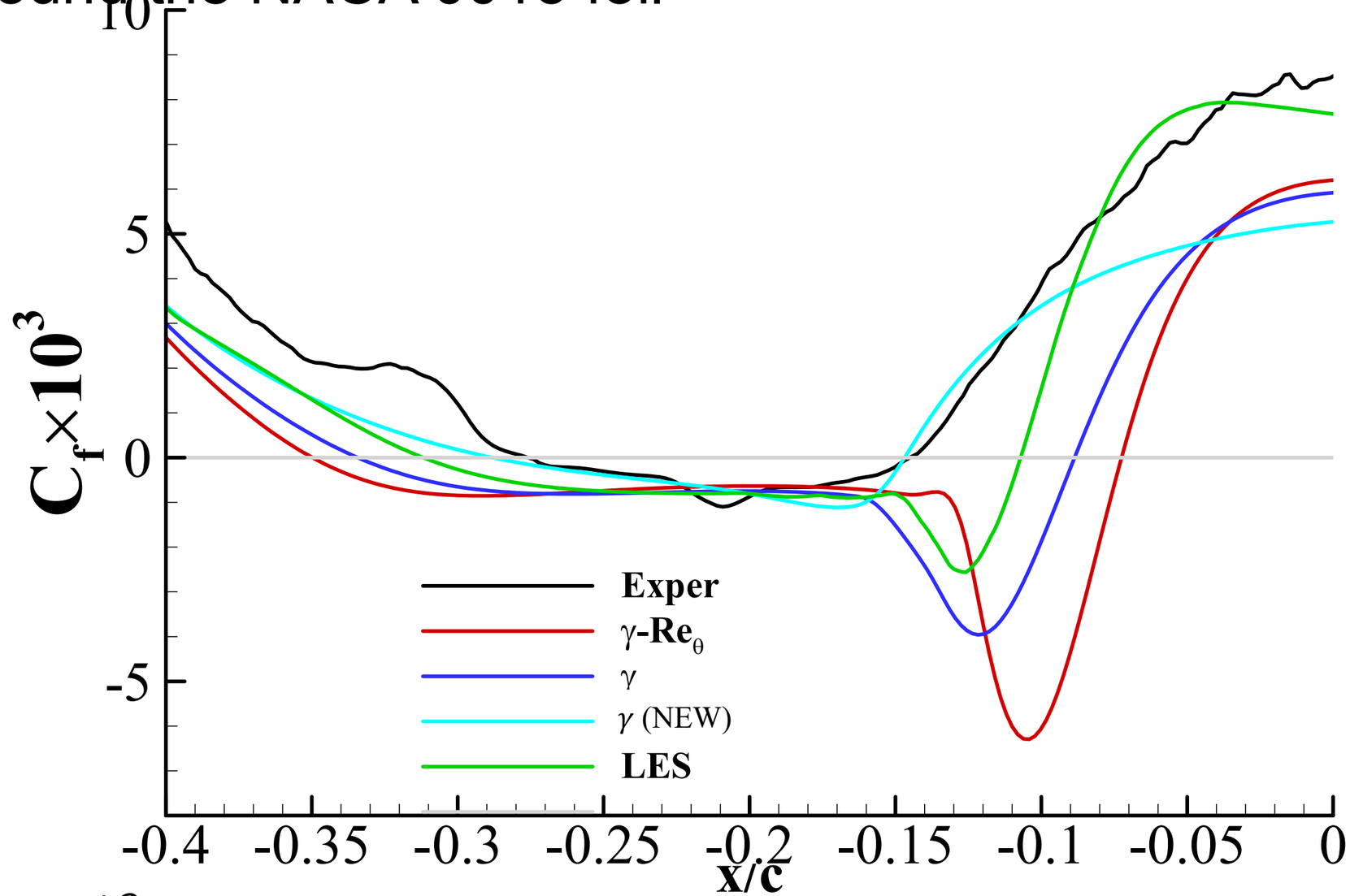

$\alpha = 5^o$

L. Eça, 9 and 12 / Upper surface, Skin friction C_f

Transition from Laminar to Turbulent Flow

AVT-313 Transition Workshop

Flow around the NACA 0015 foil

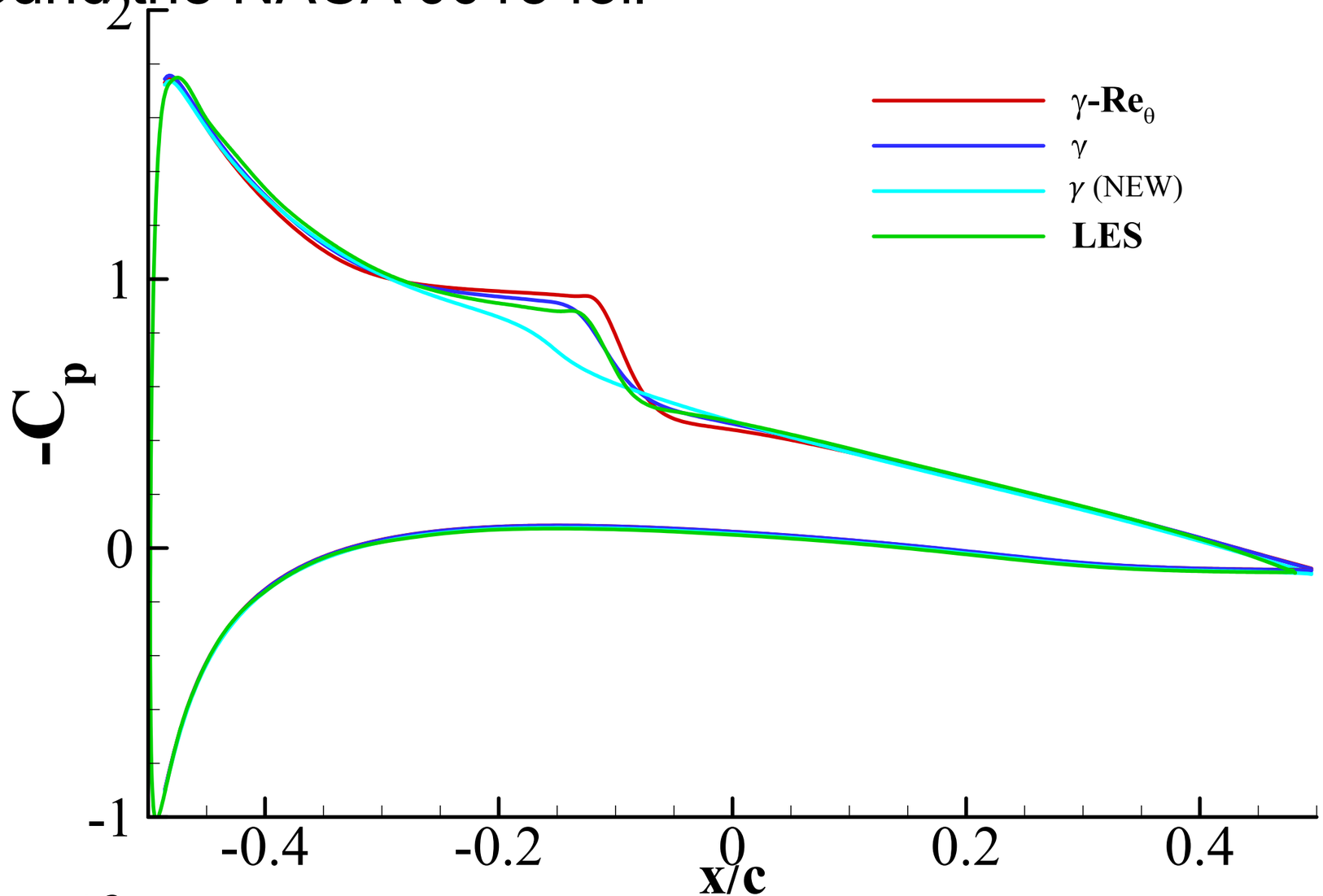

$\alpha = 5^o$

L. Eça, 9 and 12 / Upper surface, Skin friction C_f

Transition from Laminar to Turbulent Flow

AVT-313 Transition Workshop

Flow around the NACA 0015 foil

$\gamma - Re_\theta$

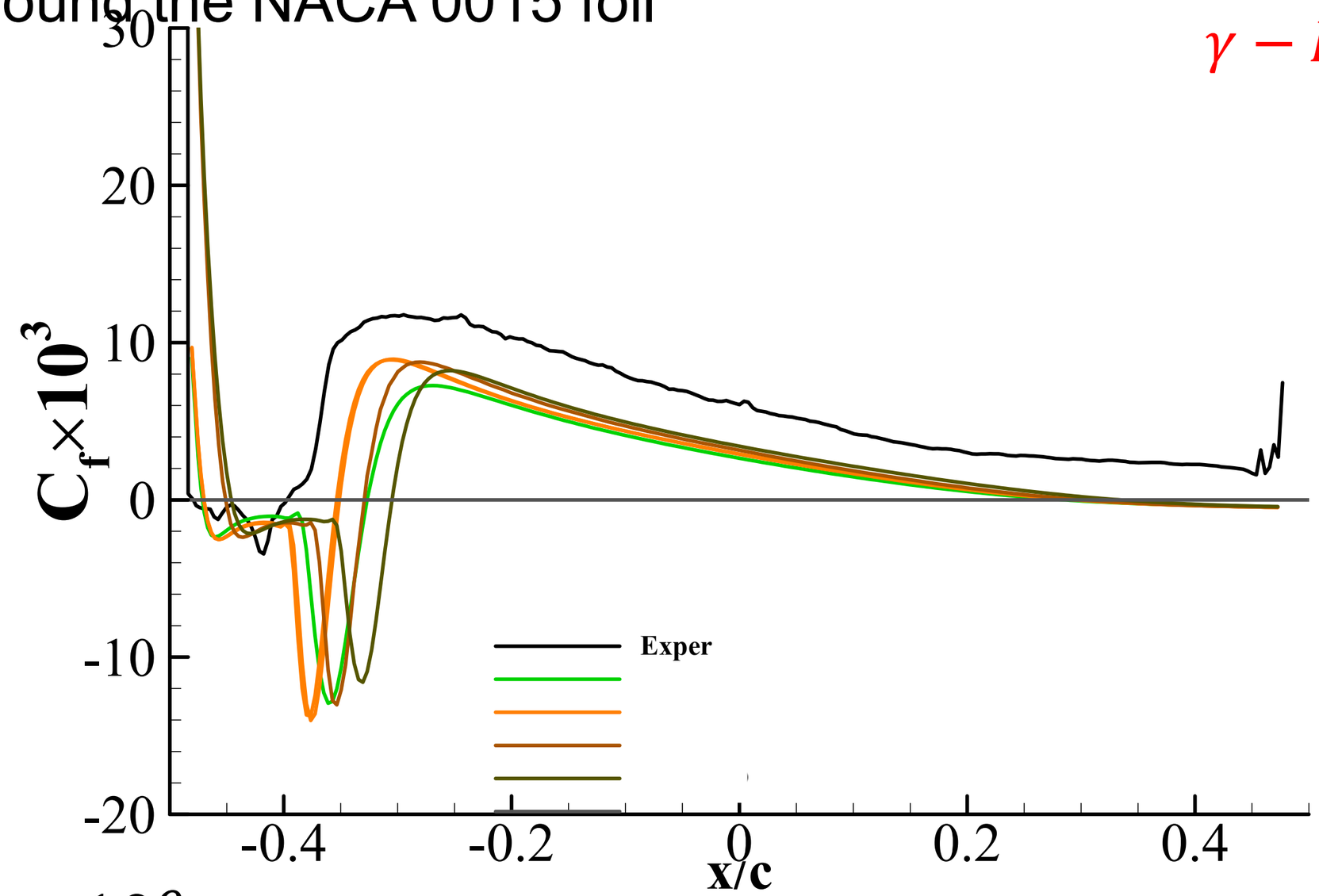

$\alpha = 10^o$

L. Eça, 9 and 12 / Upper surface, Skin friction C_f

Transition from Laminar to Turbulent Flow

AVT-313 Transition Workshop

Flow around the NACA 0015 foil

$\gamma - Re_\theta$

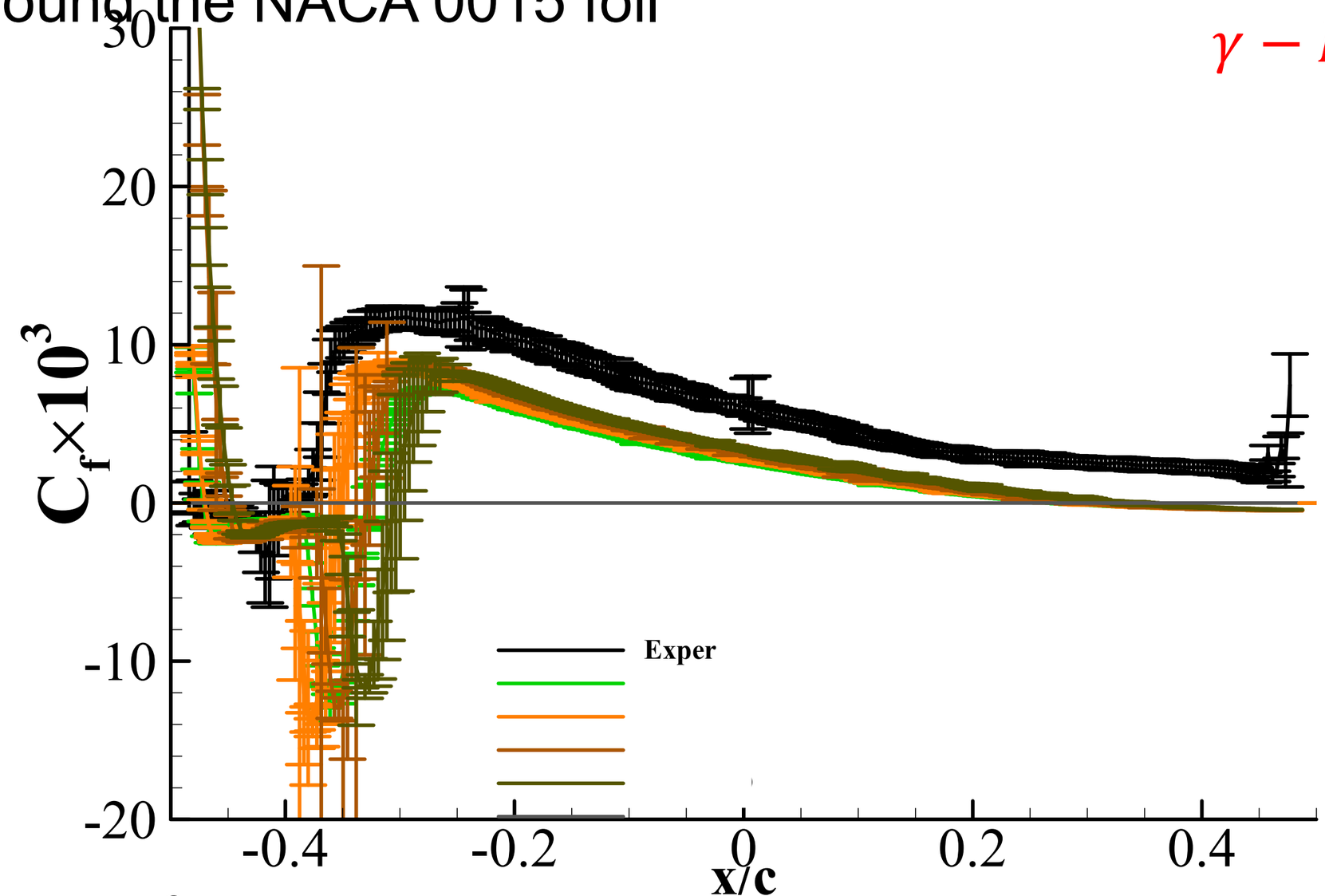

$\alpha = 10^o$

L. Eça, 9 and 12 / Upper surface, Skin friction C_f

Transition from Laminar to Turbulent Flow

AVT-313 Transition Workshop

γ

Flow around the NACA 0015 foil

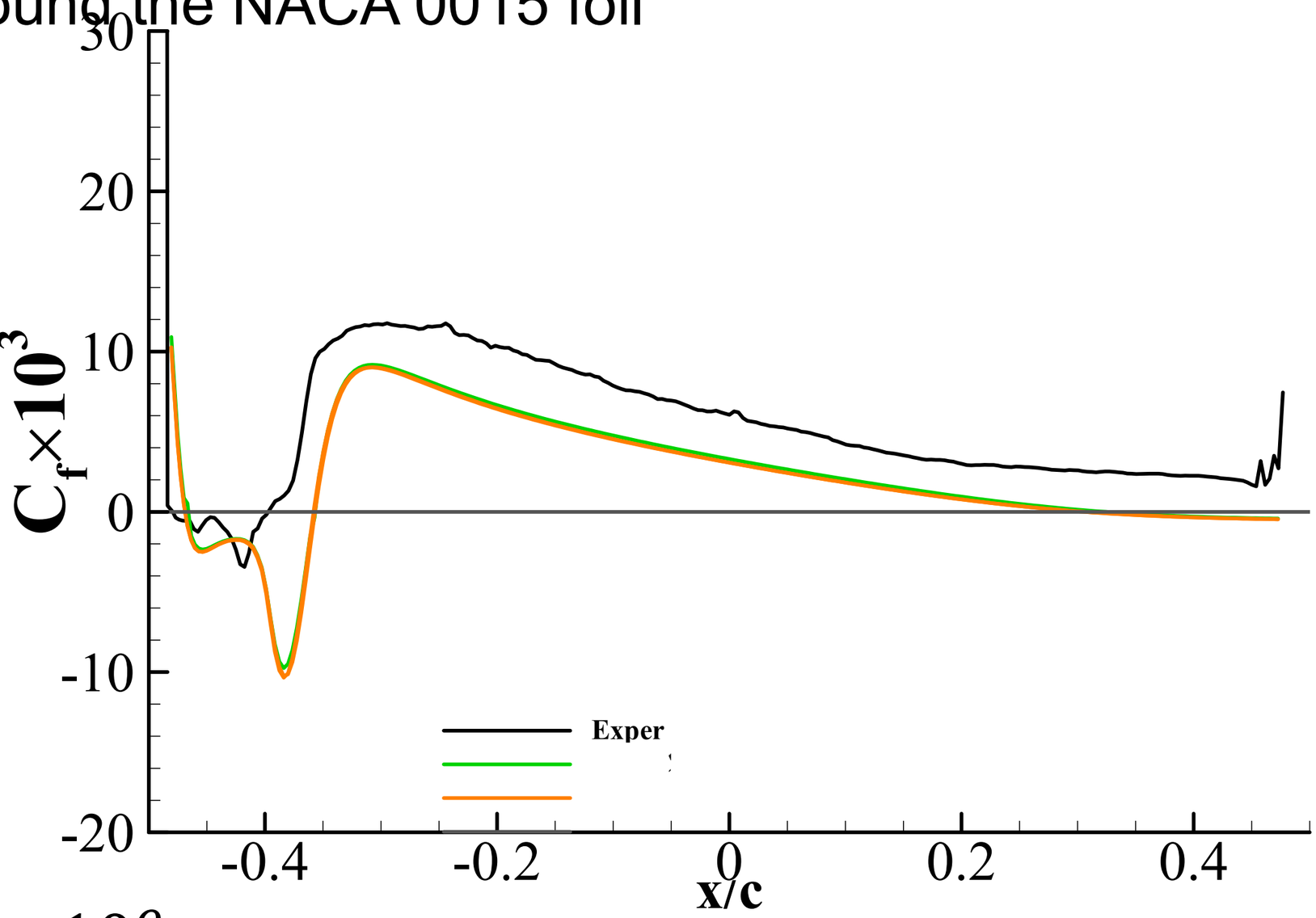

$\alpha = 10^o$

L. Eça, 9 and 12 / Upper surface, Skin friction C_f

AVT-313 Transition Workshop

γ

Flow around the NACA 0015 foil

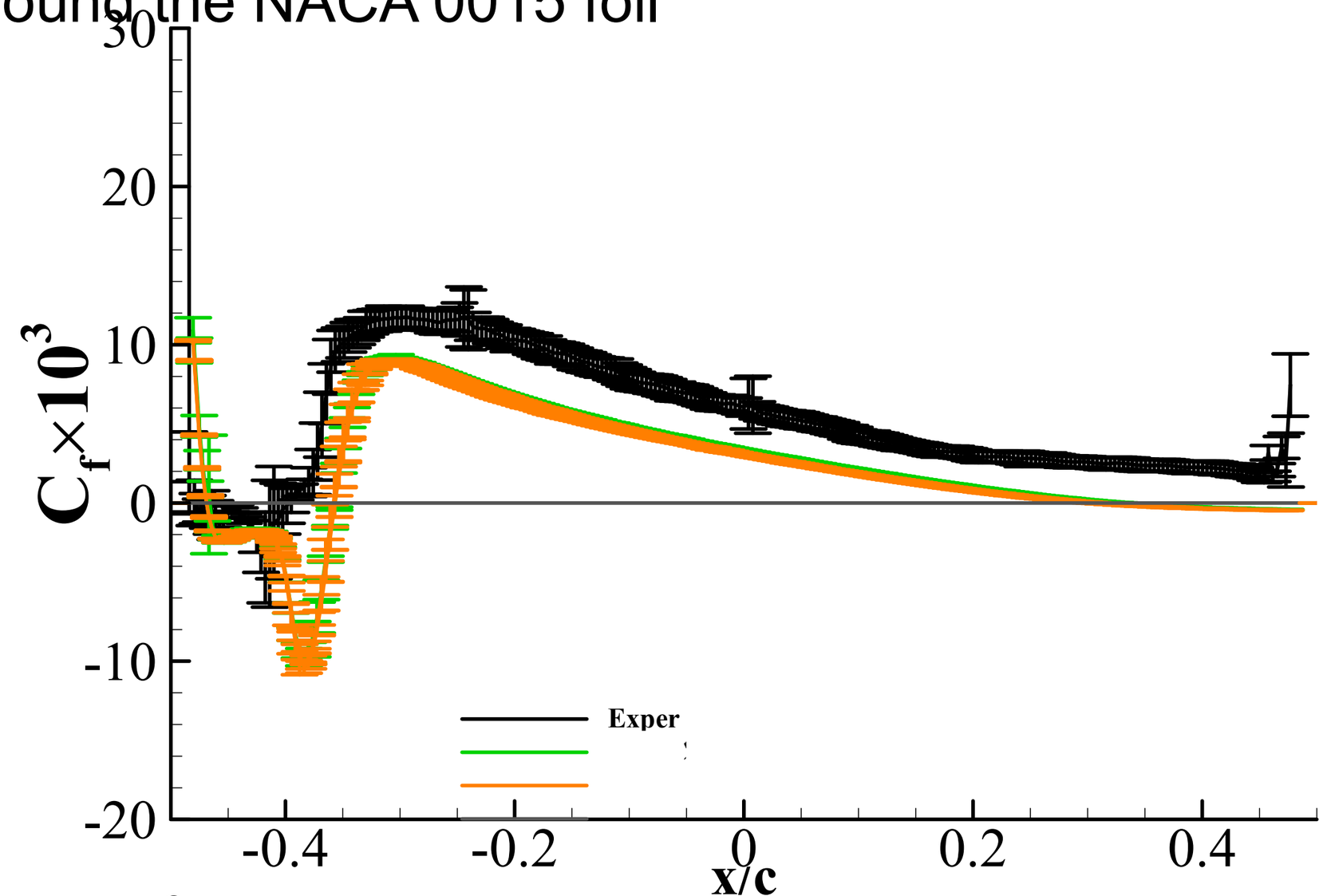

$\alpha = 10^o$

L. Eça, 9 and 12 / Upper surface, Skin friction C_f

AVT-313 Transition Workshop

Flow around the NACA 0015 foil

- General Remarks

- Largest discrepancies between all submissions;

- Experimental data needs clarification at the laminar separation bubble and downstream of $x = 0.5c$ for $\alpha = 5^o$;

- Results with the new γ model significantly different than those obtained for the Menter et al. γ model;

- Grid dependency significantly dependent on flow solver.

6:1 Prolate Spheroid

Computational Domain

- Follows workshop guidelines:
- Boundaries at $\frac{X}{L} = \pm 100$, $\frac{Y}{L} = \pm 100$ and $\frac{Z}{L} = +100$;
- Symmetry plane at the spheroid $\left(\frac{Z}{L} = 0\right)$;

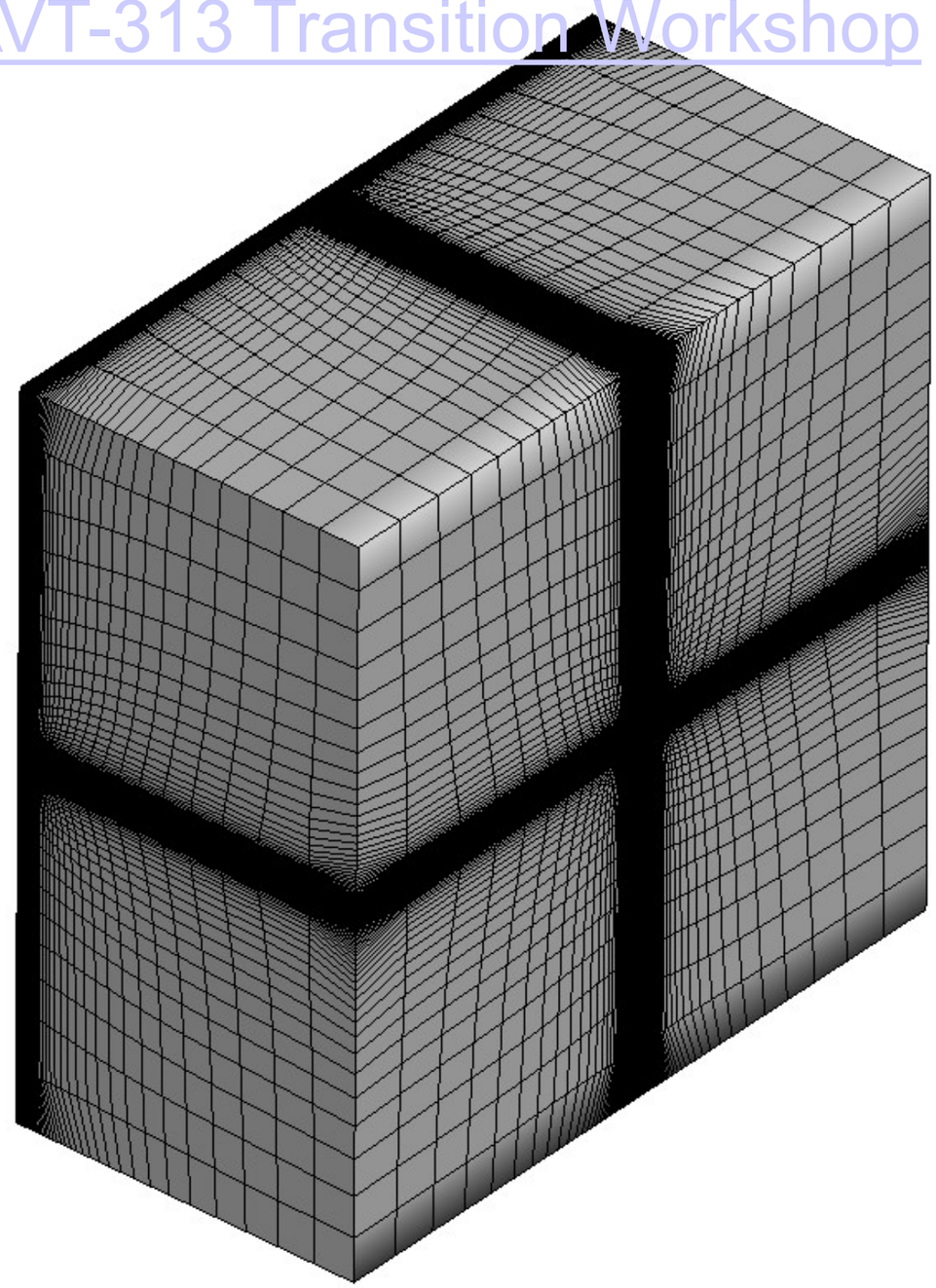

6:1 Prolate Spheroid

Grids	$r = \frac{h_i}{h_1}$	$N_{surface}$	N_{cells}
1	1	126,016	42.6M
2	1.14	95.816	28.3M
3	1.33	70,884	17.9M
4	1.61	48,750	10.3M
5	2	31,504	5.3M

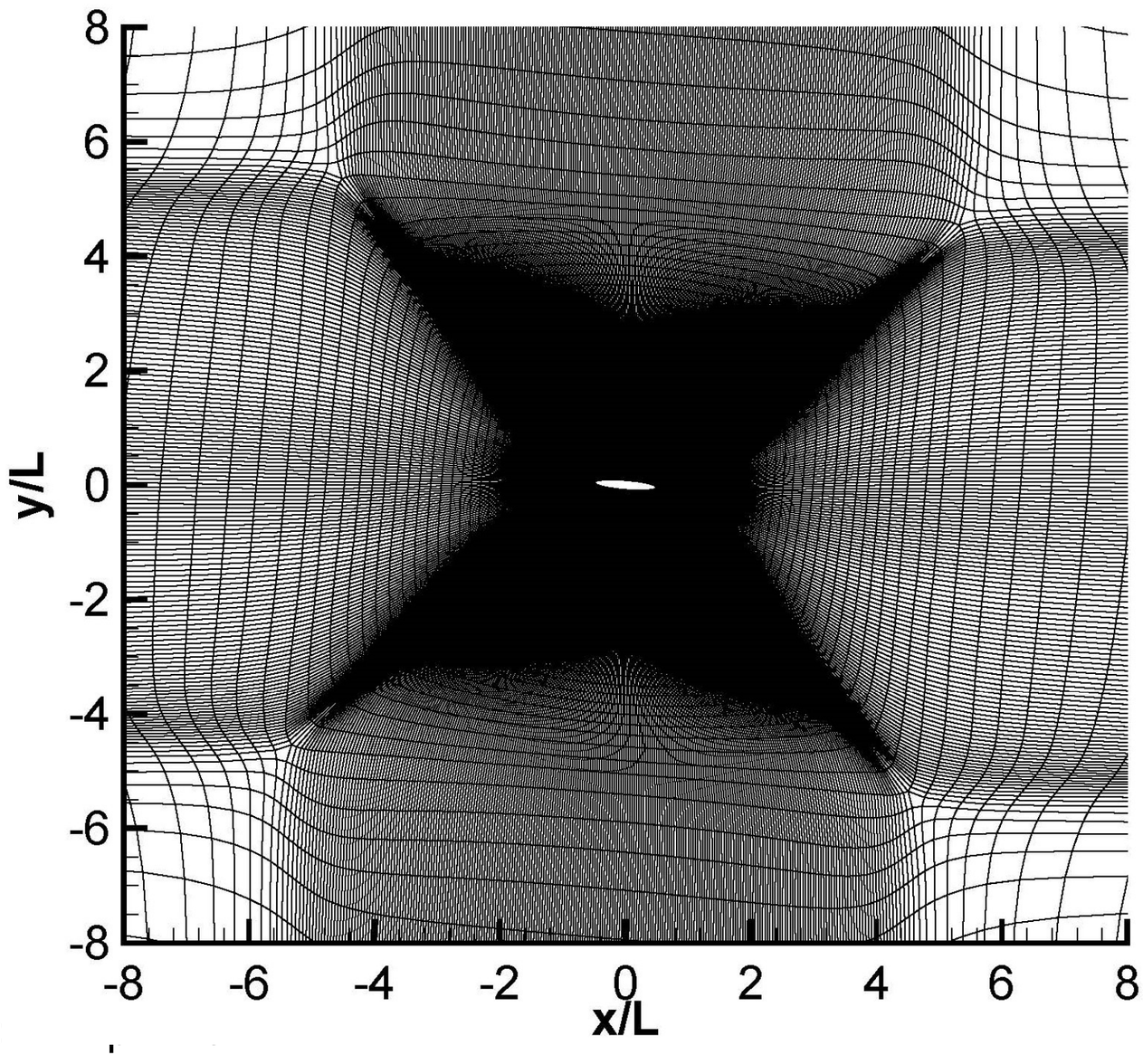

L. Eça, 9 anc

Transition from Laminar to Turbulent Flow

1st AIAA Transition Workshop and AVT-313 Transition Workshop

6:1 Prolate Spheroid

Set 1

- $I = 0.1917\%$;
- $\frac{\mu_t}{\mu} = 5.2$;
- $X_F = -1.5L$;
- Matches guideline for $I = 0.15\%$ at the nose of the spheroid.

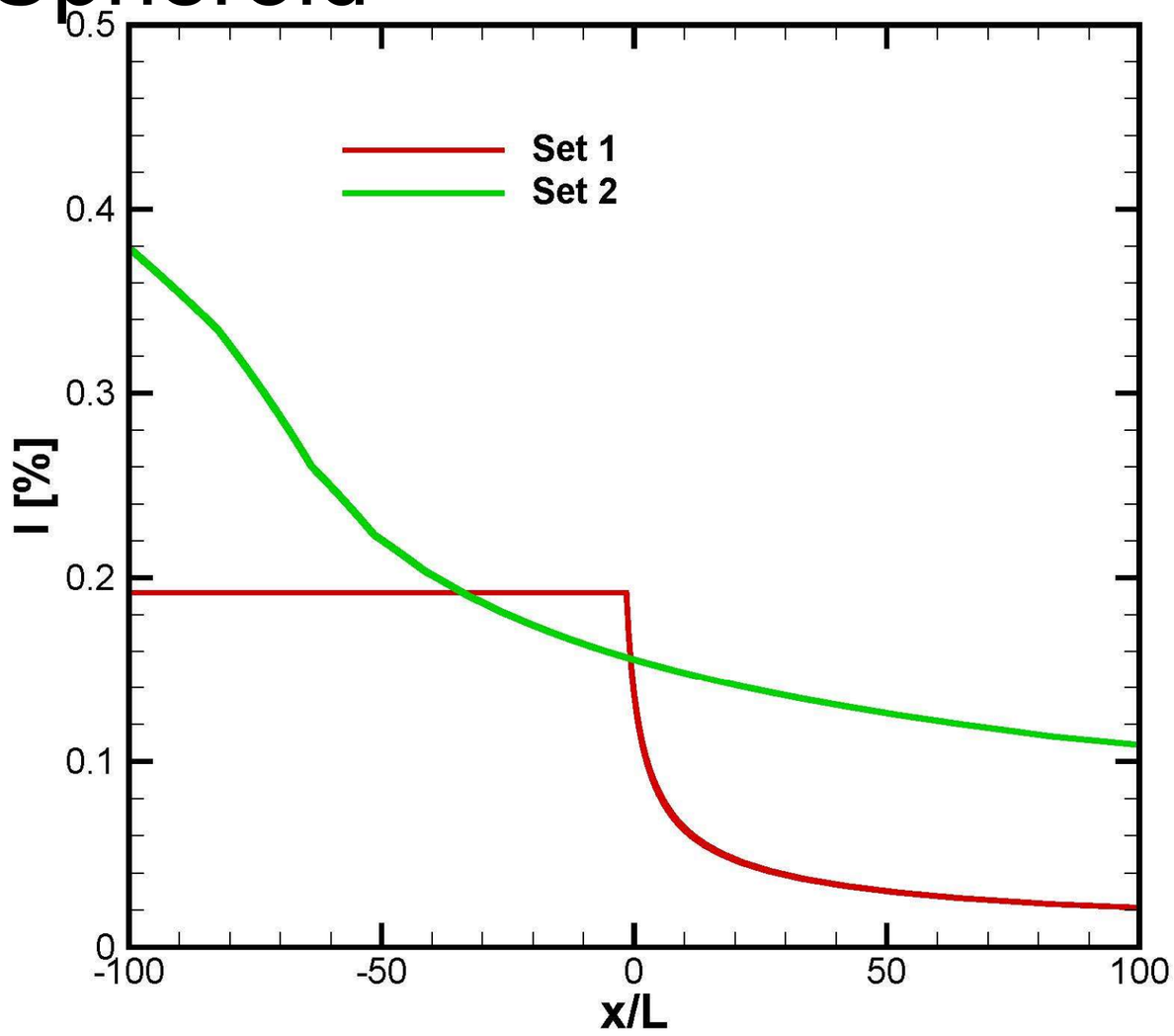

Set 2

- $I = 0.5\%$;
- $\frac{\mu_t}{\mu} = 250$;
- X_F not used;
- Matches guideline for $I = 0.15\%$ at the nose of the spheroid.

6:1 Prolate Spheroid

Boundary Conditions

- $I = 0.1917\%$;
- $\frac{\mu_t}{\mu} = 5.2$;
- $X_F = -1.5L$;
- Matches guideline for $I = 0.15\%$ at the nose of the spheroid.

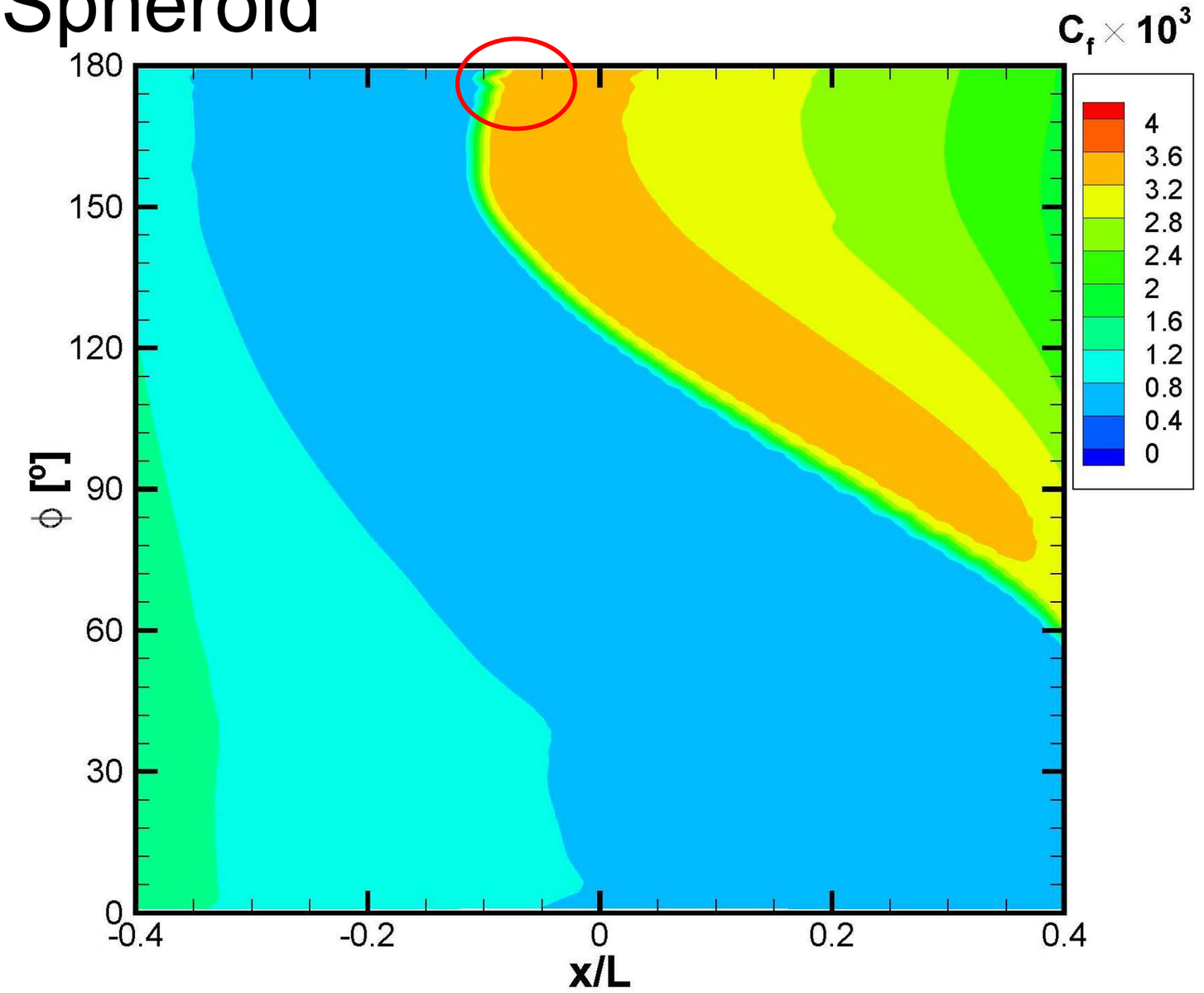

- $\alpha = 5º$
- Grid 5;
- $\gamma - Re_\theta$;

6:1 Prolate Spheroid

Boundary Conditions

- $I = 0.5\%$;
- $\frac{\mu_t}{\mu} = 250$;
- X_F not used;
- Matches guideline for $I = 0.15\%$ at the nose of the spheroid.

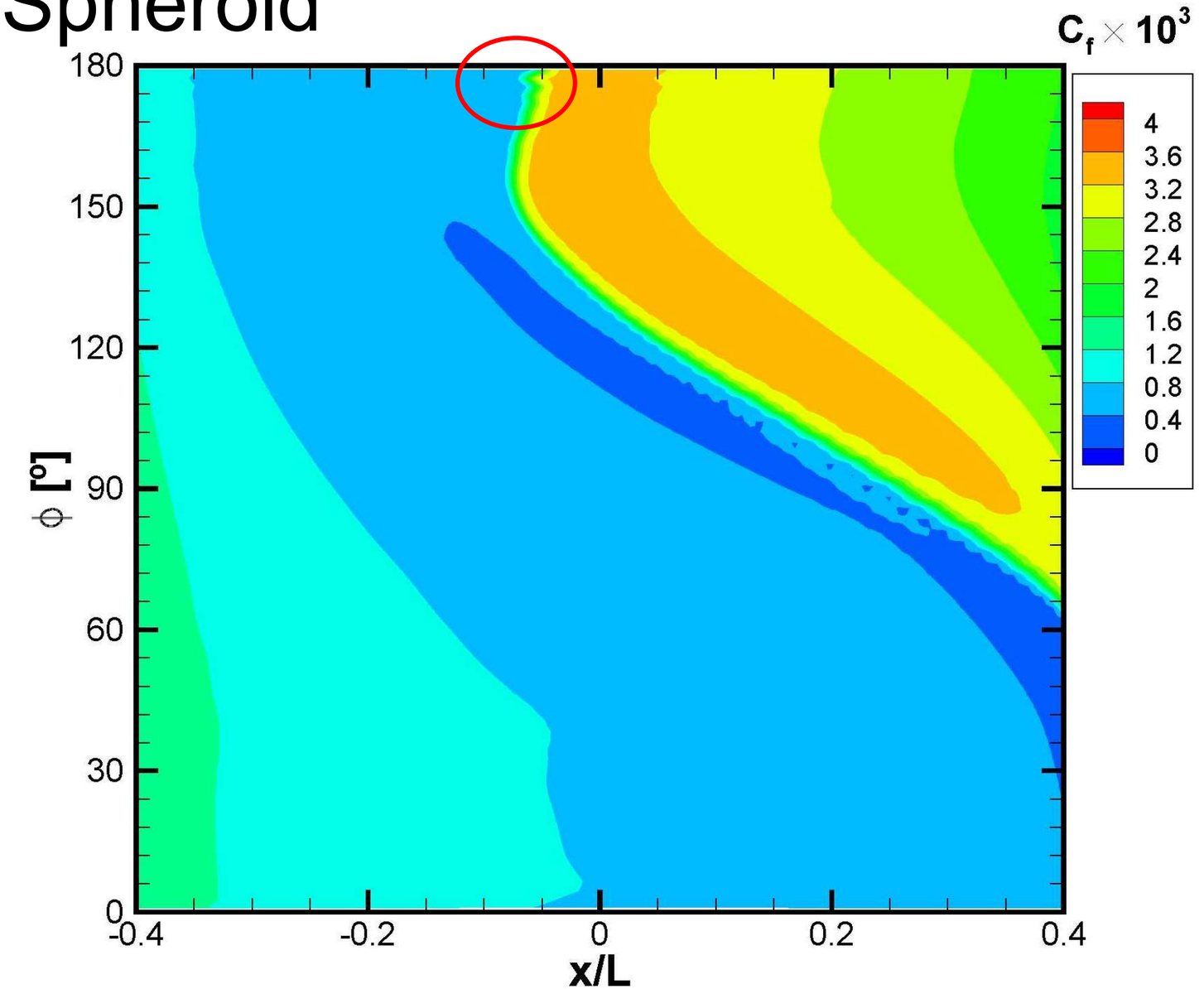

- $\alpha = 5º$
- Grid 5;
- $\gamma - Re_\theta$;

6:1 Prolate Spheroid

- $\alpha = 5º$
- Grid 5;
- $\gamma - Re_\theta$;

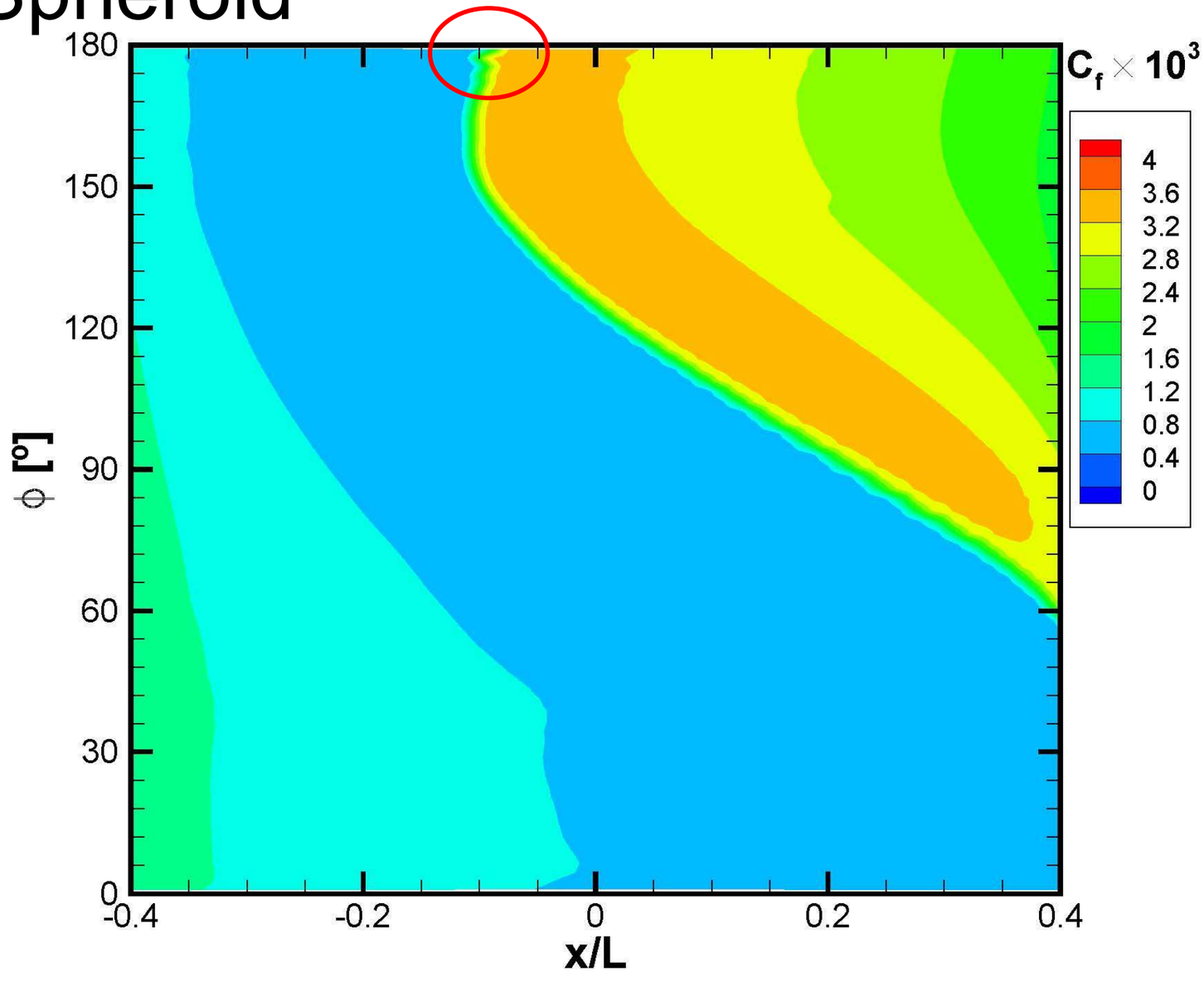

6:1 Prolate Spheroid

- $\alpha = 5º$
- Grid 3;
- $\gamma - Re_\theta$;

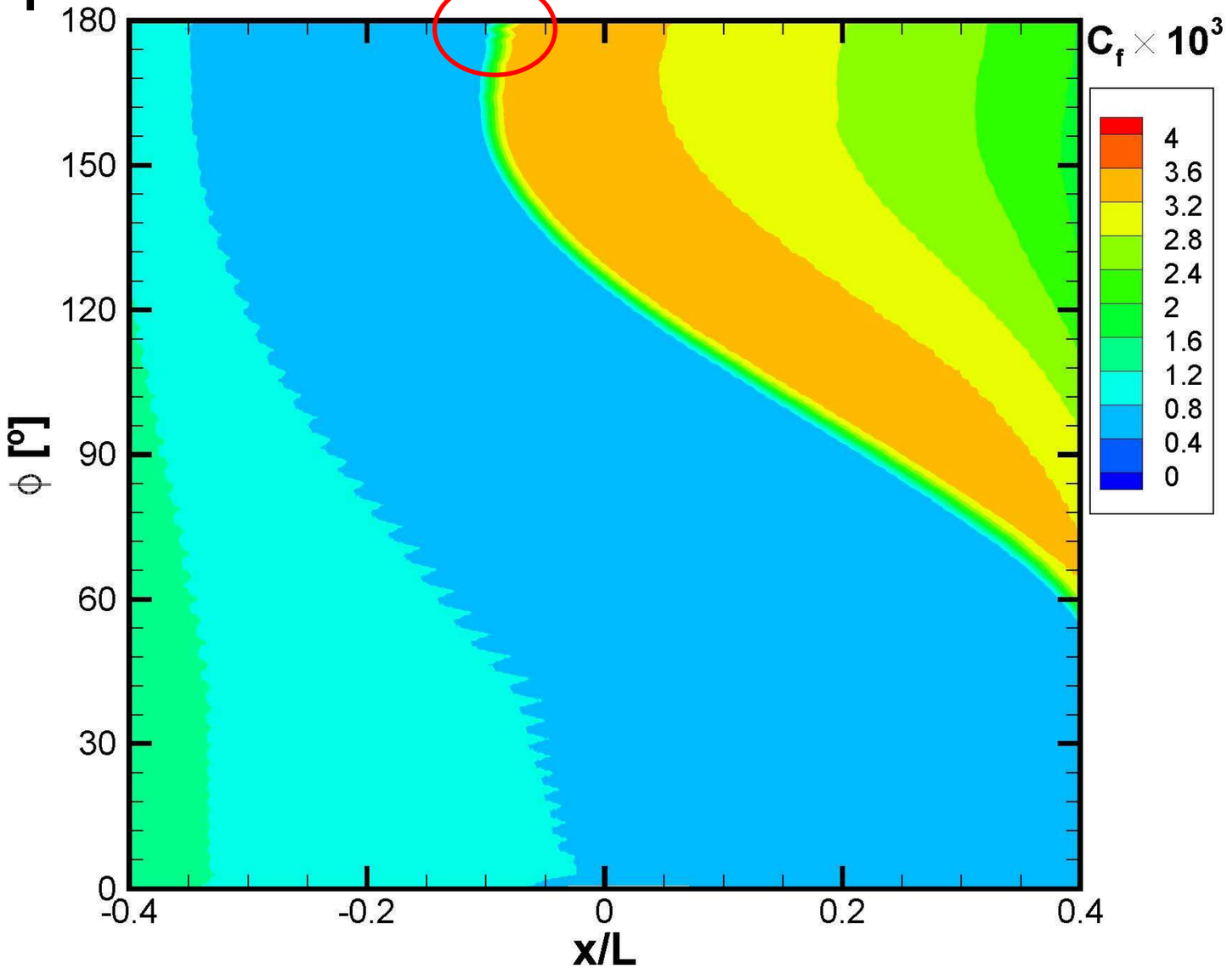

6:1 Prolate Spheroid

- $\alpha = 5º$
- Grid 1;
- $\gamma - Re_\theta$;

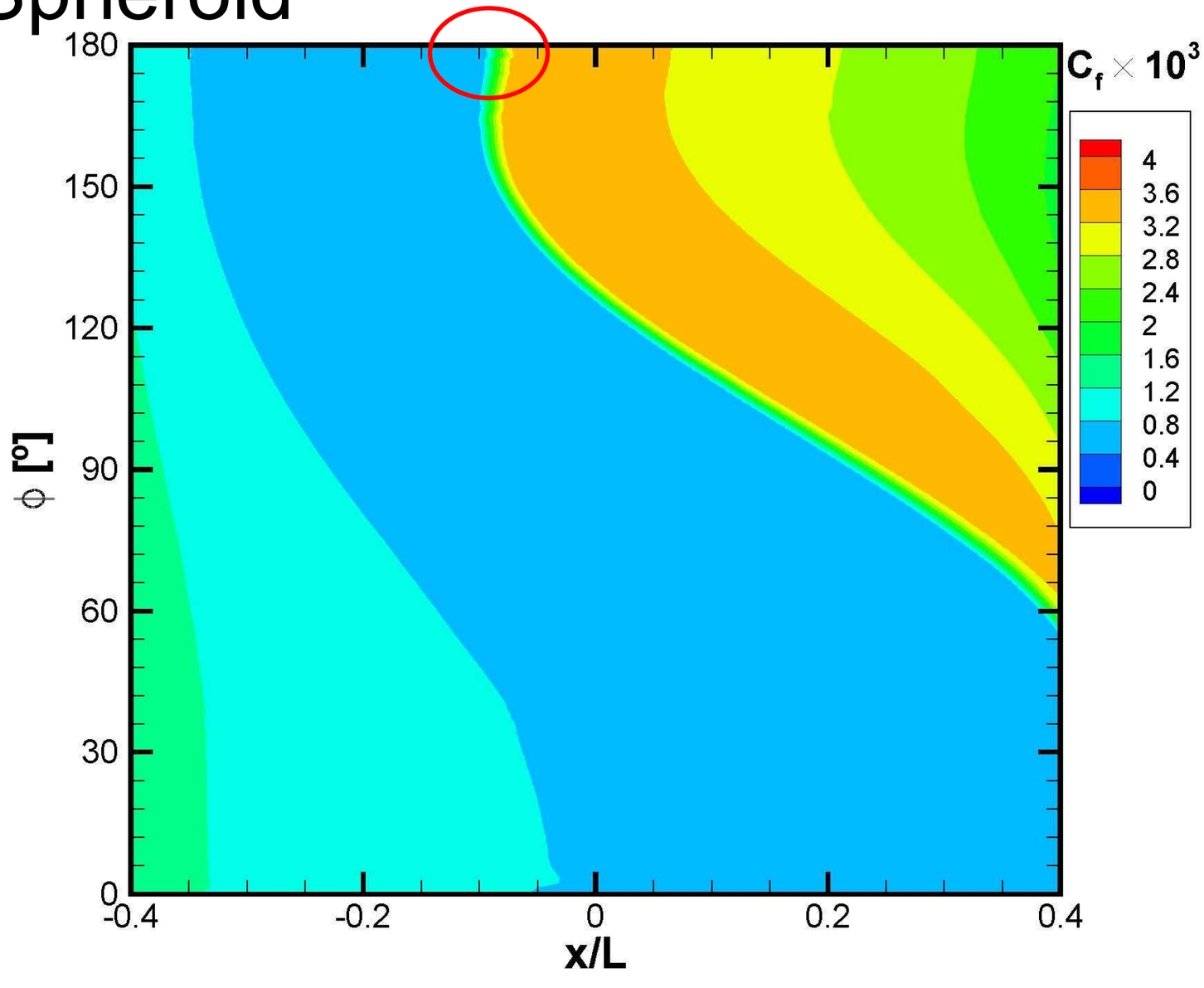

Case 3 – 6:1 Prolate Spheroid

- $\alpha = 5º$

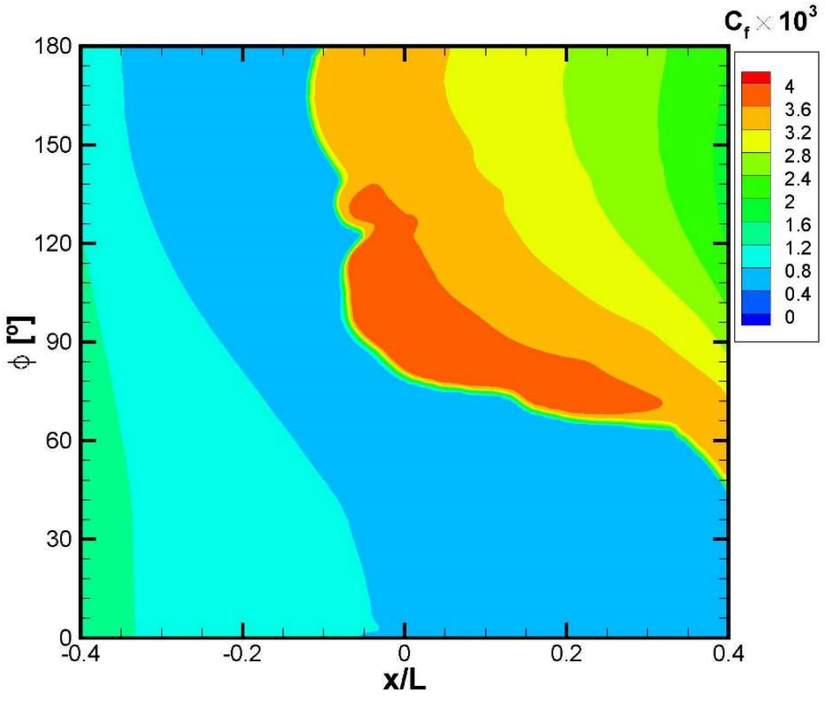

$\gamma - Re_\theta$ - CFHE

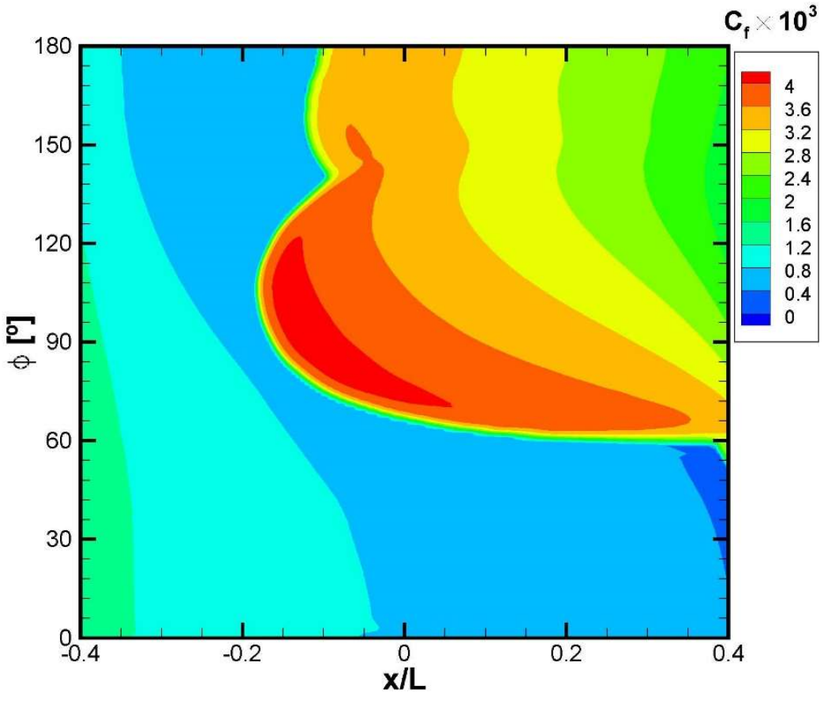

γ – CFHE

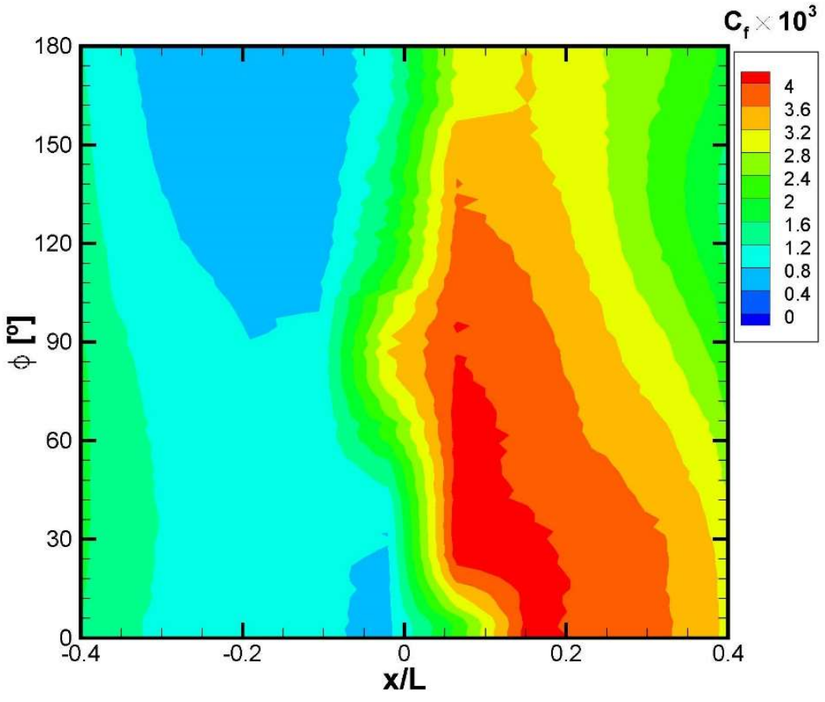

Exp.

Case 3 – 6:1 Prolate Spheroid

- $\alpha = 15º$

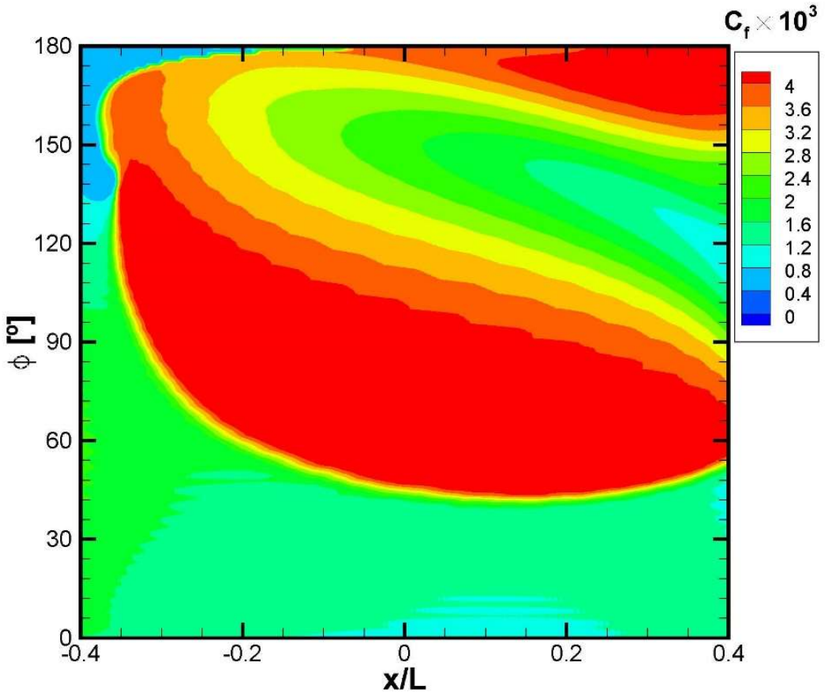

$\gamma - Re_\theta$ - CFHE

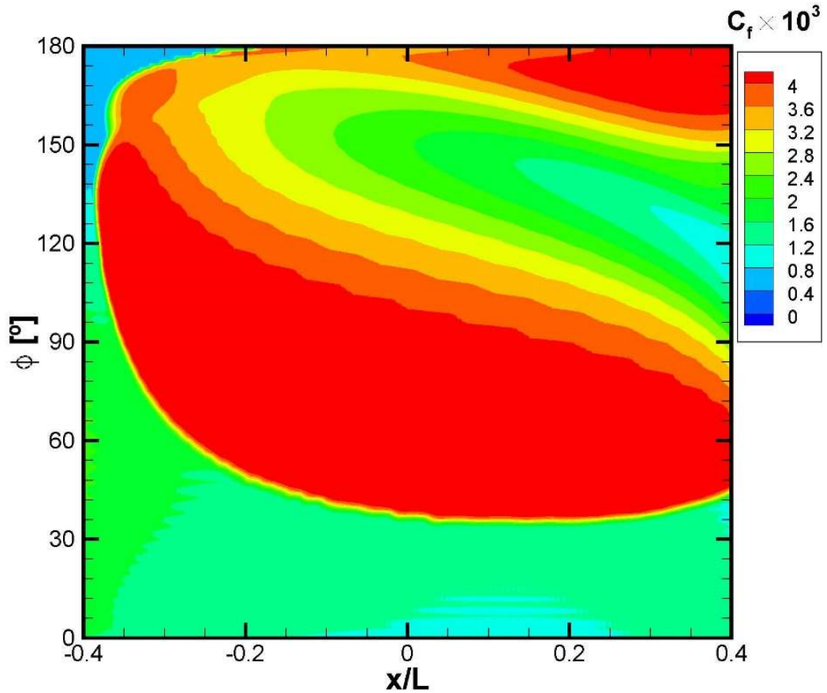

γ – CFHE

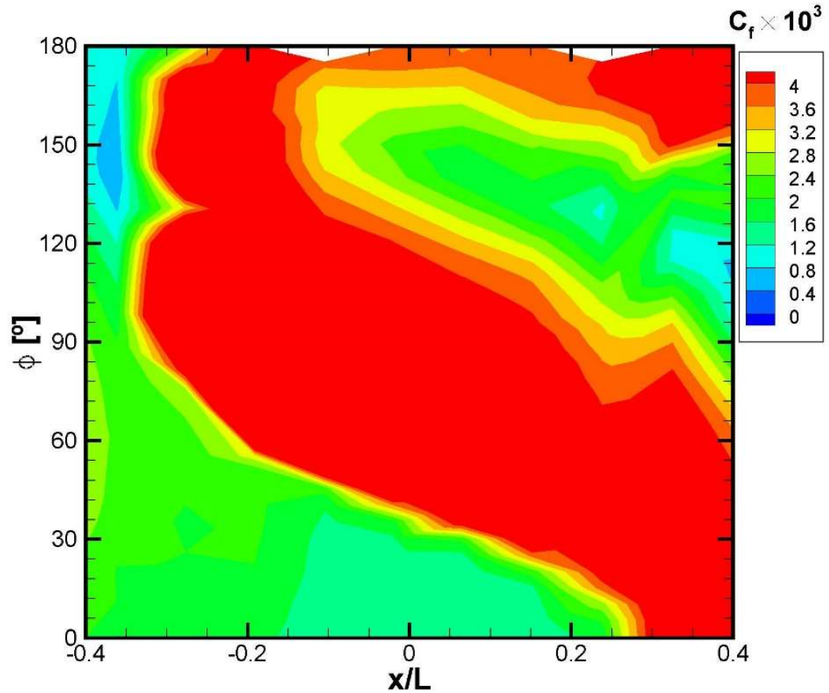

Exp.

L. Eça, 9 and 12 April 2021

6:1 Prolate Spheroid

- Complete specification of inlet boundary conditions is essential for simulations performed with transition models at low Reynolds numbers. Specifying only turbulence intensity at the leading edge is insufficient.
- Reliable comparison with experimental data depends on knowledge of complete inflow conditions and domain size (wind tunnels are not infinite domains).
- Using large (awkward) values of eddy-viscosity at the inlet is most likely an attempt to correct an error (of the underlying turbulence model) with an another error.

L. Eça, 9 and 12 April 2021

Final Remarks

- Transitional flows strongly depend on inflow conditions and other flow details (as for example surface roughness) that are not always known;
- Present RANS transition models give a clear improvement of the agreement between simulations and experiments, but a proper validation exercise (modelling error assessment) is difficult to perform;
- Extension of the present transition models to Scale Resolving Simulations is not straightforward.

Acknowledgement

- The contents of this presentation are a result of the MARIN-IST cooperation that started in October 1986;
- Most of the simulations presented were performed with the CFD solver ReFRESCO. Recent developments in the handling of transitional flows are part of the PhD thesis of Rui Lopes;
- Thanks to all the groups that submitted data to the 2-D test cases of the AVT-313 Workshops.

L. Eça, 9 and 12 April 2021